

**4/81**

CMCRCZ 10(4), 291-383 (1981)

**ΧΗΜΙΚΑ ΧΡΟΝΙΚΑ**

ΝΕΑ ΣΕΙΡΑ

**CHIMIKA CHRONIKA**

NEW SERIES

**AN INTERNATIONAL EDITION  
OF THE GREEK CHEMISTS ASSOCIATION**

# CHIMIKA CHRONIKA /NEW SERIES

Published by the Greek Chemists' Association  
27, Kaningos Street, Athens (147), Greece

## MANAGING COMMITTEE

Irene DILARIS, Yannis GAGLIAS, Vassilios M. KAPOULAS, Vassilios LAMBROPOULOS,  
Georgia MARGOMENOU - LEONIDOPOULOU, Panayotis PROUNTZOS, George SKALOS

Ex-officio Members: Panayotis PAPADOPOULOS (Asst. Gen. Secretary of G.C.S.),  
Stelios CHATZIYANNAKOS (Treasurer of G.C.S.).

## EDITORS - IN - CHIEF

V.M. KAPOULAS

G. SKALOS

G. MARGOMENOU - LEONIDOPOULOU

## EDITORIAL ADVISORY BOARD

N. ALEXANDROU

*Org. Chem., Univ. Salonica*

A. ANAGNOSTOPOULOS

*Inorg. Chem., Tech. Univ. Salonica*

P. CATSOULACOS

*Pharm. Chem., Univ. Patras*

G.D. COUMOULOS

*Physical Chemistry Athens*

C.A. DEMOPOULOS

*Biochemistry, Univ. Athens*

C.E. EFSTATHIOU

*Anal. Chem., Univ. Athens*

A.E. EVANGELOPOULOS

*Biochemistry, N.H.R.F., Athens*

S. FILIANOS

*Pharmacognosy, Univ. Athens*

D.S. GALANOS

*Food Chem., Univ. Athens*

A.G. GALINOS

*Inorg. Chem. Univ. Patras*

P. GEORGAKOPOULOS

*Pharm. Techn., Univ. Salonica*

I. GEORGATOS

*Biochemistry, Univ. Salonica*

M.P. GEORGIADIS

*Org./Med. Chem., Agr. Univ. Athens*

N. HADJICHRISTIDIS

*Polymer Chem., Univ. Athens*

T.P. HADJIIOANNOU

*Anal. Chem., Univ. Athens*

E. HADJLOUDIS

*Photochem., N.R.C. "D", Athens*

H. CHJA

*Food Technol., Univ. Salonica*

D. JANNAKLOUDAKIS

*Phys. Chem., Univ. Salonica*

N.K. KALFOGLOU

*Polymer Sci., Univ. Patras*

E. KAMPOURIS

*Polymer. Chem., Tech. Univ. Athens*

M.I. KARAYANNIS

*Anal. Chem., Univ. Ioannina*

N. KATSANOS

*Phys. Chem., Univ. Patras*

D. KIOUSSIS

*Petrochemistry, Univ. Athens*

A. KOSMATOS

*Org. Chem., Univ. Ioannina*

P. KOUROUNAKIS

*Pharm. Chem., Univ. Salonica*

G.P. KYRIAKAKOU

*Org./Phys. Chem., Univ. Ioannina*

S.B. LITSAS

*Bioorg. Chem., Arch. Museum, Athens*

G. MANOUSSAKIS

*Inorg. Chem., Univ. Salonica*

I. MARANGOSIS

*Chem. Mech., Tech. Univ. Athens*

I. NIKAKAVOURAS

*Photochem., N.R.C. "D", Athens*

D.N. NICOLAIDES

*Org. Chem., Univ. Salonica*

C.M. PALEOS

*N.R.C. "Democritos", Athens*

V. PAPADOPOULOS

*N.R.C. "Democritos" Athens*

G. PAPAGEORGIOU

*Biophysics, N.R.C. "D", Athens*

V.P. PAPAGEORGIOU

*Nat. Products, Tech. Univ. Salonica*

S. PARASKEVAS

*Org. Chem., Univ. Athens*

G. PHOKAS

*Pharmacognosy, Univ. Salonica*

S. PHILIPAKIS

*N.R.C. "Democritos", Athens*

G. PNEUMATIKAKIS

*Inorg. Chem., Univ. Athens*

C.N. POLYDOROPOULOS

*Phys./Quantum Chem., Univ. Ioannina*

K. SANDRIS

*Organic Chem., Tech. Univ. Athens*

M.J. SCOULLOS

*Env./Mar. Chem., Univ. Athens*

C.E. SEKERIS

*Mol. Biology, N.H.R.F., Athens*

G.A. STALIDIS

*Phys. Chem., Univ. Salonica*

C.I. STASSINOPOULOU

*N.R.C. "Democritos", Athens*

A. STASSINOPOULOS

*N.R.C. "Democritos", Athens*

A. STAVROPOULOS

*Ind. Technol., G.S.I.S., Piraeus*

I.M. TSANGARIS

*Inorg. Chem., Univ. Ioannina*

G. TSATSARONIS

*Food Technol., Univ. Salonica*

G.A. TSATSAS

*Pharm. Chem., Univ. Athens*

A.K. TSOLIS

*Chem. Technol., Univ. Patras*

G. VALCANAS

*Org. Chem., Tech. Univ. Athens*

A.G. VARVOGLIS

*Org. Chem., Univ. Salonica*

G.S. VASSILIKIOTIS

*Anal. Chem., Univ., Salonica*

S. VOLIOTIS

*Instrum. Analysis, Univ. Patras*

E.K. VOUDOURIS

*Food Chem., Univ. Ioannina*

I. VOURVIDOU - FOTAKI

*Org. Chem., Univ. Athens*

I.V. YANNAS

*Mech. Eng., M.T.I., U.S.A.*

Correspondence, submission of papers, subscriptions, renewals and changes of address should be sent to Chimika Chronika, New Series, 27 Kaningos street, Athens, Greece. The Guide to Authors is published in the first issue of each volume, or sent by request. Subscriptions are taken by volume at 500, drachmas for members and 1.000 drachmas for Corporations in Greece and 28 U.S. dollars to all other countries except Cyprus, where subscriptions are made on request.

Printed in Greece by FOTOKIMENO E.P.E.

Υπεύθυνος σύμφωνα με το νόμο: Παναγιώτης Ευθάλης Κάνιγγος 27, Αθήνα (147)

CONTENTS

Study of physical adsorption using the hole theory. III. Thermodynamic functions ( <i>in English</i> ) by D.A. Jannakoudakis, P.J. Nikitas, A.K. Papa-Louisi.....	293
Synthesis of carbamate esters of phenethylamines and their pharmacological action on the central nervous system ( <i>in English</i> ) by Th. Siatra-Papastaikoudi, Z. Papadopoulou - Daifoti, Ch. Spyraiki and D. Varonos.....	307
A comparative study of the oxidising power of arylodine diacetates ( <i>in English</i> ) by D. Barbas, J. Gallos and A. Vavoglis.....	315
The reaction of phenyliodine ditrifluoroacetate with aromatic ethers ( <i>in English</i> ) by S. Spyroudis and A. Vavoglis.....	323
Study of the liquid state and the vapor-liquid phase transition using a new approximate method of the hole theory ( <i>in English</i> ) by D.A. Jannakoudakis and P.J. Nikitas.....	331
Application of a new approximate method of the hole theory to binary liquid mixtures ( <i>in English</i> ) by D.A. Jannakoudakis and P.J. Nikitas.....	347
I. New series of N, N'-Bis(s-alkyl-2-ethanethio) acetamidines. II. Cyclisation of s-alkyl-benzoylaminoalkylene-sulfides in the presence of phosphorous oxychloride ( <i>in English</i> ) by G. Papaioannou and Asp. Papadaki-Valiraki.....	361
A novel angiotensin II antagonist, [sar <sup>1</sup> , dehydro-ala <sup>8</sup> ]-A-II. Purification and characterization in vitro. ( <i>in English</i> ) by S.E. Papaioannou, P-C. Vang and F. Fago.....	369
SHORT PAPERS	
Diethylaminoethyl esters of the p-[(N'-alkyl)- carbamoylamino]-benzoic acid ( <i>in English</i> ) by G. Papaioannou.....	381

## STUDY OF PHYSICAL ADSORPTION USING THE HOLE THEORY III. THERMODYNAMIC FUNCTIONS

D.A. JANNAKOUDAKIS, P.J. NIKITAS, A.K. PAPPA-LOUISI

*Laboratory of Physical Chemistry Fac. of Physics & Mathematics, University of Thessaloniki, Greece*

(Received June 25, 1980).

### Summary

The isosteric heat of adsorption, the internal energy, the integral and differential entropy of the adsorbed layer of noble gases on homogeneous surfaces are derived on the basis of the hole theory and the proposed models of the previous papers I and II of this series. The theoretical data are compared with the experimental data of the Argon adsorption on graphite and boron nitride. The agreement with experiment is found to be quite good for those models which consider the adsorbed phase as a liquid like layer. Deviations appearing at the monolayer adsorption of Argon on boron nitride are due to the heterogeneous surface of boron nitride.

**Key words:** Argon, Hole Theory, Physical adsorption.

### I. Introduction

The theoretical and experimental study of physical adsorption showed that different models often lead to theoretical isotherms which have similar mathematical form. For this reason, the agreement between experimental adsorption isotherms obtained at a single temperature and a theoretical isotherm, is insufficient evidence of the validity of a model. Thus, it is desirable to compare experimental adsorption isotherms at various temperatures and thermodynamic functions obtained from them, with the theoretical isotherms and the thermodynamic functions predicted from a certain model.

The hole theory of the liquid state<sup>1,2,3,4</sup> provides a satisfactory qualitative picture of the liquid state. The equation of state is in agreement with experimental data throughout both the liquid and dense gas regions, but the agreement with experiment becomes less satisfactory for the internal thermodynamic functions<sup>2,3,4</sup>

In previous papers<sup>5,6</sup> (hereafter referred to as I and II) the hole theory has been extended to study the physical adsorption of noble gases on solid surfaces. The adsorption isotherms predicted from the theory were found to be in good agreement with experiment. Thus, it is interesting to compare the theoretical data of the internal thermodynamic functions with the experiment.

In this paper the internal energy, the isosteric heat and the integral and differential entropy of the adsorbed phase are calculated on the basis of the hole theory and the proposed models of papers I and II. The resulting theoretical values are compared with the experimental data of the adsorption of Argon on graphite (P-33) and boron nitride (BN).

## II. Monolayer adsorption

If the adsorbed phase is considered to be a two-dimensional liquid-like layer adsorbed on a structureless energetically uniform surface, then its partition function is given by<sup>5</sup>

$$Z_{\text{ads}} = \lambda^N \cdot q_{\text{vib}}^N \cdot \exp\left(\frac{NU_0}{kT}\right) \cdot \frac{N_0!}{N!(N_0-N)!} \cdot [a_f(\bar{Y})]^N \cdot \exp\left[-\frac{\bar{Y}N\Psi(0)}{2kT}\right], \quad (1)$$

where the symbols have their usual meaning (from I).

From Eq. (1) we have the following relations which permit us to calculate all the thermodynamic properties of the adsorbed phase.

### 1. Internal Energy, E

$$E = kT^2 \left( \frac{\partial \ln Z_{\text{ads}}}{\partial T} \right)_{N, N_0, P} \quad (2)$$

$$= NkT + \frac{Nh\nu}{2} \cdot \frac{1 + e^{-h\nu/kT}}{1 - e^{-h\nu/kT}} - U_0N + \frac{N^2\Psi(0)}{2N_0} \quad (3)$$

### 2. Isosteric Heat, $Q_{\text{st}}$

From the definition<sup>7</sup> of  $Q_{\text{st}}$ , we obtain, using Eq. (2),

$$Q_{\text{st}} = H_g - \left( \frac{\partial E}{\partial N} \right)_{T, N_0} \quad (4)$$

$$= \frac{3}{2}RT - R \frac{h\nu}{2k} \cdot \frac{1 + e^{-h\nu/kT}}{1 - e^{-h\nu/kT}} + U_0 - \theta \frac{\Psi(0)R}{k}, \quad (5)$$

where  $H_g$  is the enthalpy in the bulk gas phase.

### 3. Integral Entropy, S

From the definition and Eq. (1) and (3) we have

$$S = \frac{E}{T} + k \ln Z_{ads} \tag{6}$$

or

$$\frac{S}{k} = N + \frac{N h \nu}{2kT} \cdot \frac{1+e^{-h\nu/kT}}{1-e^{-h\nu/kT}} + N \ln(\lambda q_{vib}^\omega) - \frac{N}{\theta} \ln(1-\theta) - N \ln \frac{\theta}{(1-\theta)^2} \tag{7}$$

4. Differential Entropy,  $\bar{S}$

Differentiating S of Eq. (7) with respect to N, we have

$$\bar{S} = \left( \frac{\partial S}{\partial N} \right)_{T, N_0} = \frac{1}{T} \left( \frac{\partial E}{\partial N} \right)_{T, N_0} + k \left( \frac{\partial \ln Z_{ads}}{\partial N} \right)_{T, N_0} \tag{8}$$

$$= R + \frac{R h \nu}{2kT} \cdot \frac{1+e^{-h\nu/kT}}{1-e^{-h\nu/kT}} + R \ln(\lambda q_{vib}^\omega) - R \ln \frac{\theta}{(1-\theta)^2} - R \frac{\theta}{1-\theta} \tag{9}$$

III. Multilayer adsorption

A. Modified B.E.T. model — model A.

In this model, the first adsorbed layer is regarded as a two dimensional liquid, while the molecules in subsequent layers are located on top of one another as in the B.E.T. treatment. The partition function of the adsorbed phase is given by<sup>6</sup>

$$Z = \lambda^{N_1} q_{vib}(1)^{N_1} \exp\left(\frac{N_1 U_1}{kT}\right) \frac{N_0!}{N_1! (N_0 - N_1)!} \cdot a_f^{N_1} \cdot \exp\left[-\frac{N_1^2 \Psi_1(O)}{N_0 \cdot 2kT}\right] \\ \cdot \frac{N_1!}{(N - N_1)! N_1!} \cdot j_2^{(N - N_1)} \cdot \exp\left(\frac{(N - N_1) U_2}{kT}\right) \tag{10}$$

subject to the restriction

$$\ln\left(\frac{\lambda q_{vib}(1)^\omega}{j_2}\right) + \frac{U_1 - U_2}{kT} + \ln\left(\frac{N_0 - N_1}{N_1}\right) + \ln\left(1 - \frac{N_1}{N_0}\right) - \frac{N_1}{N_0 - N_1} \\ - \frac{N_1 \Psi_1(O)}{N_0 kT} + \ln\left(\frac{N - N_1}{N_1}\right) = 0 \tag{11}$$

The isosteric heat is easily evaluated from the adsorption isotherm<sup>6</sup>

$$\ln\left(\frac{j_2}{\lambda q_{vib}(1)^\omega}\right) + \frac{U_2 - U_1}{kT} + \ln\left(\frac{\theta(1-x)^2}{x[1-\theta(1-x)]^2}\right) + \frac{\theta(1-x)}{1-\theta(1-x)} + \frac{\theta(1-x)\Psi_1(O)}{kT} = 0 \tag{12}$$

using the relation

$$q_{st} = R \left( \frac{\partial \ln(P/P_0)}{\partial (1/T)} \right)_{\theta} = R \left( \frac{\partial \ln x}{\partial (1/T)} \right)_{\theta} \quad (13)$$

Differentiating Eq. (12) with respect to T, we obtain, using Eq. (13),

$$q_{st} = \frac{U_2 - U_1 + \theta (1-x) \Psi_1(O) R/k}{\frac{x\theta \Psi_1(O)}{kT} + \frac{1+x-(1-x)(2-x)\theta+(1-x)^3\theta^2}{(1-x)[1-\theta(1-x)]^2}} \quad (14)$$

The quantity  $q_{st}$  is the isosteric heat of adsorption when the reference state is the corresponding bulk phase of the adsorbent. Thus

$$Q_{st} = q_{st} + \Delta H_{\text{sublimation}} \quad (15)$$

Alternatively  $Q_{st}$  can be obtained from Eq. (10), as in the case of monolayer adsorption. We have

$$Q_{st} = q_{st} + \left[ RT + \frac{R h \nu}{2k} \cdot \frac{1 + \exp(-h\nu/kT)}{1 - \exp(-h\nu/kT)} - U_1 \right], \quad (16)$$

where  $q_{st}$  is given by Eq.(14). It is obvious that the quantity in the brackets is the theoretical expression of  $\Delta H_{\text{sublimation}}$  for the model A.

The differential entropy is evaluated from the relation<sup>7</sup>

$$s = S_g - \frac{Q_{st}}{T}, \quad (17)$$

where  $S_g$  is the entropy of the bulk gas phase.

The integral entropy can be obtained from the definition of the differential entropy

$$s = \int_0^N \bar{s} dN \quad (18)$$

### B. Mobile model - Model B

The partition function of the adsorbed phase regarded as a system of  $j$  two-dimensional liquid-like layers, is<sup>6</sup>

$$\ln Z = \sum_i \left\{ N_i \ln(\lambda q_{\text{vib}(i)} a_f^0 e) + \frac{N_i U_i}{kT} + N_{i-1} \ln \frac{N_{i-1}}{N_{i-1} - N_i} - N_i \ln \frac{N_i}{N_{i-1} - N_i} - \frac{N_i^2}{N_{i-1}} - \frac{N_i^2 \psi_i(O)}{N_{i-1} 2kT} \right\} \quad (19)$$

The internal thermodynamic functions of the adsorbed phase can be derived following the same type of procedure as in the case of the monolayer adsorption.

1. Internal Energy, E

$$E = \sum_i N_i \left\{ \frac{k}{R} A_i - U_i + \frac{1}{2} \theta_i \psi_i(O) \right\} \quad (20)$$

where  $A_i = RT + \frac{R h \nu_i}{2k} \cdot \frac{1 + \exp(-h \nu_i / kT)}{1 - \exp(-h \nu_i / kT)} + RT^2 \frac{g_m}{g}$  (21)

$$g = \int_0^{2.757} \exp \left\{ - \left\{ \frac{3\sqrt{3} c \epsilon}{16kT} \left( \frac{3\sqrt{3}}{\omega^{*5/6}} l(y) - \frac{8}{\omega^{*3/2}} m(y) \right) \right\} \right\} dy = \frac{a_f(O)}{\frac{2\sqrt{3}\pi\omega}{3}} \quad (22)$$

and  $g_m = dg/dT$  (23)

The L-JD functions l(y), m(y) are given in paper I

2. Isosteric Heat, Q<sub>st</sub>

$$Q_{st} = \frac{5}{2} RT - \sum_i \frac{\partial N_i}{\partial N} \left\{ A_i - U_i + \theta_i \psi_i(O) \frac{R}{k} - \frac{1}{2} \theta_{i+1}^2 \psi_{i+1}(O) \frac{R}{k} \right\} \quad (24)$$

3. Integral Entropy, S

$$\frac{S}{k} = \sum_i N_i \left\{ B_i - \theta_i^{-1} \ln(1 - \theta_i) - \ln \frac{\theta_i}{1 - \theta_i} - \theta_i \right\} \quad (25)$$

where  $B_i = \frac{A_i}{RT} + \ln(\lambda q_{\text{vib}(i)} a_f^0 e)$  (26)

4. Differential Entropy,  $\bar{S}$

$$\frac{\bar{S}}{k} = \sum_i \frac{\partial N_i}{\partial N} \left\{ B_i + \ln \frac{1 - \theta_i}{\theta_i (1 - \theta_{i+1})} - 2\theta_i + \theta_{i+1}^2 \right\} \quad (27)$$



#### IV. Numerical results and comparison with experiment

##### A. Monolayer adsorption

Ross and Oliver<sup>8</sup> have studied the adsorption of Argon on graphite at relatively low pressures. They have calculated isosteric heats of adsorption by analysing their experimental data. Ross and Pultz<sup>9</sup> have determined  $Q_{st}$  and adsorption isotherms for the system Ar-BN.

To calculate differential entropies from the above experimental data, using Eq. (17), we have assumed that  $Q_{st}$  was constant. The entropy of the ideal gas  $S_g$  was calculated from the Sackur-Tetrode equation.

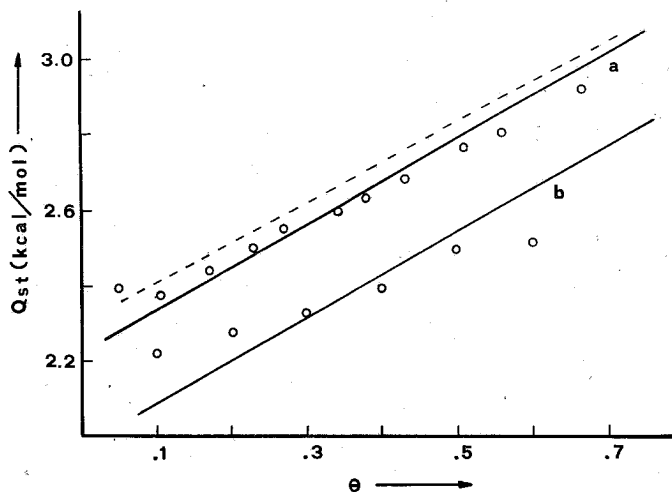


FIG. 1. Calculated and experimental isosteric heats of adsorption of Argon on graphite (a) and boron nitride (b) at  $T=84^{\circ}\text{K}$ . The solid lines represent theoretical calculations while the dotted line gives the results of the significant structures theory. Circles are experimental data from ref. (8), (9).

Figure 1 compares the theoretical values of  $Q_{st}$  obtained from Eq. (5) with the experimental results of the systems Ar-P33 and Ar-BN. Table I contains the values of  $\Psi(O)R/k$

TABLE I. Values of  $\Psi(O)R/k$  as calculated from Eq. (28).

$\theta$	.1	.2	.3	.4	.5	.6	.7	.8
$-\Psi(O)R/k$ cal/mole	1133.1	1133.1	1133.1	1138.0	1141.6	1143.8	1143.4	1127.4

calculated from the relation<sup>5</sup>

$$\frac{\Psi(0)}{k} = \frac{3\sqrt{3}c\epsilon}{16k} \left( \frac{3\sqrt{3}}{\omega^{*6}} - \frac{8}{\omega^{*3}} \right), \quad (28)$$

where  $\omega^*$  is the reduced cell area of an adsorbed molecule,  $c$  the coordination number of the adsorbed phase and  $\epsilon$  the maximum depth of the intermolecular potential. The values of the other parameters used in Eq. (5) are given in Table II of paper I.

The agreement between experimental and theoretical data is considerably good for the Argon on P-33. Included in Fig. 1 is the theoretical curve of the significant structure theory<sup>10</sup>. The results of this investigation are in a better agreement with experiment than the ones of the significant structure theory.

The agreement with experiment is less satisfactory for the system Ar-BN. The theoretical values of  $Q_{st}$  for  $\theta = 0.6$  and for  $\theta < 0.2$  deviate from the experimental values at about 120 cal/mole. The positive deviations of the experimental data of  $Q_{st}$  at low values of  $\theta$  and the negative deviations for  $\theta \geq 0.6$ , are susceptible to the following explanation<sup>11</sup>. Because of the heterogeneous surface of BN, at low values of  $\theta$  molecules are adsorbed preferentially on the most attractive sites. As adsorption proceeds and these sites become filled, the less active sites come into play.

The lack of a linear dependence of the free area<sup>6</sup> on the number of neighbouring holes at  $\theta > 0.5$  can have pronounced effects on the deviations observed at this region of adsorption.

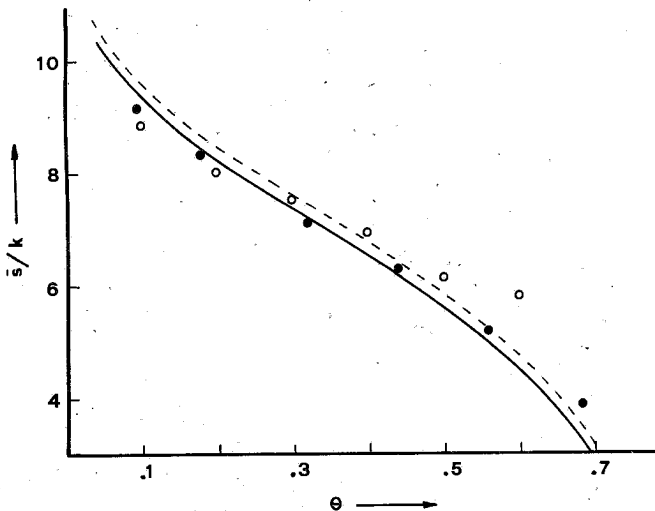


FIG. 2. Calculated and experimental differential entropies of adsorbed Argon at 90.1°K. Solid line and dotted line represent theoretical calculations for Argon on C and BN respectively. The open circles and filled circles represent experimental data of Ar-C and Ar-BN, respectively.

The theoretical differential entropies of the adsorption of Argon on P-33 and BN at 90.1°K were calculated using Eq.(9) and are shown in Fig. 2 plotted as a function of  $\theta$ . As in the case of  $Q_{st}$  against  $\theta$  plots, we have an excellent agreement between theory and experiment for the system Ar-P33 and systematic deviations for Argon on BN mainly due to the heterogeneous surface of BN.

## B. Multilayer Adsorption

### 1. Computation of experimental values of $Q_{st}$ and $\bar{S}$ .

Prenzlow and Halsey<sup>12</sup> have measured adsorption isotherms for Argon on P-33 and calculated isosteric heats and differential entropies from these data. Similarly, Pierotti<sup>13</sup> has calculated isosteric heats of adsorption of Argon on BN. In this paper we have recalculated these quantities for purposes of checking self-consistency, obtaining similar results.

The isosteric heat of adsorption was calculated using

$$\left(\frac{\partial \ln P}{\partial T}\right)_{\theta} = \frac{Q_{st}}{RT^2} \quad (29)$$

The plots of  $\ln P$  vs  $1/T$  at constant  $\theta$  for different temperatures yielded good straight lines. The experimental values of  $Q_{st}$  were evaluated using a least square procedure. This procedure has also given the errors in isosteric heat, introduced by the measurement of pressure. The errors for Argon on BN were about  $\pm 10$  cal/mol except for the region of adsorption between  $\theta = 1$  and  $\theta = 1.4$  where a rather large error,  $\pm 50$  cal/mol was found. The errors in  $Q_{st}$  were  $\pm 30$  cal/mol for the system Ar-P33. Measurements of dosage ( $\theta$ ) would appear to contribute about  $\pm 10$  cal/mol.

Experimental values of differential entropies were calculated using Eq.(17), as in the case of monolayer adsorption.

### 2. Computation of theoretical values of $Q_{st}$ and $\bar{S}$ .

We have used Eq.(15) and (17) for the theoretical calculation of  $Q_{st}$  and  $\bar{S}$  on the basis of model A. Table I of paper II contains all the molecular parameters used in this theory.

The theoretical values of  $Q_{st}$  and  $\bar{S}$ , predicted from the mobile model, have been calculated using Eq. (24) and (27) and  $g$  and  $g_m$  have been evaluated from Eq.(22) and (23) by means of an analytical integration using Simpson's rule. The differential terms  $(\partial N_i / \partial N) T N_o$  in terms of the population ratios have been obtained in the following manner: If we differentiate the adsorption isotherms Eq. (22), (23) of paper II with respect to  $N_i$ , we have

$$\left. \begin{aligned}
 & - \frac{\partial N_2}{\partial N_1} \left\{ \theta_2 \left( \frac{\Psi_2(O)}{kT} + 2 \right) + (\theta_3 + \theta_3^2) \left( \frac{\Psi_3(O)}{kT} + 2 \right) + \frac{2 - \theta_2}{1 - \theta_2} + \frac{2\theta_3}{1 - \theta_3} \right\} \\
 & + \frac{\partial N_3}{\partial N_1} \left\{ (1 + \theta_3) \left( \frac{\Psi_3(O)}{kT} + 2 \right) + \frac{1 + \theta_3}{\theta_3(1 - \theta_3)} \right\} \\
 & + \left\{ \theta_2^2 \left( \frac{\Psi_2(O)}{kT} + 2 \right) + \frac{\theta_2}{1 - \theta_2} \right\} = 0
 \end{aligned} \right\} \quad (30)$$

and

$$\left. \begin{aligned}
 & \frac{\partial N_2}{\partial N_1} \left\{ (1 + \theta_2) \left( \frac{\Psi_2(O)}{kT} + 2 \right) + \frac{\theta_2^2}{\theta_2} \left( \frac{\Psi_3(O)}{kT} + 2 \right) + \frac{1}{\theta_2(1 - \theta_3)} + \frac{2}{1 - \theta_2} \right\} \\
 & - \frac{\partial N_3}{\partial N_1} \left\{ \frac{\theta_3}{\theta_2} \left( \frac{\Psi_3(O)}{kT} + 2 \right) + \frac{1}{\theta_2(1 - \theta_3)} \right\} \\
 & - \left\{ \theta_1 \left( \frac{\Psi_1(O)}{kT} + 2 \right) + (\theta_2 + \theta_2^2) \left( \frac{\Psi_2(O)}{kT} + 2 \right) + \frac{2 - \theta_1}{1 - \theta_1} + \frac{2\theta_2}{1 - \theta_2} \right\} = 0
 \end{aligned} \right\} \quad (31)$$

From the solution of this system we obtain the quantities  $(\partial N_2 / \partial N_1)_{T, N_0}$  and  $(\partial N_3 / \partial N_1)_{T, N_0}$ .

The partial derivatives  $(\partial N_i / \partial N)_{T, N_0}$  are now easily evaluated from the relations:

$$\begin{aligned}
 \left( \frac{\partial N_1}{\partial N} \right)_{T, N_0} &= \frac{1}{\sum_i (\partial N_i / \partial N_1)_{T, N_0}} \\
 \left( \frac{\partial N_2}{\partial N} \right)_{T, N_0} &= \frac{(\partial N_2 / \partial N_1)_{T, N_0}}{\sum_i (\partial N_i / \partial N_1)_{T, N_0}} \\
 \left( \frac{\partial N_3}{\partial N} \right)_{T, N_0} &= \frac{(\partial N_3 / \partial N_1)_{T, N_0}}{\sum_i (\partial N_i / \partial N_1)_{T, N_0}}
 \end{aligned} \quad (32)$$

Table II shows the results of this procedure. The values of the molecular parameters used in this treatment are in Table II of paper II.

### 3. Comparison with experiment - Discussion.

The experimental values of isosteric heat of adsorption of Argon on P-33 and BN are given in Fig. 3 and 4, respectively.

TABLE II. Values of  $(\partial N_i / \partial N)_{T, N_0}$  as calculated from Eq.(32).

Ar-C				Ar-BN			
$\theta$	$(\frac{\partial N_1}{\partial N})_{T, N_0}$	$(\frac{\partial N_2}{\partial N})_{T, N_0}$	$(\frac{\partial N_3}{\partial N})_{T, N_0}$	$\theta$	$(\frac{\partial N_1}{\partial N})_{T, N_0}$	$(\frac{\partial N_2}{\partial N})_{T, N_0}$	$(\frac{\partial N_3}{\partial N})_{T, N_0}$
.98	.682	.312	.006	.88	.025	.014	.961
1.04	.156	.798	.045	1.01	.399	.568	.032
1.09	.052	.869	.079	1.07	.158	.772	.071
1.14	.021	.872	.106	1.13	.070	.829	.101
1.22	.009	.865	.125	1.19	.032	.843	.124
1.33	.004	.862	.134	1.29	.014	.848	.137
1.60	.001	.857	.142	1.49	.004	.856	.139
1.80	.003	.761	.235	1.75	.007	.786	.207
1.91	.004	.610	.385	1.88	.011	.636	.353
2.00	.004	.447	.549	1.98	.011	.471	.518
2.05	.003	.353	.644	2.03	.009	.374	.616
2.12	.002	.239	.758	2.11	.007	.256	.737
2.23	.001	.117	.881	2.22	.003	.127	.869
2.34	.001	.081	.919	2.33	.002	.088	.909
2.44	.001	.103	.895	2.43	.003	.111	.885

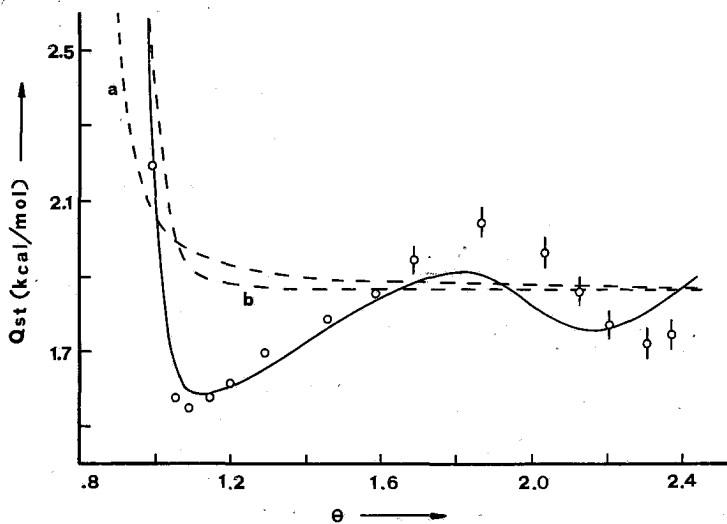


FIG. 3. Calculated and experimental isosteric heat of Argon on graphite at  $T=74.96^{\circ}\text{K}$ . Solid line represents theoretical results of the mobile model while dotted lines show the theoretical results of (a) model A and (b) B.E.T. model. Circles are experimental data.

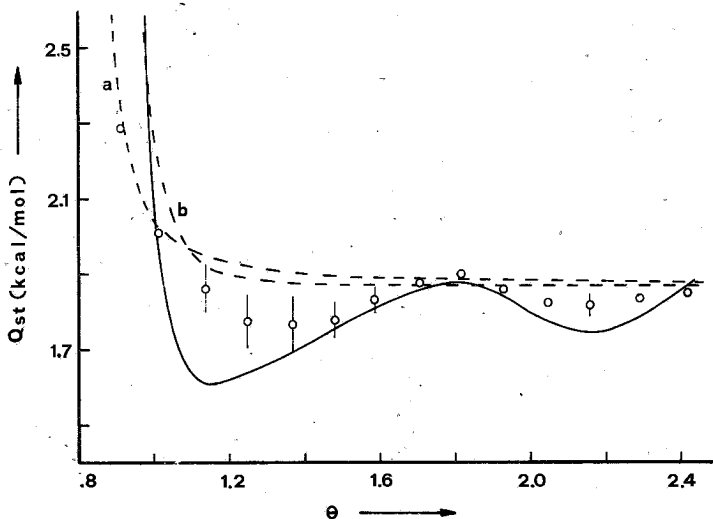


FIG. 4. Calculated and experimental isosteric heat of Argon on BN at  $T=68.9^{\circ}\text{K}$ . Solid line represents theoretical results of the mobile model while dotted lines show the theoretical results of (a) model A and (b) B.E.T. model. Circles are experimental data.

The form of plots of  $Q_{st}$  against  $\theta$  for the systems Ar-P33 and Ar-BN is that commonly observed for physical adsorption. In both systems there are two maxima and two minima. The P-33 curves have higher and sharper maxima and lower and sharper minima. For each system, as  $\theta$  increases the isosteric heat approaches the heat of sublimation of Argon.

The theoretical isosteric heat curves predicted by B.E.T. and modified B.E.T. models are almost similar in shape. They don't show maxima and minima and give a rough qualitative description of the phenomenon.

In contrast to B.E.T. and modified B.E.T. models, mobile model provides a satisfactory description of multilayer physical adsorption. The shape and the order of magnitude of the isosteric heat curves are in good agreement with experiment particularly if we take into account the order of magnitude of the experimental errors in  $Q_{st}$ .

It is interesting to observe that the system Ar-BN shows rather strong deviations around  $\theta = 1.1$ . These deviations should be attributed to the heterogeneous surface of BN.

Figures 5 and 6 compare theoretical with experimental values of differential entropies of the adsorption of Argon on P-33 and BN at  $T = 74.96^{\circ}\text{K}$  and  $68.9^{\circ}\text{K}$  respectively. The entropy curves are similar to those of isosteric heat. Thus, B.E.T. and modified B.E.T. models give a qualitative description of the entropy curves, while the mobile model provides an almost quantitative picture of these curves.

As a conclusion we may say that the mobile model seems to provide a good description of the multilayer adsorption. The satisfactory theoretical adsorption isotherms according to the experiment, the correspondence between the calculated and observed position and the height of the two maxima and minima, in plots  $Q_{st}$

—  $\theta$  and  $S-\theta$ , suggest that the general features of the mobile model are correct.

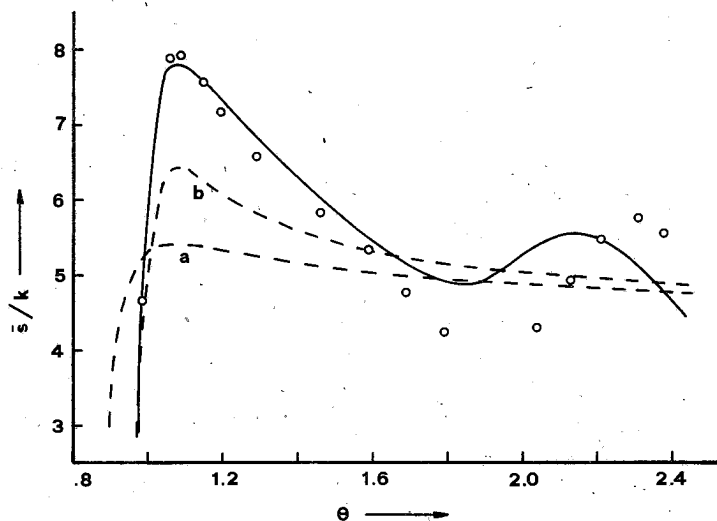


FIG. 5. Calculated and experimental differential entropies of Argon on C at  $T=74.96^{\circ}\text{K}$ . Solid line represents theoretical results of the mobile model while dotted lines show the theoretical results of (a) model A and (b) B.E.T. model. Circles are experimental data.

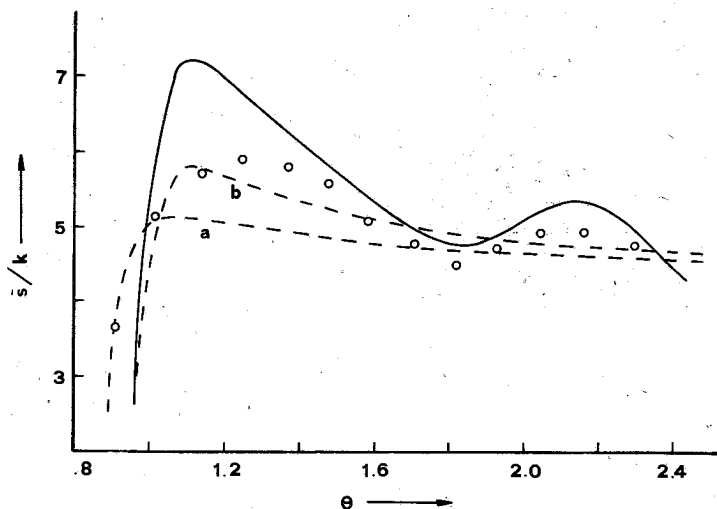


FIG. 6. Calculated and experimental differential entropies of Argon on BN at  $T=68.9^{\circ}\text{K}$ . Solid line represents theoretical results of the mobile model while dotted lines show the theoretical results of (a) model A and (b) B.E.T. model. Circles are experimental data.

## Περίληψη

Μελέτη τής φυσικής προσροφήσεως μέ τή θεωρία όπών.

### III. Θερμοδυναμικές συναρτήσεις.

Ἡ έργασία αὐτή άποτελεϊ συνέχεια καί συμπλήρωση τών δημοσιεύσεων I καί II. Οί έσωτερικές θερμοδυναμικές ιδιότητες, όπως ή θερμότητα προσροφήσεως γιά ίση έπικάλυψη, ή έσωτερική ένέργεια, ή όλοκληρωτική καί διαφορική έντροπία τής στιβάδας προσροφήσεως άδρανών άερίων πάνω σέ όμογενή έπιφάνεια, προσδιορίζονται μέ βάση τή θεωρία όπών καί τά πρότυπα προσροφήσεως πού προτείνονται στίς έργασίες I καί II.

Οί τιμές τής θερμότητας προσροφήσεως γιά ίση έπικάλυψη καί τής διαφορικής έντροπίας, οί όποίες προκύπτουν θεωρητικά, συγκρίνονται μέ τά πειραματικά δεδομένα τής προσροφήσεως τοῦ άδρανούς άερίου Ar πάνω σέ P-33 καί BN. Ἡ συμφωνία μεταξύ θεωρητικών καί πειραματικών τιμών είνai έξαιρετικά καλή γιά τά πρότυπα, τά όποία θεωροῦν τήν προσροφημένη φάση σάν ύγρη. Ορισμένες άποκλίσεις παρατηροῦνται στήν περίπτωση τής μονομοριακής προσροφήσεως τοῦ Ar πάνω στό BN. Αὐτές άποδίδονται στήν ύπαρξη σχετικής «έτερογένειας» στήν έπιφάνεια τοῦ κρυστάλλου τοῦ BN.

---

## References and Notes

- Henderson, D.: *J. Chem. Phys.* **37**, 631 (1962).
- Henderson, D.: *J. Chem. Phys.* **39**, 54 (1963).
- McLellan, A.G.: *J. Chem. Phys.* **40**, 567 (1964).
- Blomgren, G.E.: *J. Chem. Phys.* **34**, 1307 (1961); **38**, 1714 (1963).
- Jannakoudakis, D.A., & Nikitas, P.J.: *Chimika Chronika*, New Series, **10**, 23 (1981).
- Jannakoudakis, D.A., Nikitas, P.J. & Pappa-Louisi, K.A.: *Chimika Chronika*, New Series, in press.
- Hill, T.L.: *J. Chem. Phys.* **18**, 246 (1950).
- Ross, S. & Olivier, J.P.: *J. Phys. Chem.* **65**, 608 (1961).
- Ross, S. & Pultz, W.W.: *J. Colloid Sci.* **13**, 397 (1958).
- McAlpin, J.J. & Pierotti, R.A.: *J. Chem. Phys.* **41**, 68 (1964).
- Young, D.M. & Crowell, A.D.: *Physical Adsorption of Gases* (Butterworth, Inc., Washington, D.C. 1962).
- Prenzlow, C.F. & Halsey, G.D.: *J. Phys. Chem.* **61**, 1158 (1957).
- Pierotti, R.A.: *J. Phys. Chem.* **66**, 1810 (1962).



## **SYNTHESIS OF CARBAMATE ESTERS OF PHENETHYLAMINES AND THEIR PHARMACOLOGICAL ACTION ON THE CENTRAL NERVOUS SYSTEM**

TH. SIATRA - PAPASTAIKOUDI\*, Z. PAPADOPOULOU - DAIFOTI, CH. SPYRAKI and D. VARONOS\*\*

\* *Laboratory of Pharmaceutical chemistry, University of Athens.*

\*\* *Laboratory of Experimental Pharmacology, University of Athens. (Greece).*

(Received June 4, 1980; Revised December 17, 1980).

### **Summary**

The synthesis of novel carbamate esters of phenethylamine phenylethylamine derivatives is described.

These N-substituted derivatives are prepared from phenethylamines with chloroformate esters.

The toxicity and the possible central pharmacological action of these compounds on CNS was studied in animals.

In most of the tested compounds, although the phenethylamine system remains in the dextrorotatory conformation, the particular changes reduce the central stimulant effects.

**Key words:** Phenethylamines; Carbamate esters.

### **Introduction**

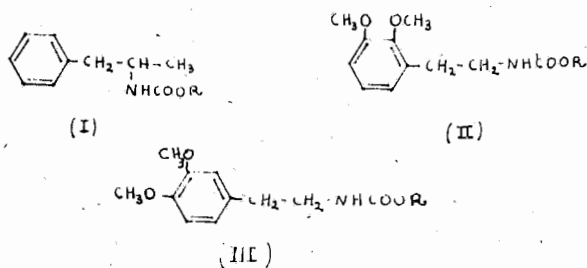
In this paper we study mono- and 2,3- or 3,4-disubstituted phenethylamine derivatives.

This work is an extension to previous research carried out in the Laboratory of Pharmaceutical Chemistry<sup>1-3</sup> and deals with the synthesis and pharmacological studies of mono- and disubstituted phenethylamines, as part of an extended research project on the effect of disubstitution on the pharmacological activity of the above compounds.

In the present work various carbamate esters of ( $\pm$ )-amphetamine and 2,3-or

3,4-dimethoxy substituted -phenethylamines were prepared and their pharmacological activity was determined.

The compounds synthesized and tested correspond to the general formulas I, II, III.



The procedure followed for the preparation of the above compounds is shown in Fig. 1. The parent compounds for the synthesis of the 2,3- and 3,4-disubstituted derivatives were 4-methoxy-3-hydroxy-benzaldehyde and 2-hydroxy-3-methoxy-benzaldehyde (1, 1a).

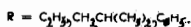
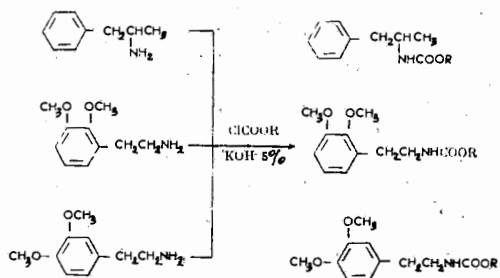
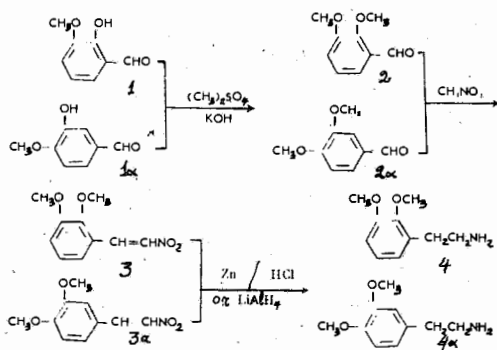


Fig. 1

Methylation of these compounds with dimethyl sulfate in alkaline medium<sup>4,5</sup> gave the corresponding substituted benzaldehydes (2,2a) which were converted to the corresponding nitrostyrenes (3, 3a) with the aid of nitromethane<sup>6</sup>.

Reduction of the above mentioned nitrostyrenes with zinc in hydrochloric acid<sup>6,7</sup> or lithium aluminium hydride<sup>8</sup> gave the corresponding phenethylamines (4, 4a).

Reaction of the substituted phenethylamines and ( $\pm$ )-amphetamine with chloroformate esters in alkaline media under nitrogen yielded I, II, III.

### Experimental Part.

N- (2,3-Dimethoxy) - $\beta$ -phenethyl isobutylcarbamate.

(2,3 Dimethoxy) - $\beta$ -phenethylamine (1g, 0.005 mol) was dissolved in 100 ml of ether. Into the solution was added dropwise 0.6 ml (0.005 mol) of isobutyl chloroformate dissolved in 10 ml ether. The mixture was stirred for 30 min. The reaction took place under a nitrogen atmosphere.

The ether solution was then washed with dilute hydrochloric acid followed by water until neutral reaction. The solution was dried over anhydrous sodium sulfate and the solvent was evaporated.

The yellow oil (1.25 g, 85%) was distilled under reduced pressure (110°C/80mm. Hg) to give an off-white oil.

$n_D^{31}$ : 1.478,  $C_{15}H_{23}NO_4$  (1)

Found: C:63,88 H:8,60 N:4,60

Calculated: C:64,02 H:8,24 N:4,99

The following were prepared as described above.

N- (3,4-Dimethoxy) - $\beta$ -phenethyl isobutyl carbamate.

$C_{15}H_{23}NO_4$  (2) m.p. : 50-52°C (petr. ether) yield 85%.

Found: C:64,00 H:8,00 N:4,51

Calculated: C:64,02 H:8,24 N:4,99

N- (3,4-Dimethoxy) - $\beta$ -phenethyl Phenyl carbamate.

$C_{17}H_{19}NO_4$  (3) m.p. : 127°C (Me<sub>2</sub>CO) yield 68%.

Found: C:68,04 H:6,60 N:4,20

Calculated: C:67,75 H:6,36 N:4,65

N- ( $\alpha$ -Methyl,  $\beta$ -phenethyl), ethyl carbamate.

$C_{12}H_{18}NO_2$  (4)  $n_D^{32}$ : 1,449 yield 70%.

Found: C:69,59 H:8,35 N:6,65

Calculated: C:69,19 H:8,71 N:6,72

N- ( $\alpha$ -Methyl,  $\beta$ -phenethyl), isobutyl carbamate.

$C_{14}H_{22}NO_2$  (5)  $n_D^{30}$ : 1,484 yield 73%.

Found: C:71,40 H:9,60 N:5,63

Calculated: C:71,16 H:9,38 N:5,93

N- ( $\alpha$ -Methyl,  $\beta$ -phenethyl)-phenyl carbamate.

$C_{16}H_{18}NO_2$  (6)  $n_D^{30}$ : 1,488 yield 79%.

Found: C:74,96 H:6,86 N:5,00

Calculated: C:74,96 H:7,08 N:5,46

N- (2,3-Dimethoxy) -phenethyl, phenyl carbamate.

$C_{17}H_{19}NO_3$  (\*)  $n_D^{30}$ : 1,481 yield 79%.

Found: C:67,80 H:6,80 N:4,00

Calculated: C:67,75 H:6,36 N:4,65

### Pharmacological tests

Methods: Albino mice (18-22 g) and rats (200-220 g) bred in the laboratory animal house were employed regardless of sex.

Experiments in mice and rats were done at a room temperature of  $25 \pm 1^\circ C$ .

Mice and rats were used in groups of 10 animals each unless indicated otherwise.

All tested compounds were administered i.p. immediately before performance of the test.

Wherever activity was observed at dose levels chosen on a logarithmic scale (10,30 and 100 mg/Kg) graded doses were given to calculate  $ED_{50}$ .

Acute toxicity: Acute toxicity of the compounds was determined by the i.p. route in mice. Graded doses of compounds were given to groups of 10 animals each and percent mortality over the next 24 hrs was recorded.

The  $LD_{50}$  was calculated graphically in mortality percentage according to the administered dose (10).

Behavioural observations: Behavioural observations were carried out in mice according to the general screening procedure described by Irwin<sup>11</sup>.

Groups of seven animals placed in plastic transparent cages were injected with each of the test compounds. The animals were observed 30 min afterwards for 5 hours.

Motor Activity: An activity recording system (Ugo Basile, Milano, Italy) was used to measure motor activity in rats.

This system consisted of three parts: The animal chamber, the electric unit and a recorder which were incorporated into the electric unit. The sides of the chamber were opaque and the ceiling transparent in order to allow observation. The floor consisted of a stainless steel sheet, the even bars were active.

Movements of the animals were thus recorded continuously on a counter, as well as on paper every 15 min. during a session of 3 hours.

The counts for the first 10 minutes were rejected.

Results were expressed as the percentage change from control and compared by the student - t - test (two tails).

(Table I).

**Stereotypy:** Groups of 6 male rats were injected i.p. with each compound and were observed every 30 min for 3 hours after administration.

Searching movements of the head, circling, walking backwards and grooming were recorded<sup>12</sup>.

**Body Temperature:** Male mice weighing 18-22 g were used. After two initial hourly control readings of the rectal temperature the tested compounds were administered i.p. in a range of doses.

Subsequent measurements were made at 1,2,3 and 4h after drug administration.

The differences in mean temperature between the control group and the treated group was calculated.

**Motor Coordination:** Mice weighing 18-23g, selected for use by their ability to maintain their position on a rotating rod, for two consecutive days, were injected with the test compounds.

One hour after i.p. administration the mice were checked for their ability to maintain their position on the rotating rod.

**Anorexia:** The details of our method have been described by Gosh<sup>13</sup>.

All tested compounds were injected i.p. into rats which had been fasted overnight.

Groups of 4 animals were used at each dose level.

Water was available at all times.

The consumption of solid food by each group of rats was determined over one hour, beginning 15 min after injection.

Anorexia was measured as the reduction in the food consumption of starved, drug-treated rats compared with that of starved, saline-treated rats determined on the same day.

The results are expressed as the percentage change from control.

## Results

The intraperitoneal LD<sub>50</sub> of the tested compounds in mice are listed in Table I.

The isobutyl derivatives showed less toxicity than the other derivatives, which was in parallel with the potency of these compounds.

The behavioural observations for all test compounds evoked alertness, slightly increased respiration rate, restless and in high doses vocalizations.

"Chewing" movements and grooming were recorded. All test compounds (except the isobutyl derivatives) produced a marked lowering of the motor activity (Table I).

On the contrary, motor coordination of the mice was not affected as measured on the rotating rod.

The substances tested evoked stereotypy of amphetamine type, that is searching movements of the head<sup>12</sup>.

TABLE I. *Pharmacological properties of the compounds tested.*

Comp. No	LD <sub>50</sub> mg/Kg	Anorexia change %	Motor activity change %
1	100	-63	- 45
2	200	-40	- 28 N.S.
3	150	-52	- 42
4	200	-52	- 35
5	400	-15	- 12 N.S.
			- 25 N.S.
6	200	-20	- 20
7	250	-47	- 380

The isobutyl derivatives of all the series did not disturb the behaviour of animals in this respect.

All test compounds produced a rather limited increase in body temperature ( $1 \pm 0.5^{\circ}$  C), only at a few time intervals (5' - 30 min) after drug administration.

The anorectic activity effects in mice are summarized in Table I.

The effects of the compounds synthesized were recorded always in comparison with a group of saline treated mice or rats.

The behavioural observations made according to blind screening evoked an amphetamine like response, but less potent.

In most of the tested compounds, although the phenethylamine system remains in the dextrorotatory configuration, the particular structural changes reduce the central stimulant effects.

This finding supports the view that they probably act through a dopaminergic and not noradrenergic mechanism<sup>14, 15</sup>.

Horn (16) has shown that dopaminergic sites are less sensitive to structural changes than are noradrenergic ones. Thus particular structural changes to a molecule might substantially reduce the noradrenergic system effect and yet leave the dopaminergic largely intact.

The compounds synthesized in this work seem to be not stimulant anorectics, the mechanism of their action should be further studied.

## Περίληψη

Είς τήν παροῦσαν ἐργασίαν περιγράφεται ἡ σύνθεσις καρβαμιδικῶν ἐστέρων τῶν φαινυλαιθυλαμινῶν.

Τά Ν-ὀποκατεστημένα αὐτά παράγωγα παρασκευάζονται ἐκ τῶν ἀντιστοιχῶν φαινυλαιθυλαμινῶν διά μετατροπῆς των εἰς ἐστέρας τῆ ἐπιδράσει

χλωρομυρμικικών εστέρων εις αλκαλικόν περιβάλλον.

Ἡ τοξικότης καί ἡ φαρμακολογική δράσις ἐπὶ τοῦ Κ.Ν.Σ. τῶν νεοσυντεθεισῶν οὐσιῶν ἐμελετήθησαν ἐπὶ πειραματοζῶων.

Τὰ ἀποτελέσματα ἔδειξαν ὅτι τὰ ἰσοβουτυλοπαράγωγα εἶχαν μικροτέρα τοξικότητα ἀπὸ τὰ ἄλλα, ἀλλὰ ὅλα γενικῶς (ἄν καί τυπικά ἀμφεταμινικά παράγωγα) παρουσίασαν μικρὴ διεγερτικὴ δράση ἐπὶ τοῦ Κ.Ν.Σ.

---

## References

1. Papadaki-Valiraki A., Guioca V., Tsatsas G.: *Chim. Ther.*, **308** (1973).
2. Tsatsas G., Foscolos G., Papaconstantinou-Garoufalias S.: *Praktica of Acad. of Athens* **53**, 485 (1978).
3. Papadaki-Valiraki A., Guioca V., Papaioannou G., Tsatsas G.: *Chim. Chron., N.S.*, **7**, 3 (1978).
4. Delaby R., Tsatsas G., Jendrot M.C.: *Bull. Soc. Chim. France*, 231 (1960).
5. Buck, J.S.: *Org. Synth. Coll. Vol.* **11**, 620 (1947).
6. Delaby R., Tsatsas G., Jendrot M.C.: *Bull. Soc. Chim. France*, 1830 (1956).
7. Tsatsas G.: *Bull. Soc. Chim. France*, 884 (1949).
8. Erne, M., Ramirez F.: *Helv. Chim. Acta.*, **33**, 912 (1950).
9. Dornow, A., Petsch, G.: *Arch. Pharm.* **285**, 323 (1952).
10. Litchfield, J.T., Wilcoxon, F.: *J. Pharmacol. exptl. Ther.*, **96**, 99, (1949).
11. Irwin, S. Gordon Res.: *Conf. on Medicinal Chem.* 133 (1959).
12. Randrap, A., Munkrad J.: *Psychopharmacologia II*, 300 (1967).
13. Ghosh, P., Bolt, A.G., Mrongoriorious R.T.: *Arzneim.-Forsch. Drug. Res.* **28**, 156, (1978).
14. Clineschmidt, B.V., McGuffin J.C., Werner A.B.: *Eur. J. Pharmacol.* **27**, 313 (1974).
15. Kruk Z.L., Smith L.A., Zarrindast M.R.: *Brit. J. Pharmacol.* **58**, 468 (1976).
16. Horn A.S.: *Brit. Pharmacol.* **47**, 332 (1973).

## A COMPARATIVE STUDY OF THE OXIDISING POWER OF ARYLIODINE DIACETATES

D. BARBAS, J. GALLOS and A. VARVOGLIS

*Laboratory of Organic Chemistry, University of Thessaloniki, Thessaloniki (Greece).*

(Received February 2, 1981).

### Summary

Several aryliodine diacetates were used to effect the oxidation of ethyl hydrazodicarboxylate to ethyl azodicarboxylate. Measurements of oxidation rates revealed that various substituents in the phenyl ring have not any significant influence on reactivity. The acyloxy moiety of the oxidants enhances moderately its reactivity, when it comes from a strong acid. Apparently conflicting results from the literature along with the present results are discussed and explained taking into account the different mechanisms which hold for the various reactions.

### Introduction

Phenyliodine diacetate,  $C_6H_5I(OCOCH_3)_2$ , hereafter abbreviated as PID, is a well known oxidising agent. It has been found to react with alkenes forming 1,2-diacetoxy alkanes and to cleave glycols to carbonyl compounds<sup>1,2</sup>. Also, it oxidises analines to azocompounds<sup>3</sup>, thiols to disulfides<sup>4</sup>, thioethers to sulfoxides<sup>5</sup> and a variety of other substrates to different kinds of products<sup>6</sup>. Several inorganic reductants are also oxidised by PID, which is thus suitable for potentiometric titrations<sup>7</sup>.

Recently, phenyliodine ditrifluoroacetate,  $C_6H_5I(OCOCF_3)_2$ , abbreviated as PIT, has been found to possess considerably more pronounced oxidising power than PID. Not only it effects oxidations under milder conditions than PID<sup>8,9</sup> but also it can oxidise substrates not oxidisable by PID<sup>8,10,11,12</sup>.

Criegee and Beucker<sup>1</sup> as early as 1939 investigated kinetically the reaction of PID and also  $C_6H_5I(OCOCH_2Cl)_2$ ,  $C_6H_5I(OCOCHCl_2)_2$  and  $C_6H_5I(OCOCCL_3)_2$  with isohydrobenzoin, i.e. the racemic form of 1,2-diphenyl ethanediol. They found a 5-fold increase in the reaction rate from PID to  $C_6H_5I(OCOCCL_3)_2$ . The same authors studied the reaction of a series of phenyl substituted PID with



isohydrobenzoin and they found that electron donors decreased moderately reaction rates, while electron acceptors increased considerably (up to almost 100-fold) reaction rates. This influence of substituents was reversed in the reactions of substituted PID with anethole,  $p\text{-CH}_3\text{O-C}_6\text{H}_4\text{-CH=CHCH}_3$ , and oxalic acid: here electron acceptors decreased reaction rates, although the differences were not as great as with isohydrobenzoin. A similar situation has been found to hold in the  $\text{H}_2\text{SO}_4$  catalysed reaction of substituted PID and toluene, where iodonium salts are formed<sup>13</sup>.

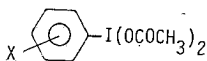
The reaction of isohydrobenzoin with substituted PID was reexamined by Pausacker<sup>2</sup>, who agreed with the above results and suggested a concerted mechanism, similar to that for lead tetraacetate cleavage of glycols.

A third study with substituted PID's has been performed by Johnson and Riggs<sup>14</sup> who examined the reaction between PID and N-(4-substituted-aryl) acetamides, resulting to the acetoxylation of the benzene ring at position 3. These workers found that only small erratic changes in reaction rates were caused by the various substituted PID.

This unsatisfactory state of affairs has led us to the present study, in order to elucidate the influence of both the acid moiety and the phenyl substituents on the oxidising power of aryl iodine diacetates. We have chosen a hydrazine derivative as a suitable substrate and we have measured its reaction rates, which were used as a criterion of the oxidising power of aryl iodine diacetates. It must be emphasised that the present results do not constitute a thorough kinetic study of the reaction but rather an exploratory effort into the reactivity of this interesting class of compounds.

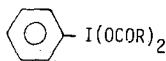
## Results and Discussion

Two series of aryl iodine diacetates were prepared, with variations either in the phenyl ring (1a-h) or in the acid part (2a-e).



1

- a: X=H, b: X=p-CH<sub>3</sub>, c: X=m-CH<sub>3</sub>  
 d: X=m-Cl, e: X=p-Cl, f: X=m-NO<sub>2</sub>  
 g: X=o-CH<sub>3</sub>, h: X=o-Cl



2

- a: R=CH<sub>3</sub>, b: R=CH<sub>2</sub>Cl, c: R=CHCl<sub>2</sub>  
 d: R=CCl<sub>3</sub>, e: R=CF<sub>3</sub>

Ethyl hydrazodicarboxylate,  $\text{C}_2\text{H}_5\text{OOCNHNHCOOC}_2\text{H}_5$ , was chosen as a suitable reductant, because it is oxidised quantitatively according to the equation:



The resulting ethyl azodicarboxylate has been found to be exclusively in the trans-configuration<sup>6</sup> and it has an absorption maximum at 410 nm, which allows

for its easy monitoring spectrophotometrically. At this wavelength there is not any interference from the starting materials or from the other reaction products. The reactions with 1 were studied at 25°C while those with 2 were too fast at this temperature and they were studied at 1°C. All reactions were followed in the thermostated cell of a spectrophotometer for approximately three half-lives. Using equimolecular quantities of reactants it was found that the reaction rates follow first-order kinetics in respect to ethylhydrazodicarboxylate. These rate constants are brought out in the Table.

TABLE. . Rate Constants of the Reaction of Aryliodine Diacetates with Ethyl Hydrazodicarboxylate in Chloroform.

$\text{ArI}(\text{OCOCH}_3)_2$	$10^4 \text{ k s}^{-1}$	$\text{C}_6\text{H}_5\text{I}(\text{OCOR})_2$	$10^4 \text{ k s}^{-1}$
1a	8.04	2a	1.34
1b	4.87	2b	1.47
1c	8.28	2c	2.84
1d	11.50	2d	8.36
1e	7.72	2e	7.37
1f	5.33		
1g	6.15		
1h	4.10		

The above results show clearly that (i) the more acidic is the acid whose acyloxy group is bound to iodine, the faster is the reaction and (ii) the influence of the substituents in the benzene ring on the reaction rate is unimportant.

The enhanced reactivity of aryl iodine diacetates with increasing acidity of their acyloxy groups is rather moderate, since only a six-fold rate enhancement has been measured from PID to PIT or  $\text{C}_6\text{H}_5\text{I}(\text{OCOCCl}_3)_2$ . This difference in reactivity is almost identical with the reported for the oxidation of hydrobenzoin. In both cases no linear relationship could be established between rate constants ( $k$  or  $\log k$ ) and  $\text{pK}_a$  of the acid.

The insensitivity of the reaction rate to the nature of the aryl group is remarkable, since only a three-fold difference has been observed between the slower and the faster reaction. Practically any substituted aryl iodine diacetate is almost equally effective in the oxidation of ethyl hydrazodicarboxylate. Even the *o*-substituted oxidants, i.e. *o*- $\text{CH}_3$  and *o*- $\text{Cl-C}_6\text{H}_4\text{I}(\text{OCOCH}_3)_2$  show insignificant difference between them. A Hammett plot for these reactions has a  $\rho$  value of 0.08, by contrast to the oxidation of isohydrobenzoin, which has  $\rho=+1.36$  and the reaction of anethole, where  $\rho=-1.05$ . In Fig. 1 reaction rates are plotted against  $\rho$  values for all three reaction and it is obvious that there are three different ways in which substituents influence the velocity of these reactions.

The oxidation of ethyl hydrazodicarboxylate is presumably a homolytic reaction. When the reaction of *o*- $\text{CH}_3$ -PID is run in the presence of 5% acrylonitrile, which is a radical scavenger, a decrease in its rate is observed, from  $6.15 \times 10^{-4} \text{ s}^{-1}$  to  $3.8 \times 10^{-4} \text{ s}^{-1}$ . The final optical density of the oxidation product is

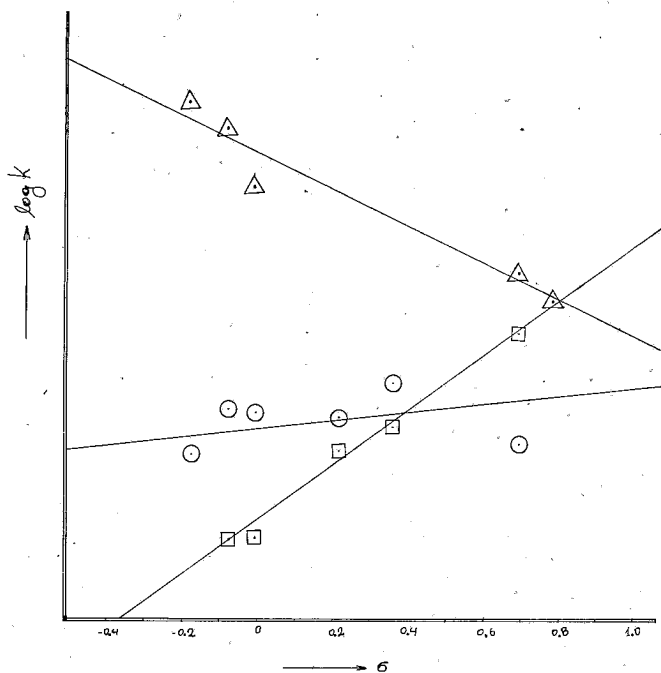
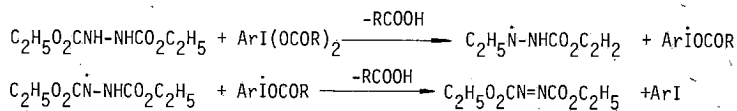


FIG. 1. Hammett plots for the reactions of aryliodine dicarboxylates with ethyl hydrazodicarboxylate (○), anethole<sup>1</sup> (Δ) and isohydrobenzoin<sup>2</sup> (□). Different scales are used for the three reactions.

also lowered, from 0.415 to 0.380. Both these low values in acrylonitrile suggest a free-radical pathway, according to the general sequence:

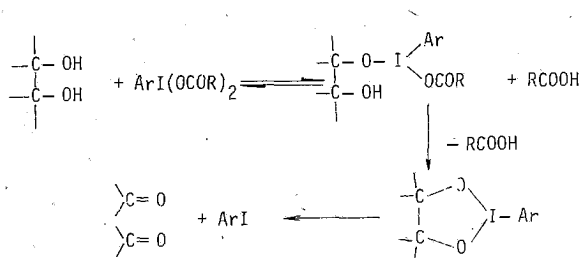


A free-radical mechanism has also been proposed for the oxidation of anilines to azocompounds with PID<sup>3</sup>; an intermediate of that reaction is hydrazo-benzene, which is further oxidised homolytically.

Homolytic reactions are generally only to a small degree sensitive to substituent effects. In the present case the iodine radical, ArIOCOR, is not expected to be particularly stabilised by conjugation, since iodine is reluctant to form double bonds with carbon. This reluctance has been demonstrated<sup>16</sup> from a<sup>19</sup>F-NMR study of a series of *m*- and *p*-fluorocompounds of the type FC<sub>6</sub>H<sub>4</sub>IX<sub>2</sub>, where X=OCOCH<sub>3</sub>, OCOF<sub>3</sub>, Cl, F. Therefore the influence of the substituents could be only of inductive nature. Since though even ortho substituents have practically no influence, it is concluded that the rate determining step of the reaction is the initial electron transfer to iodine. Concerning the rate increase with increasing acidity of

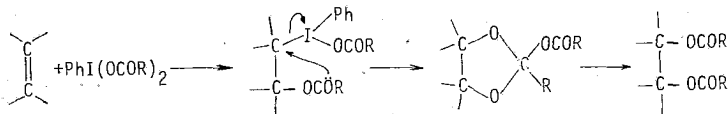
the acid moiety, it is reasonable to assume that stronger electron acceptors, such as  $\text{CF}_3\text{COO}$  vs  $\text{CH}_3\text{COO}$  reduce the electron density of iodine, which can accept more easily the electron.

In order to explain the behaviour of isohydrobenzoin and anethole towards aryl iodine diacetates, one must consider the mechanisms of these reactions, for which adequate bibliographic data exist. The cleavage of isohydrobenzoin has been shown to be a concerted reaction of the following mechanism<sup>2</sup>:



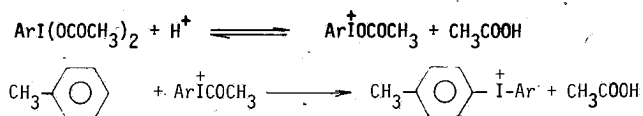
The rate determining step is the second, where electron acceptors in the benzene ring favour attack by oxygen to iodine, to form the cyclic intermediate. The Hammett  $\rho$  value of +1.36 is in accordance with this mechanism; the fastest reaction is sixteen times faster than the slowest. Particularly effective is the *o*- $\text{NO}_2$  group, which causes a 100-fold acceleration of the reaction rate. In this reaction the benzene ring substituents play surprisingly a more pronounced role than the acid moiety.

The reaction of anethole with aryl iodine diacetates must follow a different and more complex mechanism, although no detailed mechanistic study has been done so far. In the case of some reactions of PIT with alkenes<sup>6</sup> it was suggested that initially PIT adds to the double bond under formation of an intermediate, which may lose  $\text{C}_6\text{H}_5\text{I}$  as follows:



The second cyclic intermediate is eventually isomerized to the isolated reaction product, i.e. the vic-trifluoroacetate derivative of the alkene. If the rate determining step was the initial attack of the alkene to iodine, then electron acceptors would accelerate the reaction rate. Since the opposite has been observed, it follows that the second step is rate determining. The sensitivity of the reaction of anethole with aryl iodine diacetates is somewhat less than that of isohydrobenzoin, i.e. a twelve-fold difference in rates was observed between the slowest and the fastest reaction.

In the case of the reaction of substituted PID with toluene the main product is the *p*-iodonium salt, in a typical electrophilic aromatic substitution. The reaction does not proceed without  $\text{H}_2\text{SO}_4$ , which acts as a catalyst, promoting the dissociation of PID to the effective electrophile:



Thus electron donors in PID will increase its basicity, leading to greater ionisation, which further increases with increasing  $\text{H}_2\text{SO}_4$  concentration.

The nature of the reaction of substitute PID with N-(4-substituted-aryl) acetamides, which was initially thought to be of a radical character<sup>14</sup> and then an electrophilic displacement involving an acetoxy cation<sup>15</sup>, has recently been elucidated<sup>17</sup>. The reaction is especially complex with no less than eight discrete steps; the acetoxy group enters the aromatic ring as a nucleophile and an intermediate dienone imine has been isolated. Thus the observed insensitivity of the reaction to the substituents of PID is hardly surprising.

Finally, it has been reported that substituted PID with electron donors accelerate the reaction rate in the oxidation of oxalic acid to carbon dioxide<sup>1</sup>. The mechanism of this reaction was thought to involve a cyclic intermediate, but no explanation can presently be offered for the role of substituents in this system.

## Conclusion

Aryliodine dicarboxylates are emerging as useful oxidising agents of wide applicability. Variations in their structure can exert a significant change in their reactivity. As aryliodine dicarboxylates may react via homolytic, heterolytic or concerted pathways, sometimes quite complex, no general conclusion can be drawn about relations between structure and reactivity. Nevertheless in a given system one may moderate or enhance the oxidising power of the oxidant by suitable variations to its structure.

Generally it may be concluded that (i) the stronger the acid, the more efficient is the oxidant and (ii) o-substituted oxidants exert the more pronounced changes in reactivity, provided that the reaction has a polar step.

## Experimental

*Materials.* All iodine compounds were known from the literature. Aryliodine diacetates and bis chloroacetates were prepared by oxidation of aryl iodides with peracetic acid, according to Pausacker's method<sup>2</sup>. The other phenyliodine dicarboxylates were prepared by exchange of PID with an excess of haloacetic acid<sup>8</sup>.

Ethyl hydrazodicarboxylate was prepared from hydrazine and ethyl chloro-

formate, m.p. 130°C (lit.<sup>18</sup> m.p. 130 °C). Its oxidation product, ethyl azodicarboxylate, was a yellow-orange coloured oil, in one only diastereomeric form, apparently trans. A sample of it from an oxidation run in a preparative scale was converted to the trans-azodicarboxamide, m.p. 225–228 °C (lit.<sup>19</sup> m.p. 224–230 °C). *Kinetic measurements.* Stock solutions of the substrate and oxidants in chloroform were thermostated, mixed in the appropriate equimolecular quantities and placed in the jacketed thermostated cell of a Zeiss PMQ II spectrophotometer. The formation of ethyl azodicarboxylate was monitored by measuring the increase of optical density at 410 nm, which is the wavelength of its absorption maximum. The “pseudo-first-order” rate constants were calculated after following the reactions for about three half-lives, while final readings were taken after at least ten half-lives. The differences of the final optical density and optical densities measured at various intervals were plotted logarithmically against time and the rate constants calculated from the slopes of the straight lines obtained.

## Περίληψη

*Συγκριτική μελέτη της οξειδωτικής ισχύος υποκατεστημένων διακετοξυ-ιωδοβενζολίων*

Σ' αυτή την εργασία εξετάζεται η επίδραση των υποκαταστατών X και της ομάδας R στην οξειδωτική ισχύ μιάς σειράς διακετοξυ-ιωδοβενζολίων, του γενικού τύπου  $X-C_6H_4I(OCOR)_2$ . Αρχικά γίνεται μιά μελέτη της οξειδώσεως  $C_2H_5OOCNHNHCOOC_2H_5$  προς  $C_2H_5OOCN=NCOOC_2H_5$  και στή συνέχεια τ' αποτελέσματα συγκρίνονται με βιβλιογραφικά δεδομένα των αντιδράσεων διακετοξυ-ιωδοβενζολίων με γλυκόλες (σχάση προς καρβονυλικές ενώσεις), άνηθόλη (άνορθωση διπλού δεσμού) και τολουόλιο (σχηματισμός ιωδωνιακών αλάτων).

Τά κύρια συμπεράσματα είναι: 1) όσο ισχυρότερο είναι τό όξύ της άκετοξυομάδας, τόσο αξάνει ή οξειδωτική ισχύς του οξειδωτικού και 2) δέν ισχύει γενικός κανόνας γιά την επίδραση των υποκαταστατών του βενζολικού δακτυλίου, πού εξαρτάται από τό μηχανισμό της αντίδρασης.

Στό σύστημα πού εξετάζεται,  $-NH-NH-$   $-N=N-$ , ή επίδραση των υποκαταστατών είναι άμελητέα. Στή σχάση των γλυκολών δέκτες ήλεκτρονίων αξάνουν τή δραστικότητα του οξειδωτικού, ενώ δότες τήν έλαττώνουν. Τά αντίθετα ισχύουν στήν άνορθωση του διπλού δεσμού και στήν ήλεκτρονιόφιλη υποκατάσταση του τολουολίου.

---

## References

1. Criegee R., Beucker H.: *Ann. Chem.* **541**, 218 (1939).
2. Pausacker K.H.: *J. Chem. Soc.* 107 (1953).
3. Pausacker K.H.: *J. Chem. Soc.* 1989 (1953).

4. Mukaiyama T., Endo T.: *Bull. Chem. Soc. Japan* **40**, 2388 (1967).
5. Szmant H.H., Suld G.: *J. Am. Chem. Soc.* **78**, 3400 (1956).
6. Spyroudis S., Ph. D. Thesis.: University of Thessaloniki, 1981.
7. Sivasankara Pillai V.N., Ramachandran Nair C.G.: *Talanta* **22**, 57 (1975).
8. Spyroudis S., Varvoglis A.: *Synthesis* 445 (1975).
9. Radakrishna A.S., Parham M.E., Riggs R.M., Loudon G.M.: *J. Org. Chem.*, **44**, 1746 (1979).
10. Spyroudis S., Varvoglis A.: *Synthesis* 837 (1976).
11. Spyroudis S., Varvoglis A.: *J. Chem. Soc. Chem. Commun.* 615 (1979).
12. Merkushev E.B., Karpitskaya L.G., Novoseltseva G.I.: *Dokl. Akad. Nauk. SSSR*, **245**, 607 (1979).
13. Briody J.M.: *J. Chem. Soc. B*, 93 (1968).
14. Johnson W.D., Riggs N.V.: *Australian J. Chem.* **17**, 787 (1964).
15. Johnson W.D., Sherwood J.E.: *Australian J. Chem.* **25**, 1213 (1970).
16. Lyalin V.V., Syrova G.P., Orda V.V., Alekseeva L.A., Yagupolskii L.M.: *Zhur. Org. Khim.* **6**, 1420 (1970); *C.A.* **73**, 87298 (1970).
17. Kokil P.B., Patil S.D., Ravindranathan T., Madhavan Nair P.: *Tetrahedron Letters* 989 (1979).
18. Beilstein's Handbuch der organischen Chemie, **3**, H. 98.
19. Beilstein's Handbuch der organischen Chemie, **3**, III 234.

## THE REACTION OF PHENYLIODINE DITRIFLUOROACETATE WITH AROMATIC ETHERS

S. SPYROUDIS and A. VARVOGLIS

*Laboratory of Organic Chemistry, University of Thessaloniki, Thessaloniki (Greece).*

(Received February 11, 1981).

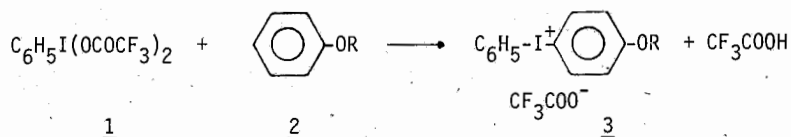
### Summary

The reaction of phenyliodine ditrifluoroacetate with eight aromatic ethers has been studied. The main product of the reaction is an iodonium salt, provided that the aromatic nucleus is not sterically hindered and not deactivated. It is remarkable that the *p*-isomers are exclusively formed and no acid catalysis is required, unlike with some other related reactions.

### Theoretical

The oxidative properties of phenyliodine ditrifluoroacetate (hereafter abbreviated as PIT) have been demonstrated recently in a number of cases<sup>1-8</sup>. We describe here the reaction of PIT with aromatic ethers of various types.

PIT (1) reacts with most aryl ethers (2) under mild conditions, the main product of the reaction being an iodonium salt (3), according to the equation:



The ethers used and the resulting iodonium salts along with some by-products appear in the Table. As the above equation implies, phenyl ethers give exclusively *p*-substituted iodonium salts, in yields ranging between 52 and 75%, while aryl ethers may give also other products, depending on the nature of the substituent of the phenyl ring.



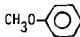
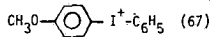
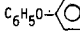
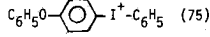
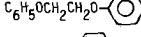
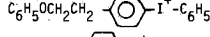
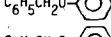
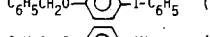
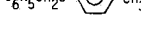

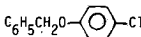
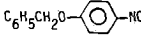
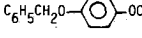
The reaction appears to be a typical aromatic-electrophilic substitution, where the electrophilic species is the cation of bivalent iodine, which results from dissociation of PIT:



Analogous reactions are known with phenyliodine diacetate (PID). Beringer and his coworkers<sup>9</sup> among the various methods which they developed for the preparation of iodonium salts used also PID and various activated arenes in the presence of strong acids. The reactions of PID with toluene<sup>10,11,12</sup> and thiophene<sup>13</sup> have been studied in detail kinetically, while in several patents the preparation of iodonium salts of thiophene has been described from its reactions with various aryl iodine diacetates<sup>14</sup>. A similar reaction is that of toluene with some perfluoroalkyliodine ditrifluoroacetates<sup>15</sup>, resulting to the formation of iodonium salts, while the reaction of iodine tris(trifluoroacetate),  $\text{I}(\text{OCOCF}_3)_3$ , with arenes<sup>16</sup> leads to aryl iodine ditrifluoroacetates.

In the previous reactions with PID, there is no detectable reaction in the absence of acid ( $\text{H}_2\text{SO}_4$ ). In the reaction of PIT with aromatic ethers, there is no need for an acid catalyst; presumably, trifluoroacetic acid formed along with the

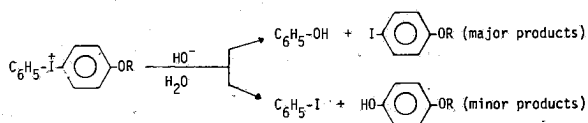
TABLE. Reaction Products from Aryl Ethers and PIT.

Ether	Iodonium Salt <sup>1</sup> (yield %)	Benzaldehyde(yield %)
2a 	 (67)	—
2b 	 (75)	—
2c 	 (64)	—
2d 	 (56)	(3)
2e 	 (52)	(4)
2f 	—	(5)
2g 	—	—
2h 	unstable <sup>2</sup>	(30)

<sup>1</sup>The anion is always  $\text{CF}_3\text{COO}^-$ .

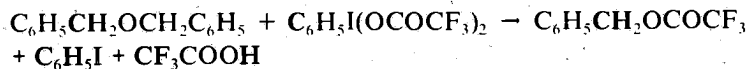
<sup>2</sup>For isolated products see text.

iodonium salt may serve as a catalyst. Actually when a 5-10% of trifluoroacetic acid is added to the reaction mixture, the reaction is completed in 2-6 h, instead of the usual 24-36 h required, at room temperature. The reactions of toluene with PID have been shown to give a mixture of p- and o-methyl diphenyl iodonium salts, in a ratio of 9:1. In the present study the exclusive formation of p-isomers was established from the alkaline hydrolysis of the iodonium salts, which generally proceeds in two directions as follows:

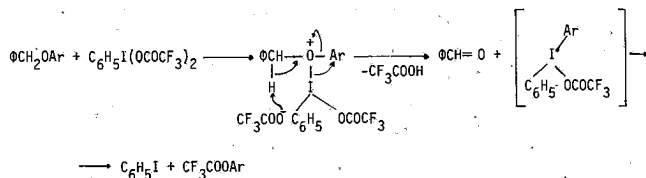


All four products have been isolated and characterised in most cases, but no o-substituted iodoether nor o-monoether of pyrocatechol could be detected. Thus, the formation of o-substituted iodonium salts at detectable amounts has been ruled out. The bulkiness of both the  $\text{C}_6\text{H}_5\text{I}^+\text{OCOCF}_3$  group and the alkoxy (phenoxy, benzyloxy) group apparently precludes the attachment of the former group in ortho position to the latter. This steric inhibition is probably the reason why p-chlorophenyl benzyl ether does not form an iodonium salt. Of course chlorine is a mild deactivator, but under the drastic conditions used in this case (prolonged heating, addition of trifluoroacetic acid), one would have expected the formation of some iodonium salt in o-position to the benzyloxy group, unless steric inhibition was dominant. This inhibition is more obvious in the case of p-tolyl benzyl ether, where only the iodonium salt ortho to the methyl group is formed.

A by-product of the reaction of PIT with aryl benzyl ethers is benzaldehyde, which is always formed in small yields, 3-5%, with the exception of p-nitrophenyl benzyl ether, which is completely inert in its reaction with PIT. The formation of benzaldehyde is quantitative in the reaction of PIT with dibenzyl ether and other substituted dibenzyl or related ethers. In those cases a trifluoroacetate of benzylic alcohol is also formed, according to the equation:



The mechanism of the above reaction has been discussed<sup>3</sup> and a similar pathway probably operates with aryl benzyl ethers:

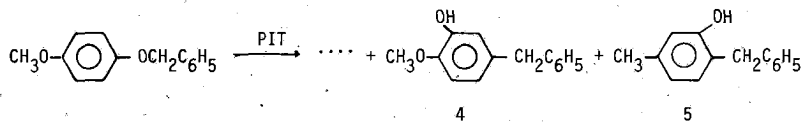


The expected phenyl(aryl) trifluoroacetates though have not been isolated, possibly because they are easily hydrolysed to phenols, which are then oxidised by PIT to resinous material. The inertness of p-nitrophenyl benzyl ether is easily explained, as the etheral O has not anymore available its bonding electron pair because of interaction with the nitro group:

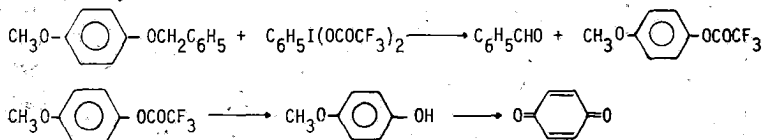


Especially noteworthy was the reaction between p-benzyloxy anisole and PIT. Upon mixing of the reagents a deep green colour was formed which soon turned to

yellow. When the reaction was carried out in an nmr tube, a complete disappearance of all peaks was observed and only after approximately 1 h the peaks of the final products did appear. The reaction products turned out to be p-benzoquinone (10%), benzaldehyde (30%) and a mixture of the isomeric phenols 4 and 5 (7%). No iodonium salt could be isolated or detected. This reaction undoubtedly follows a homolytic pathway, as the disappearance of the nmr peaks points out.

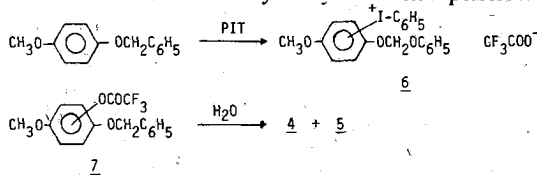


The free radicals involved must be of considerable stability, since they suppress all nmr signals for a relatively long period of time. The formation of benzaldehyde and p-benzoquinone may be accounted for by the following series of reactions, where initially a mixture of benzaldehyde and p-methoxyphenyl trifluoroacetate are normally formed:



The ester may be hydrolysed to p-hydroxy anisole, which is further oxidised by PIT to the quinone or alternatively it may undergo a homolytic scission to a p-methoxy phenoxy radical, which is also oxidised to the quinone. Independent experiments showed that both p-hydroxy anisole and p-methoxy anisole react with PIT and they give p-benzoquinone as the main product. During these reactions the same colours develop and again the nmr signals disappear. There is little doubt that free radicals, probably of the quinhydrone type, are involved in the stages of the oxidation of these compounds.

The formation of phenols 4 and 5 is best explained assuming that initially two unstable iodonium salts (6) are formed. Under expulsion of iodobenzene the esters 7 are formed, which hydrolyse to the phenols.



The instability of 6 is probably due to the greatly enhanced  $\pi$  electron density of the benzene ring, which favours the expulsion of a neutral molecule, i.e.  $C_6H_5I$ , and the formation of a stabilised carbonium ion, which combines with the trifluoroacetate anion.

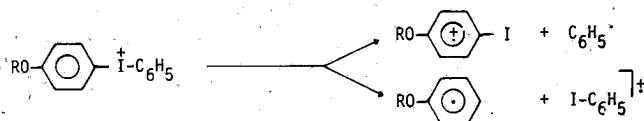
The formation of both phenols 4 and 5 was established from the nmr spectrum of their mixture, where two sets of protons for the groups  $-OCH_3$  and  $-OCH_2-$  were present. The mixture could not be separated by chromatography; after repeated

recrystallisations one phenol was obtained in pure form, but it was not possible to assign its correct structure on the basis of spectroscopic data. It is of interest that p-methoxyphenyl benzyl ether gives initially two iodonium salts, despite the steric hindrance of the benzyloxy group. We believe that this system is extremely activated and the reaction of aromatic substitution is so rapid, that the steric factor becomes unimportant and the two phenols which finally result are in a ratio of 2.5:1. The isolated phenol was the minor constituent and it is plausible to assume that because of the greater steric hindrance of the benzyloxy group was the isomer 4.

### Mass Spectra of Iodonium Salts

The mass spectra of iodonium salts have not been described in the literature. From the limited data available presently we cannot draw general conclusions yet. In any case we observe in two from the four compounds studied iodonium ions with very low intensity. It should be noted that rarely cations of various types of salts give in their mass spectra the corresponding ion.

The fragmentation pattern is mainly a C-I scission occurring in both directions with almost equal probability, i.e.



The other fragments of high mass must be the products of thermal reactions, as it has been observed with ammonium salts<sup>17</sup>. The trifluoroacetate anion may attack either C in  $\alpha$ -position to iodine, so that again two kinds of trifluoroacetate esters are formed:



Fragments arising from the above esters are mainly the  $[M-CO]^+$  ions and the tropylium ion.

### Experimental

**Measurements.** Melting points have been obtained on a Kofler hot stage apparatus and they are uncorrected. IR spectra were obtained from neat liquids or nujol mulls with a Perkin-Elmer Model 257 spectrophotometer. <sup>1</sup>H NMR spectra were recorded on a Varian A-60A spectrometer, in CDCl<sub>3</sub> or CCl<sub>4</sub> with TMS as an internal standard. Mass spectra were obtained with a Hitachi-Perkin-Elmer Model RMU-6L spectrometer, with ionisation energy of 70 eV.

**Materials.** PIT was prepared as previously described<sup>1</sup>. All ethers were known compounds and prepared by standard methods.

**General procedure.** The ether (0.1 mmole) is dissolved in dry chloroform (10

ml) and an excess of PIT (0.13 mmols) is added with stirring, until it dissolves. The reaction mixture is allowed to stand at room temperature for 36 h, when the ether has been consumed. The solvent is then removed and the residue is chromatographed on a silica gel column, using chloroform-hexane (6:4). Iodobenzene is first collected and then, where appropriate, benzaldehyde. The iodonium salt was usually not possible to be eluted from the column, even with the use of pure alcohols. In these cases the upper 1/3, of the silica gel was removed from the column and it was extracted with a hot mixture of chloroform-methanol (1:1) and the iodonium salt could be obtained crude after filtration and evaporation of the solvents. All salts were purified by recrystallisation from chloroform-hexane. The following compounds were obtained:

- 3a. M.p. 168°C (lit. m.p.<sup>9</sup> 166-168°C), with decomposition.
- 3b. M.p. 155-156°C (dec.). IR (nujol) 1655 (C=O), 1230, 1180, 1150 (C-F, CF<sub>3</sub>) cm<sup>-1</sup>. NMR (CDCl<sub>3</sub>) 86.80-8.02 (m). Mass spectrum, m/e (relative intensity) 373 (trace) 296 (82), 282 (20), 204 (100), 190 (15), 185 (34), 149 (71), 141 (44), 139 (35), 119 (70), 117 (72), 77 (15), 76 (15), 69 (21).  
Anal. Calculated for C<sub>20</sub>H<sub>14</sub>F<sub>3</sub>IO<sub>3</sub> C 49.38, H 2.88. Found C 49.16, H 2.99.
- 3c. M.p. 120-122°C (dec.). IR (nujol) 1655 (C=O), 1230, 1180, 1150 (C-F, CF<sub>3</sub>) cm<sup>-1</sup>. NMR (CDCl<sub>3</sub>) 4.55 (s, 4H), 6.91-7.95 (m, 10H). Mass spectrum (rel. int.) m/e 417 (1), 340 (100), 326 (25), 246 (7), 204 (39), 190 (19), 162 (6), 121 (14), 112 (10), 83 (18), 77 (18), 70 (20), 69 (9).  
Anal. Calculated for C<sub>22</sub>H<sub>18</sub>F<sub>3</sub>IO<sub>4</sub> C 49.81, H 3.39. Found C 49.64, H 3.21.  
M.p. 149-151°C (dec.). IR (nujol) 1655 (C=O), 1230, 1170, 1150 (C-F, CF<sub>3</sub>) cm<sup>-1</sup>. NMR (CDCl<sub>3</sub>) 5.05 (s, 2H), 6.98 (d, 2H, J=8Hz), 7.38 (s, 5H), 7.49-7.98 (m, 7H). Mass spectrum (rel. int.) m/e 310 (18), 296 (6), 204 (20), 190 (17), 162 (9), 91 (100), 77 (25).  
Anal. Calculated for C<sub>21</sub>H<sub>16</sub>F<sub>3</sub>IO<sub>3</sub> C 50.40, H 3.20. Found C 50.11, H 3.28.
- 3e. M.p. 151-153°C (dec.). IR (nujol) 1660 (C=O), 1230, 1180, 1150 (C-F, CF<sub>3</sub>) cm<sup>-1</sup>. NMR (CDCl<sub>3</sub>) 2.29 (s, 3H), 5.15 (s, 2H), 6.96 (d, 1H), 7.33-7.97 (m, 12H). Mass spectrum (rel. int.) m/e 324 (100), 310 (12), 234 (60), 204 (79), 190 (36), 162 (15), 91 (30), 77 (74), 69 (56).  
Anal. Calculated for C<sub>22</sub>H<sub>18</sub>F<sub>3</sub>IO<sub>3</sub> C 51.36, H 3.50. Found C 51.40, H 3.39.
- Phenols 4 and 5: The mixture had an NMR spectrum (CCl<sub>4</sub>) with two singlets at 3.81 and 3.74 and two singlets at 4.93 and 4.90. The isolated phenol, believed to be 4, had m.p. 106-107°C (from petroleum ether). IR (nujol) 3450 (OH), 1600, 1230 (C-O) cm<sup>-1</sup>. NMR (CCl<sub>4</sub>) 3.81 (s, 3H), 4.93 (s, 2H), 5.38 (s, br. 1H), 6.21-6.77 (m, 3H), 7.33 (m, 5H). Mass spectrum (rel. int.) m/e 230 (100)M<sup>+</sup>, 215 (2), 197 (2), 139 (40), 111 (10), 91 (99).

*Hydrolysis of 3.* The iodonium salt (0.1 mmole) was refluxed in 10% NaOH for 10 min. The hydrolysate was extracted with ether and the residue was chromatographed on a silica gel column; the iodocompounds were thus obtained. The aqueous layer of the hydrolysate was acidified, extracted with ether and chromatographed; in this way the phenols were obtained.

## Περίληψη

*Η αντίδραση διτριφθορακετοξυιωδοβενζολίου με αρωματικούς αιθέρες.*

Στήν εργασία αυτή μελετάται η αντίδραση μερικῶν αρωματικῶν αιθέρων (2) με τὸ διτριφθορακετοξυιωδοβενζόλιο (1). Τὸ κύριο προϊόν πού σχηματίζεται σέ ικανοποιητικές ἀποδόσεις εἶναι τὸ ιωδωνιακὸ ἄλας τοῦ αιθέρα (3), σέ μιὰ κανονικὴ ἀντίδραση ἠλεκτρονιόφιλης ὑποκατάστασης.

Χαρακτηριστικὰ τῆς ἀντίδρασης εἶναι ὁ σχηματισμὸς μόνο τῶν π-ισομερῶν καὶ τὸ γεγονός ὅτι δέ χρειάζεται ὀξινὴ κατάλυση, σέ ἀντίθεση μεῖ ἄλλες ἀνάλογες ἀντιδράσεις. Αἰθέρες μεῖ ὑποκαταστάτες πού ἀνενεργοποιοῦν τὸ δακτύλιο δέν ἀντιδροῦν μεῖ τὸ (1).

Μιὰ παράπλευρη ἀντίδραση τῶν βενζυλο-αρυλοαιθέρων ὁδηγεῖ στό σχηματισμὸ βενζαλδεϋδης.

Τὸ ιωδωνιακὸ ἄλας τῆς π-βενζυλοξυ-ανισόλης (2h) εἶναι ἀσταθές καὶ διασπᾶται σέ διάφορα προϊόντα.

## References

1. Spyroudis S., Varvoglis A.: *Synthesis*, 445 (1975).
2. Spyroudis S., Varvoglis A.: *Synthesis*, 837 (1976).
3. Spyroudis S., Varvoglis A.: *J. Chem. Soc. Chem. Commun.*, 615 (1979).
4. Varvoglis A., Spyroudis S.: *Proceedings of the 5th Panhellenic Chemical Congress*, Athens, 1980, Vol. A, p. 152.
5. Ohsawa A., Arai H., Igeta H., Akimoto T., Tsuji A., Litaka Y.: *J. Org. Chem.*, **44**, 3254 (1979).
6. Merkushev E.B., Karbitskaya L.G., Novoseltseva G.I.: *Dokl. Akad. Nauk. S.S.S.R.*, **245**, 605 (1979).
7. Axiotis B., Spyroudis S., Varvoglis A.: *Chim. Chron, New Series*, **10**, 185 (1981).
8. Spyroudis S., Ph. D. Thesis, Thessaloniki (1981).
9. Beringer F.M., Falk A.R., Karniol M., Lilien I., Masullo G., Mausner M., Sommer E.: *J. Am. Chem. Soc.*, **81**, 342 (1959).
10. LeCount D.J., Reid J.A.W.: *J. Chem. Soc. C*, 1298 (1967).
11. Briody J.M.: *J. Chem. Soc. B*, 93 (1968).
12. Hoffelner H., Schneider H., Wendt H.: *Chem.-Zeitung*, **102**, 53 (1978); *C.A.* **88**, 189534 (1978).
13. Yamada Y., Okawara M.: *Bull. Chem. Soc. Jap.*, **45**, 2515 (1972).
14. These iodonium salts have a potential use as bactericides, fungicides and algicides.
15. Lyalin V.V., Orda V.V., Alekseyeva L.A., Yagupolskii L.M.: *Zh. Org. Khim.*, **7**, 1473 (1971); *C.A.* **75**, 140390 (1971).
16. Maletina I.I., Orda V.V., Yagupolskii L.M.: *Zh. Org. Khim.*, **10**, 294 (1974); *C.A.* 120418 (1974).
17. Budzikiewicz H., Djerassi C., Williams D.H.: *Mass Spectrometry of Organic Compounds*, Holden-Day, San Francisco, 1967, p. 330.

*Chimika Chronika, New Series, 10, 331-346 (1981)*

## **STUDY OF THE LIQUID STATE AND THE VAPOR-LIQUID PHASE TRANSITION USING A NEW APPROXIMATE METHOD OF THE HOLE THEORY**

D.A. JANNAKOUDAKIS and P.J. NIKITAS

*Laboratory of Physical Chemistry, Faculty of Physics & Mathematics, University of Thessaloniki (Greece).*

(Received February 17, 1981).

### **Summary**

A new analytical expression for the free volume of the hole theories of liquids is derived from the comparison of theoretical and experimental isotherms by means of the Bragg-Williams approximation.

It is shown that this method constitutes a more satisfactory approach to the prediction of the equilibrium thermodynamic properties of liquids and vapor-liquid phase transition, compared to the already existing hole theories. The agreement with experimental and machine-calculated data is generally good and in most cases comparable to the results of the most important new mathematical theories of the liquid state.

**Key words:** Lattice statistics, Hole theory, Liquid state.

### **I. Introduction**

The central problem in the statistical thermodynamics of fluids is the prediction of the observed equilibrium properties of liquids from a knowledge of the way in which the constituent molecules interact. The theoretical interpretation of the liquid state phenomena has advanced through the development of two basic categories of methods concerning the application of the statistical thermodynamics.

The first category, namely the mathematical modelling, includes the perturbation theories and the methods for the direct calculation of the radial distribution function. The application of these methods was greatly simplified by the use of the modern computing machines leading to a highly accurate description of the liquid state.

The second category, namely the physical modelling, has developed parallel to the first one, offering a reasonable alternative for the cases where purely

mathematical methods become ineffective. Physical models are generally simple, they lead to analytical solutions and they are very useful for the analysis of more complicated systems such as mixtures, adsorbed molecules, phase transitions and order - disorder problems in general.

The major disadvantage of the mathematical modelling is that as abstraction proceeds further, the physical picture of the starting point is gradually lost. On the other hand, physical modelling although it usually involves assumptions of more or less empirical nature, is more realistic to the extent it never loses contact with the physical world.

The most widely acceptable physical theories of the liquid state are the various versions of the free volume theory of Lennard-Jones and Devonshire<sup>1</sup>. Hole theories result from the modification of the free volume theory which allows for the existence of empty cells in the system. They have been investigated by several authors<sup>1-6</sup> and attention was given mainly to the determination of a simple analytical expression of the free volume,  $v_f$ . In the previous hole theories a certain mathematical expression for the  $v_f$  was proposed in an empirical or semiempirical way. On the basis of this expression the partition function and the properties of the liquid state were determined.

In the present work, we avoid the application of the above procedure. Alternatively an analytical expression for  $v_f$  is derived from the comparison of theoretical and experimental isotherms. This method leads to an almost quantitative description not only of the dense gas region but also of the liquid region even at relatively low temperatures. It also entails a satisfactory description of the thermodynamic equilibrium existing between the liquid state and its vapors.

## II. Equilibrium properties of simple liquids

### a. Approximation to the free volume

The fundamental assumptions of the hole theories are the following<sup>1</sup>:

1. The volume  $V$  of the liquid, occupied by  $N$  molecules is divided into  $L$  identical cells, where  $L \geq N$ . The cell size,  $\omega = V/L$ , is selected sufficiently small so that configuration with more than one molecule in any cell can be neglected entirely. The number of cells  $L$  depends on either temperature and density.
2. The centres of cells form a regular face - centred cubic lattice.
3. The molecules are regarded as moving independently in their cells.
4. It is supposed that interactions between molecules in cells, that are not nearest neighbours, can be neglected.

Assuming that the intermolecular potential is given by the 6:12 potential of Lennard-Jones,

$$u(r) = 4\epsilon [(\sigma/r)^{12} - (\sigma/r)^6], \quad (1)$$

where  $\epsilon$  is the depth of the minimum in the potential curve and  $\sigma$  is the diameter of the particles, then the potential  $\Psi(0)$  of a molecule at the center of its cell is given by



$$\psi(0) = 12 \epsilon [(1/\omega^*)^3 - 2(1/\omega^*)^2], \quad (2)$$

where  $\omega^* = \omega/\sigma^3$ .

Furthermore, assuming that holes and molecules are randomly distributed within the system, the hole model leads to the following expression for the partition function<sup>3</sup>:

$$Q = \frac{L!}{N!(L-N)!} \cdot \lambda^{3N/2} \cdot v_f^N \cdot \exp\left(-\frac{\omega N \psi(0)}{2kT}\right), \quad (3)$$

where  $\lambda = 2\pi \cdot m \cdot k \cdot T / h^2$ ,  $v = V/N$  and  $v_f$  is the free volume.

Because each molecule moves into its cell under the influence of the field of the nearest - neighbour molecules, the free volume  $v_f$  can be given by

$$\begin{aligned} (v_f)_i &= \omega - b_{1i} y_i \\ &= \omega (1 - b_{2i} y_i) \end{aligned} \quad (4)$$

where  $b_{1i}$  and  $b_{2i}$  are functions of  $\omega, v$ , and  $T$ , while  $y_i$  is defined by

$$y_i = 1 - \frac{j}{c},$$

where  $j$  is the number of the vacant nearest-neighbour cells to the  $i$ th molecule and  $c$  the coordination number of the lattice. Accounting for the random distribution assumption, we can consider an average free volume  $v_f$ , for which we have

$$y_i = \frac{N}{L} = \frac{\omega}{v} = \theta. \quad (5)$$

In order to be able to use Eq. (4) for the calculation of the various thermodynamic functions of the liquid state it is necessary to assume that  $b_2$  is given by a simple functional expression. Although  $b_2$  may be calculated by numerical methods under certain approximations, it is necessary for the analytical determination of  $Q$  to assume that  $b_2$  is given by a simple relation. Here, we'll assume that  $b_2$  is a function of temperature only,

$$b_2 = b(T)$$

$$\text{or} \quad v_f = \omega \cdot [1 - b(T) \cdot \theta] \quad (6)$$

The dependence of  $b_2$  on  $T$  will be determined from the comparison between theoretical and experimental isotherms. If we substitute Eq.(6) into Eq.(3) we obtain the Helmholtz free energy, expressed as a function of  $V, N, L, T$  and  $b$ :

$$\begin{aligned} \frac{A}{NkT} &= -\ln(\lambda^{3/2} \omega \cdot q_{int.}) + \ln\left(\frac{\theta}{1 - b(T) \cdot \theta}\right) + \left(\frac{1}{\theta} - 1\right) \ln(1 - \theta) \\ &+ \theta \frac{\psi(0)}{2kT} \end{aligned} \quad (7)$$

The equation of state may be calculated from

$$\frac{PV}{NkT} = - \omega \left( \frac{\partial A/NkT}{\partial \omega} \right)_{T, \omega} \quad (8)$$

which yields

$$\frac{PV}{NkT} = \frac{b(T) \cdot \theta}{1 - b(T) \cdot \theta} - \frac{1}{\theta} \ln(1 - \theta) + \frac{6\theta \epsilon}{kT} \left( \frac{1}{\omega^{*4}} - \frac{2}{\omega^{*2}} \right) \quad (9)$$

where the volume per cell  $\omega$  is determined by minimizing A:

$$\left( \frac{\partial A}{\partial \omega} \right)_{\omega, T} = 0 \quad (10)$$

or

$$-1 + \frac{b(T) \cdot \theta}{1 - b(T) \cdot \theta} - \frac{1}{\theta} \ln(1 - \theta) + \frac{6\theta \epsilon}{kT} \left( \frac{2}{\omega^{*2}} - \frac{3}{\omega^{*4}} \right) = 0 \quad (11)$$

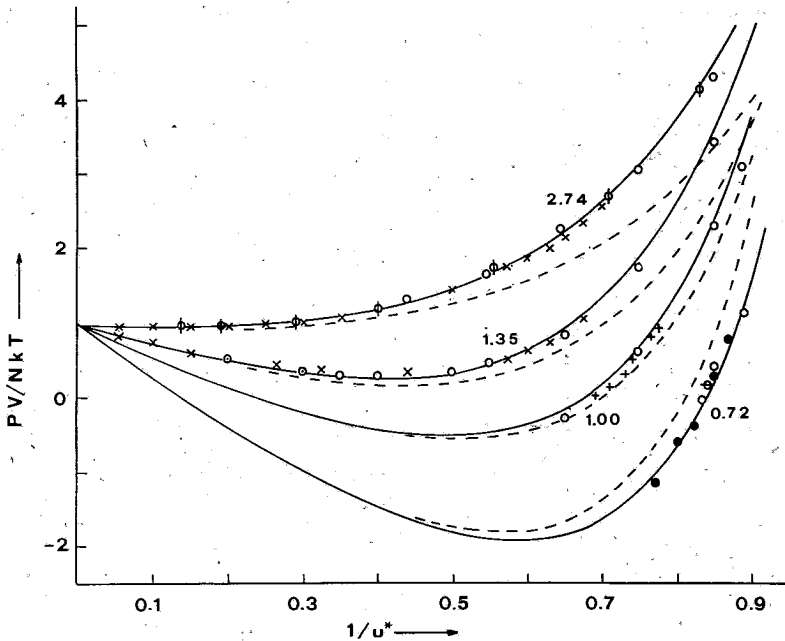


FIG. 1. Equation of state for 6:12 fluid. The curves are isotherms as labeled with  $T^*$ , the related temperature. The solid curves are calculated from Eq.(9) while the broken curves are the results of Henderson's theory. The points shown by  $o$ ,  $\phi$  and  $\bullet$  are machine-calculated values. The points given by  $\odot$  were calculated using a five-term virial expansion and the points given by  $x$ ,  $\ominus$  and  $+$  are experimental values. See Fig. 5 of Ref.(8) for the data references.

Eqs. (9) and (10) reveal that the theoretical isotherms are functions of  $V, N, T$  and  $b$ . From preliminary comparisons between theoretical data for various values of  $b$  with experimental isotherms of Argon and machine - calculated data<sup>7</sup> (see Fig. 1), we come to the following conclusions: (a) if  $b$  is determined at every temperature so that the best agreement between theoretical and experimental data is achieved, the hole theory in an almost quantitative manner describes the experimental isotherms, and (b)  $b$  is exponentially dependent on temperature. This dependence is accurately described by the relation

$$b(T) = 1.1718 \exp\left(-\frac{0.1361}{T^*}\right) \quad (12)$$

where  $T^* = kT/\epsilon$ .

#### *b. Calculations and comparison with experiment and previous theories*

Once the free volume has been formulated, we can proceed to a detailed comparison of the results obtained from the present hole theory with experimental and machine - calculated data taken from the literature. We will also compare our results with those obtained from Henderson's theory<sup>3</sup> - which is one of the most successful hole theories - as well as with the results of the most important new mathematical theories of the liquid state. These theories are: The second order perturbation theory of Barker and Henderson<sup>8</sup>, BH2, the perturbation theory of Weeks - Chandler - Anderson<sup>9</sup>, WCA, the variation theories of Mansoori-Canfield<sup>10</sup>, Var. (PY), and Rasaiah-Stell<sup>11</sup>, Var. (VW). Finally our results are compared with the results obtained by the application of the Percus - Yenick equation<sup>12</sup>, PY. In these comparisons we used the parameters  $\epsilon/k = 119.8$  K and  $\sigma = 3.405$  Å derived by Michels *et al.*<sup>13</sup> from second virial coefficients.

Figure 1 displays the comparison of the theoretical and experimental values of the compressibility factor. The agreement of the theoretical results with molecular dynamics, Monte - Carlo and experimental results is quite satisfactory at temperatures above the critical temperature and remains equally satisfactory even at very low temperatures. In Fig. 1 the results of Henderson's theory are also included.

In Fig. 2 the calculated compressibility factor for Argon at 0 °C is compared with the experimental data of Michels *et al.*<sup>14,15</sup> and the prediction of Henderson's theory. The compressibility factor has also been calculated for hydrogen at 0 °C and in the same figure it is compared with the theoretical data of Henderson and the experimental data of Michels and Goudek<sup>16</sup>. It is pointed out that the results of our method give the best agreement with the experimental data.

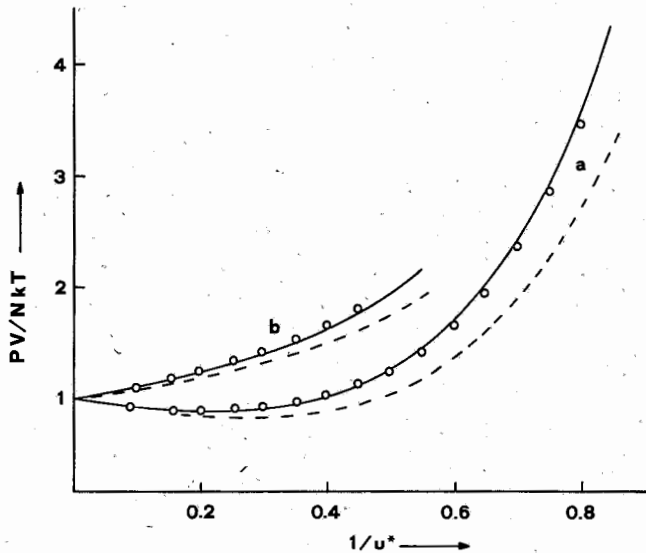


FIG. 2. Calculated and experimental values of the compressibility factor of argon (a) and hydrogen (b) at  $0^{\circ}\text{C}$ . The solid lines give the authors' results, the broken lines are the results of Henderson taken from Ref.(3), and the experimental points are taken from Ref. (14), (15) and (16).

In table I we have compared the theoretical values of  $PV/kT$  predicted by the present method with the corresponding results of the theories BH2, Var.(PY), Var.(VW), WCA, PY and also with simulation data. Regardless of the approximate nature of our method, it leads to results which are comparable to the results of the above theories.

Expanding Eq.(9) in powers of  $1/u$  we obtain for the second virial coefficient

$$B_2 = \omega \left( b(T) + \frac{1}{2} + \frac{\Psi(0)}{2kT} \right) \quad (13)$$

or in a reduced form

$$B_2^* = \frac{3B_2}{2\pi\sigma^3} = \frac{3\omega^*}{2\pi} \cdot \left\{ b(T) + \frac{1}{2} + \frac{\Psi(0)}{2kT} \right\} \quad (14)$$

In Fig. 3 the reduced second virial coefficient is compared with the exact values. The value of Boyle Temperature obtained by our method is found to be equal to 3.68. This value if compared to the value of 3.95 obtained by Henderson's theory reveals a closer approximation to the experimental value of 3.42.

The excess Helmholtz free energy is given by

$$\frac{A'}{NkT} = \frac{A}{NkT} + \frac{3}{2} \ln \lambda + \ln u + 1 + \ln q_{\text{int}} \quad (15)$$

TABLE I. Values of  $PV/NkT$  for 6:12 potential<sup>a</sup>

T*	t/v*	Simul.	PY (E)	BH2	Var (PY)	Var (VW)	WCA (PY)	Present Calc.
2.74	0.65	2.22	2.23	2.22	2.48	2.54	2.21	2.23
	0.75	3.05	3.11	3.10	3.43	3.54	3.11	3.12
	0.85	4.38	4.42	4.44	4.79	4.98	4.50	4.49
	0.95	6.15	6.31	6.40	6.69	6.97	6.57	6.56
1.35	0.10	0.72	0.72	0.74	0.78	0.78	0.77	0.72
	0.20	0.50	0.51	0.52	0.56	0.56	0.53	0.48
	0.30	0.35	0.36	0.36	0.39	0.39	0.32	0.32
	0.40	0.27	0.29	0.26	0.31	0.32	0.17	0.26
	0.50	0.30	0.33	0.27	0.39	0.43	0.18	0.34
	0.55	0.41	0.43	0.35	0.53	0.58	0.27	0.47
	0.65	0.80	0.85	0.74	1.08	1.19	0.71	0.95
	0.75	1.73	1.72	1.64	2.14	2.34	1.70	1.91
	0.85	3.37	3.24	3.36	3.92	4.24	3.51	3.63
0.95	6.32	5.65	6.32	6.67	7.16	(6.58)	6.55	
1.00	0.65	- 0.25	- 0.22	- 0.36	- 0.10	+ 0.04	- 0.51	- 0.13
	0.75	+ 0.58	+ 0.57	+ 0.53	+ 0.95	+ 1.20	+ 0.48	+ 0.73
	0.85	2.27	2.14	2.25	2.90	3.32	2.41	2.46
	0.90	~ 3.50	3.33	3.53	4.34	4.84	(3.96)	3.81
0.72	0.85	0.40	0.33	0.25	1.05	1.59	0.43	0.22
	0.90		1.59	1.63	2.73	3.39	(2.24)	1.51

a. See Table IX of Ref.(12) for the data references.

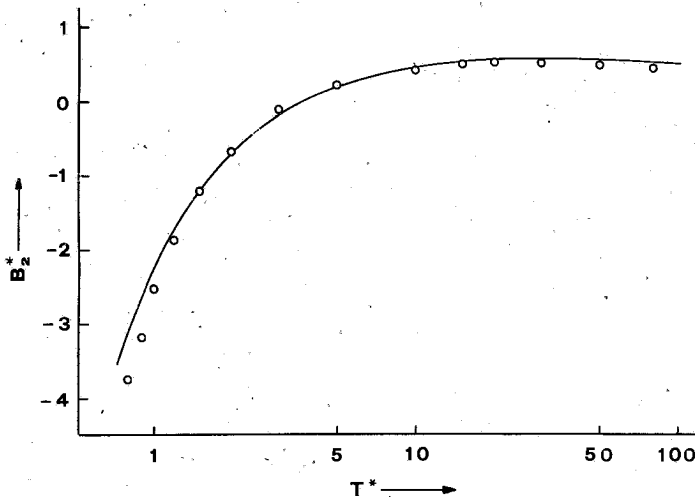


FIG. 3. Second virial coefficient for the 6:12 potential. The points are exact values taken from Ref.(19). The solid line gives the results of Eq. (14).

TABLE II. Values of  $A^*/NkT$  for 6:12 potential<sup>a</sup>

T*	1/v*	Simul.	PY (E)	BH2	Var (PY)	Var (VW)	WCA (PY)	Present Calc.
2.74	0.60	- 0.34	- 0.33	- 0.33	- 0.19	- 0.18	- 0.32	+ 0.13
	0.70	+ 0.01	+ 0.01	+ 0.01	+ 0.20	+ 0.21	+ 0.02	+ 0.32
	0.80	0.43	0.43	0.42	0.65	0.69	0.43	0.61
	0.90	0.93	0.95	0.95	1.21	1.27	0.97	1.02
	1.00	1.59	1.61	1.62	1.92	2.01	1.66	1.61
1.35	0.60	- 1.77	- 1.75	- 1.75	- 1.59	- 1.57	- 1.73	- 1.27
	0.70	- 1.65	- 1.62	- 1.63	- 1.42	- 1.39	- 1.62	- 1.28
	0.80	- 1.41	- 1.37	- 1.41	- 1.13	- 1.07	- 1.39	- 1.15
	0.90	- 1.02	- 0.99	- 1.01	- 0.67	- 0.57	- 0.98	- 0.84
	0.95	- 0.72	- 0.72	- 0.72	- 0.35	- 0.23	(- 0.67)	- 0.59
1.15	0.60	- 2.29	- 2.28	- 2.30	- 2.10	- 2.09	- 2.25	- 1.78
	0.70	- 2.25	- 2.23	- 2.26	- 2.02	- 1.99	- 2.23	- 1.86
	0.80	- 2.06	- 2.06	- 2.10	- 1.81	- 1.74	- 2.08	- 1.82
	0.90	- 1.79	- 1.74	- 1.76	- 1.40	- 1.29	- 1.73	- 1.56
0.75	0.60	- 4.24		- 4.29	- 4.01	- 3.99	- 4.17	- 3.64
	0.70	- 4.53	- 4.50	- 4.28	- 4.24	- 4.24	- 4.51	- 4.04
	0.80	- 4.69	- 4.60	- 4.74	- 4.38	- 4.30	- 4.69	- 4.30
	0.90		- 4.55	- 4.67	- 4.22	- 4.08	(- 4.60)	- 4.35

a. See Table VII of Ref.(12) for the data references.

In Table II the theoretical values of the excess Helmholtz free energy obtained from the theories BH2, Var.(PY), Var. (VW), WCA, PY, the present method and simulation "experiments" are compared. This comparison reveals that the results of our method are equally satisfactory with the results of the variational theories.

Eqs. (6) and (12) combined with Eq.(7) lead to the following expressions for the internal functions of the liquid state:

The entropy can be calculated from

$$S = -(\partial A/\partial T)_{\omega, \nu} \quad (16)$$

which gives

$$\frac{S}{Nk} = \ln(\lambda^{3/2} \omega) - \ln\left(\frac{\theta}{1-b(T)\theta}\right) - \left(\frac{1}{\theta} - 1\right) \ln(1-\theta) + \frac{3}{2} + \ln q_{int.} \\ - \frac{0.1361b(T)\theta}{T^*[1-b(T)\theta]} + T \frac{d \ln q_{int.}}{dT} \quad (17)$$

The internal entropy being in excess to the internal entropy of a perfect gas at the same temperature and volume is

$$S^* = \frac{S}{Nk} - \frac{5}{2} - \ln \lambda^{3/2} - \ln u - \ln q_{int.} - T \frac{d \ln q_{int.}}{dT} \quad (18)$$

or

$$S^* = -1 + \ln[1 - b(T)\theta] - \left(\frac{1}{\theta} - 1\right) \ln(1 - \theta) - \frac{0.1361b(T)\theta}{T^* [1 - b(T)\theta]} \quad (19)$$

The internal energy is determined from

$$U = -T^2 \left( \frac{\partial A/T}{\partial T} \right)_{\omega, u} \quad (20)$$

which yields

$$\frac{U}{N\epsilon} = \frac{3}{2} T^* - \frac{0.1361b(T)\theta}{1 - b(T)\theta} + 6\theta \left( \frac{1}{\omega^{*4}} - \frac{2}{\omega^{*2}} \right) + T \cdot T^* \frac{d \ln q_{int.}}{dT} \quad (21)$$

The excess internal energy is

$$U^* = \frac{U}{N\epsilon} - \frac{3}{2} T^* - T \cdot T^* \frac{d \ln q_{int.}}{dT} \quad (22)$$

or

$$U^* = -\frac{0.1361b(T)\theta}{1 - b(T)\theta} + 6\theta \left( \frac{1}{\omega^{*4}} - \frac{2}{\omega^{*2}} \right) \quad (23)$$

In Figures 4 and 5 the values of excess entropy and internal energy calculated by our method are compared with those of Henderson's theory and with experimental and machine - calculated data at three temperatures. Although the agreement is somewhat less satisfactory than the agreement for the values of  $PV/kT$ , it is still quite remarkable. On the contrary, Henderson's results remarkably deviate from the experimental and machine - calculated data.

The critical properties of the liquid state have been calculated from the relations

$$\left( \frac{\partial P}{\partial u} \right)_{\omega, T} = 0$$

$$\left( \frac{\partial^2 P}{\partial u^2} \right)_{\omega, T} = 0 \quad (24)$$

and they are provided in Table III. In the above table we also provide the experimental data of Argon<sup>16</sup>, the molecular dynamics results of Verlet<sup>17</sup> and the results of Henderson's theory. It can be seen that the agreement of our results is quite satisfactory especially with Verlet's results.

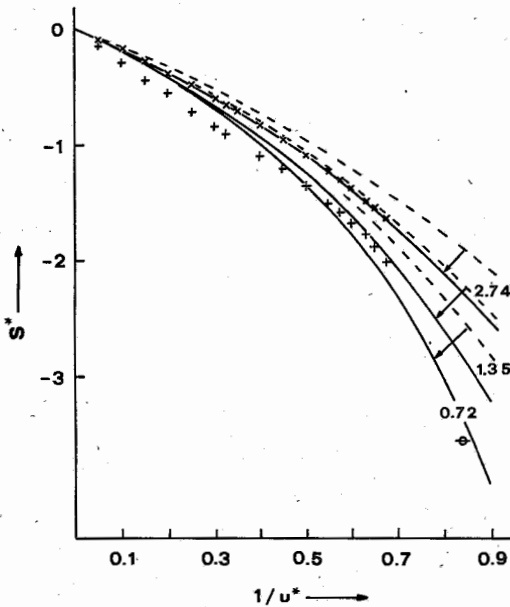


FIG. 4. Internal entropy for 6:12 potential. The curves are isotherms and are labeled with the appropriate value of  $T^*$ . The solid curves are calculated from Eq.(19) while the broken curves are the results of Henderson. The points given by  $x$ ,  $+$  and  $\odot$  are experimental values for  $T^* = 2.74$ ,  $1.35$  and  $0.72$ , respectively. See Fig. 8 of Ref (8) for the data references.

TABLE III. Critical constants for the 6:12 potential

	Present calc.	Henderson	Verlet <sup>a</sup>	Exptl (Argon) <sup>b</sup>
$T^*_c$	1.37	1.42	1.32 - 1.36	1.26
$1/u^*_c$	0.28	0.29	0.32 - 0.36	0.316
$P^*_c$	0.14	0.14	0.13 - 0.17	0.117
$\theta_c$	0.30	0.32		$\sim 0.5$
$(P^*_c u^*_c / T^*_c)$	0.37	0.33	0.30 - 0.36	0.293

a. Reference (17)

b. Reference (18)



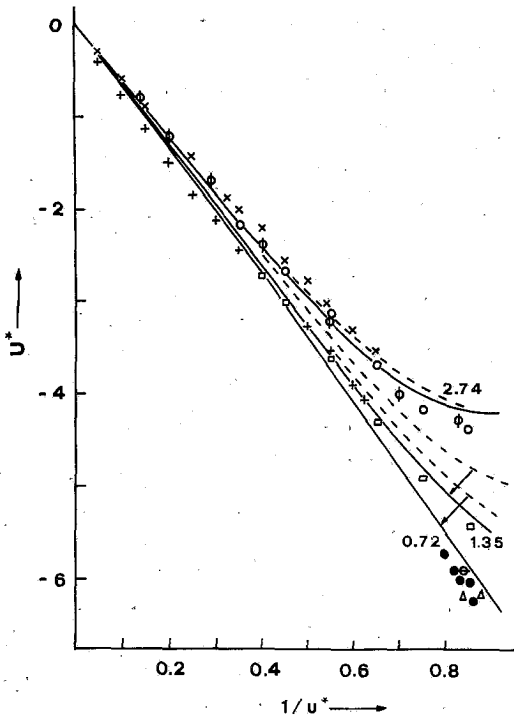


FIG. 5. Internal energy for 6:12 potential. The curves are isotherms and are labeled with the appropriate values of  $T^*$ . The solid curves are calculated from Eq.(23) while the broken curves are the results of Henderson. The points  $\circ$  are machine - calculated data for  $T^*=2.74$ . The points given by  $\square$  and  $\Delta$  are machine - calculated values for  $T^*=1.35$  and  $0.72$ , respectively. The points shown by  $x$ ,  $+$ , and  $\oplus$  are experimental values for  $T^*=2.74, 1.35$  and  $0.72$  respectively. See Fig. 9 of Ref.(8) for the data references.

### III. Liquid - vapor phase transition

Since the hole theory of the liquid state in the form which is developed in the previous section describes not only the liquid region but also the dense gas region, it is expected to give a good prediction for the liquid - vapor transition.

When two phases are at equilibrium, the temperatures, the pressures and the chemical potentials of them must be equal. Then the phase equilibria properties are found by solving the following system of two equations at a given temperature to obtain  $1/u_l$  and  $1/u_g$  i.e. the densities of the coexisting liquid and vapor respectively:

$$\begin{aligned}
 P_l &= P_g \\
 (A+PV)_l &= (A+PV)_g
 \end{aligned}
 \tag{25}$$

Pressures  $P_l, P_g$  can be calculated from Eq.(9) while the Helmholtz free energies  $A_l$  and  $A_g$  are determined from Eq.(7).

At a given temperature Eqs.(25) are equivalent to a system of two equations with four unknowns namely  $1/u_l, 1/u_g, \omega_l$  and  $\omega_g$ . Therefore for the solution of the

above system an additional relationship for  $\omega$  is necessary. This relationship is the Eq.(11).

An approximate solution for this system can be obtained by plotting the quantity  $A'' = [A / NkT + \ln(\lambda^3/2 \cdot \sigma^3 \cdot q_{int.})]$ , at a given temperature, as a function of the reduced volume  $v^*$  (see Fig. 6). The volumes at the points of common tangency are the reduced volumes of the corresponding phases and the pressure is given by the slope of the tangent.

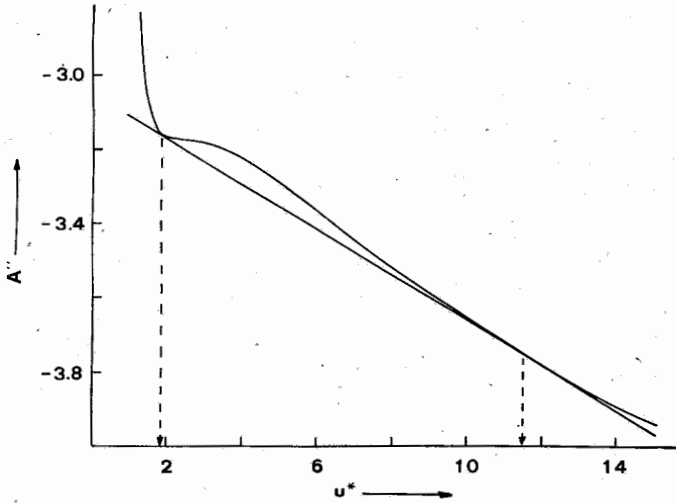


FIG. 6. Dependence of  $A'' = [A/NkT + \ln(\lambda^3/2 \cdot \sigma^3 \cdot q_{int.})]$  on the reduced volume  $v^*$  at  $T^* = 1.2$ .

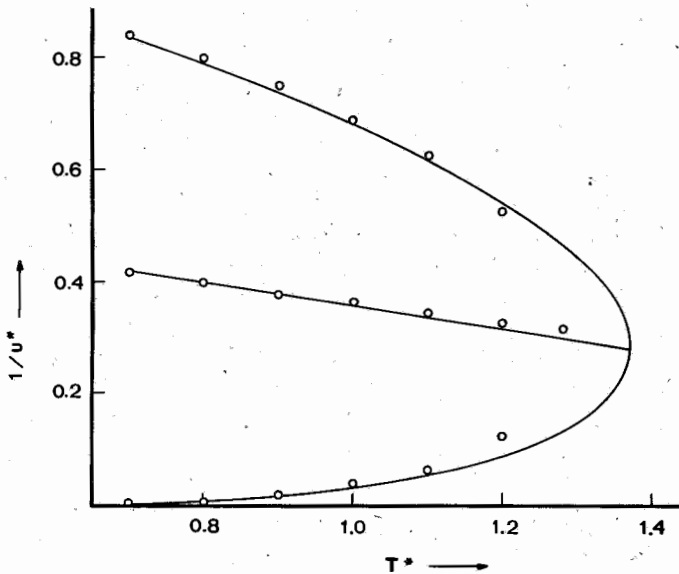


FIG. 7. Rectilinear diameters plot. The curve gives the results of the solution of the system of Eqs.(25), based upon the Helmholtz free energy calculated from Eq.(7). The points are experimental values which are calculated from the empirical formulas of Guggenheim.<sup>20</sup>

The approximate solutions obtained from these diagrams were used as initial values for the numerical solution of the system of Eqs.(25). The results of coexisting phases are shown in Figures 7-10.

The values of densities of the two coexisting phases are given in Fig. 7 in a rectilinear diameters plot and they are compared with the experimental values of Argon. The agreement is quite good except in the neighborhood of the critical point. The calculated slope of the rectilinear diameter is  $-0.210$ , while the experimental slope is<sup>3</sup>  $-0.186$ .

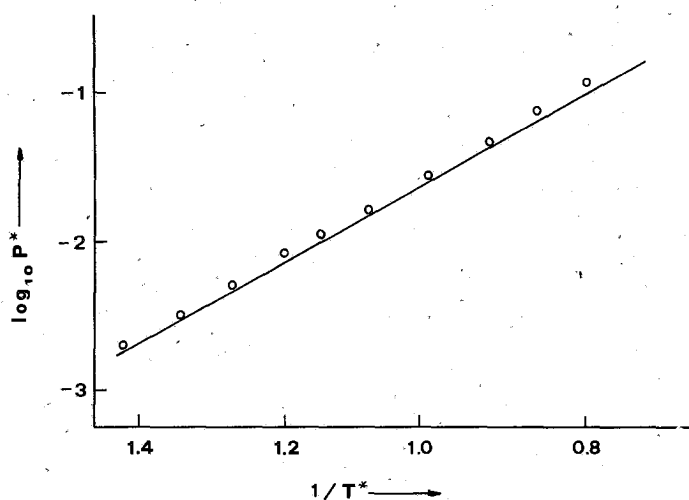


FIG. 8. Reduced vapor pressures for the 6:12 potential. The curve gives the results of Eq.(9) and the points are experimental values taken from Ref.(18).

The calculated values of the reduced vapor pressure,  $P^* = P \cdot \sigma^2 / \epsilon$ , are compared in Fig. 8 with the experimental values. The calculated logarithm of  $P^*$  varies linearly with  $1/T^*$  and this function can be represented by

$$\log_{10} P^* = 1.19 - \frac{2.79}{T^*} \quad (26)$$

The experimental relation between  $\log_{10} P^*$  and  $1/T^*$  is<sup>3</sup>

$$\log_{10} P^* = 1.29 - \frac{2.84}{T^*} \quad (27)$$

while Henderson's theory gives

$$\log_{10} P^* = 1.00 - \frac{2.62}{T^*} \quad (28)$$

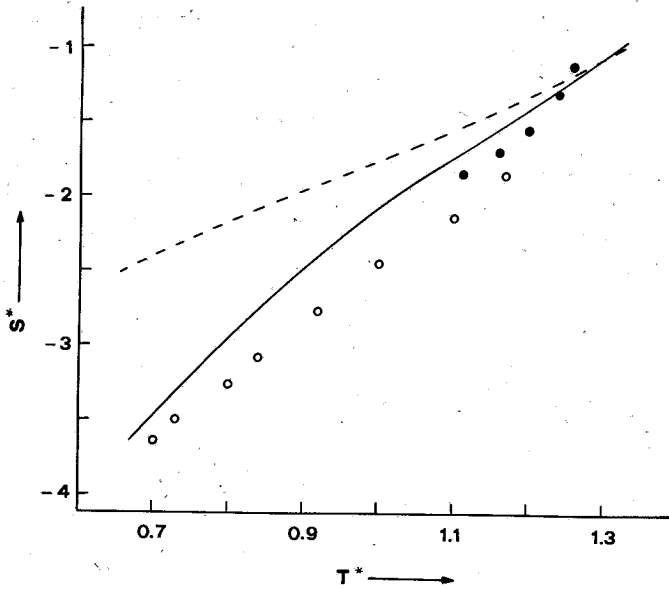


FIG. 9. Internal entropy at saturated vapor pressure for 6:12 liquid vs temperature. The solid curve is from Eq.(19) with the theoretical liquid densities as calculated from Eqs.(25). The broken curve gives the results of Henderson. The points  $\bullet$  and  $\circ$  are experimental data from two different sources. See Fig. 10 of Ref.(8) for the data references.

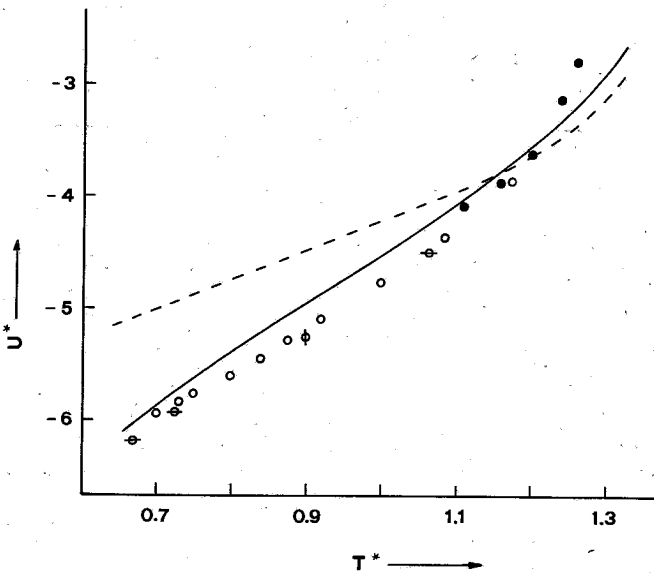


FIG. 10. Internal energy at saturated vapor pressure for 6:12 liquid vs temperature. The solid curve is from Eq. (23) with the theoretical liquid densities as calculated from Eqs.(25). The broken curve gives the results of Henderson. The points  $\phi$  and  $\odot$  are machine calculated data, while points  $\bullet$  and  $\circ$  are experimental data from two different sources. See Fig. 11 of Ref.(8) for the data references.

The excess entropy and the excess internal energy for the liquid in equilibrium with its vapor at various temperatures are plotted in Figs. 9 and 10, respectively. Although the agreement between the present calculations and the experimental values is more qualitative than quantitative, there is a remarkable improvement in relation to the results of the previous hole theories.

#### IV. Discussion

The above comparisons and results reveal that the present method of the hole theory leads to quite satisfactory results for the overall temperature range from liquid to gaseous state. The good agreement of the theoretical values of the internal thermodynamic functions with experimental and machine - calculated data indicates that even at low temperatures the temperature dependence of the free volume, Eq.(6), is also predicted to a quite satisfactory degree.

However, our attention must be focused to a critical point of this theory. The hole theory is a lattice theory. In this kind of theories the successful description of a phenomenon does not depend only on the choice of the appropriate approximations, but also on the elimination of the errors introduced by these approximations. In the present method it must be pointed out that the minimization of the free energy leads to very small values for the volume of the lattice cells. This is in agreement with the assumption that each cell contains at most one molecule but in anyway it does not agree with the approximation of the free volume Eq. (6)<sup>5,21</sup> as in the case of Henderson's theory. If we improve the random approximation and incorporate the effect of nonnearest - neighbour interactions into the hole theory, then it is possible for our method to give a more realistic expression of the free volume.

As it was mentioned earlier, lattice theories can effectively be applied to the study of problems of much more complex nature. The properties of binary liquid mixtures as well as other properties of liquids, such as the melting process and surface tension are subject to further investigation, currently carried out in our laboratory.

#### Περίληψη

*Μελέτη της υγρής καταστάσεως και της ισορροπίας μεταξύ αερίου και υγρής φάσεως με μία νέα προσεγγιστική μέθοδο της θεωρίας όπών.*

Η επιτυχής περιγραφή των φαινομένων της υγρής καταστάσεως με τις θεωρίες όπών εξαρτάται από την κατάλληλη έκλογή του ελεύθερου όγκου κινήσεως των μορίων του υγρού. Στην εργασία αυτή προσδιορίζεται μία νέα αναλυτική έκφραση για τον ελεύθερο όγκο από την σύγκριση πειραματικών με θεωρητικές ισόθερμες. Ο αναλυτικός καθορισμός της συναρτήσεως κατανομής του συστήματος στηρίχθηκε στην υπόθεση της υπάρξεως τυχαίας κατανομής μορίων και όπών στο όλο σύστημα.

Ἡ καταστατική ἐξίσωση καὶ οἱ ἐσωτερικὲς θερμοδυναμικὲς συναρτήσεις πού λαμβάνονται ἀπὸ τὴ συνάρτηση κατανομῆς πού προέκυψε ἐλέγχονται μὲ πειραματικὰ δεδομένα καθὼς καὶ μὲ δεδομένα μηχανῆς (Monte - Carlo καὶ μοριακῆς δυναμικῆς).

Ἡ συμφωνία μεταξύ θεωρητικῶν καὶ πειραματικῶν δεδομένων εἶναι σ' ὅλες τὶς περιπτώσεις ἐξαιρετικὴ καὶ ἀποδεικνύει ὅτι ἡ μέθοδος αὐτὴ ὀδηγεῖ σὲ πῶς ἱκανοποιητικὰ ἀποτελέσματα ἀπὸ τὶς προηγούμενες θεωρίες ὅπων σ' ὅ,τι ἀφορᾷ τὴν περιγραφή τῶν ιδιοτήτων τῆς ὑγρῆς καταστάσεως καθὼς καὶ τῆς θερμοδυναμικῆς ἰσορροπίας μεταξύ ὑγρῆς φάσεως καὶ τῶν ἀτμῶν μιᾶς οὐσίας. Ἐπίσης τὰ θεωρητικὰ ἀποτελέσματα πού λαμβάνονται εἶναι στὶς περισσότερες περιπτώσεις παραπλήσια μὲ τὰ ἀποτελέσματα τῶν κυριότερων νέων θεωρητικῶν ἀπόψεων γιὰ τὴν ὑγρὴ κατάσταση.

## References and Notes

1. Barker, J.A.: *Lattice Theories of the Liquid State*, Pergamon Press 1963.
2. Rowlinson, J.S. & Curtiss, C.F.: *J. Chem. Phys.* **19**, 1519 (1951).
3. Henderson, D.: *J. Chem. Phys.* **37**, 631 (1962); **39**, 54 (1963).
4. McLellan, A.G.: *J. Chem. Phys.* **40**, 567 (1964).
5. Blomgren, G.E.: *J. Chem. Phys.* **34**, 1307 (1961); **38**, 1714 (1963).
6. Fukuda, Y. & Kobayashi, R.: *J. Chem. Phys.* **46**, 2661 (1967).
7. See ref. 8 for data sources.
8. Barker, J.A. & Henderson, D.: *J. Chem. Phys.* **47**, 4714 (1967).
9. Weeks, J.D., Chandler, D. & Andersen, H.C.: *J. Chem. Phys.* **54**, 5237 (1971); **55**, 5422 (1971).
10. Mansoori, J.A. & Canfield, F.B.: *J. Chem. Phys.* **51**, 4958 (1969).
11. Rasaiah, J.C. & Stell, G.: *Mol. Phys.* **18**, 249 (1970); *Chem. Phys. Lett.* **4**, 651 (1970).
12. Barker, J.A. & Henderson, D.: *Reviews of Modern Physics*, **48**, 587 (1976).
13. Michels, A., Wijker, H. & Wijker, H.: *Physica* **15**, 627 (1949).
14. Michels, A., Levett, J.M. & Wolkers, G.J.: *Physica* **24**, 769 (1958).
15. Levett, J.M.: *Physica* **26**, 361 (1960).
16. Michels, A. & Goudeked, M.: *Physica* **8**, 347 (1941).
17. Verlet, L.: *Phys. Rev.* **159**, 98 (1967).
18. Rowlinson, J.S.: *Liquids and Liquid Mixtures*, Butterworth & Co. Publishers Ltd., London, (1969).
19. Barker, J.A. Leonard, P.J. & Pompe, A.: *J. Chem. Phys.* **44**, 4206 (1966).
20. Guggenheim, E.A.: *J. Chem. Phys.* **13**, 253 (1945).
21. Weissmann, M.: *J. Chem. Phys.* **40**, 175 (1964).

## APPLICATION OF A NEW APPROXIMATE METHOD OF THE HOLE THEORY TO BINARY LIQUID MIXTURES

D.A. JANNAKOUDAKIS and P.J. NIKITAS

*Laboratory of Physical Chemistry, Faculty of Physics & Mathematics, University of Thessaloniki (Greece).*

(Received February 17, 1981).

### Summary

The method of the hole theory proposed earlier for the calculation of the equilibrium thermodynamic properties of simple pure fluids, is extended to binary mixtures of simple fluids. It is assumed that the constituents are spherical molecules having the same size but different fields of interaction and that the holes and molecules are randomly distributed within the system. Calculated excess Gibbs energies, enthalpies and volumes are in a quite satisfactory agreement with experimental data, for seven binary systems containing simple nonpolar molecules.

**Key words:** Lattice statistics, Hole theory, Liquid mixtures.

### I. Introduction

The statistical thermodynamics of solutions has been one of the most interesting problems in physical chemistry. A large number of qualitative and quantitative theories have been proposed to predict the properties of solutions, when a knowledge of the respective properties of pure components is available.

This paper continues our previous work<sup>1</sup> on liquid state phenomena. The hole theory in the form given in Ref.(1) leads to good results for all the thermodynamic properties of liquid state. In the present work, the hole theory of pure systems is extended to binary mixtures of simple fluids. The thermodynamic excess properties of mixed systems are calculated and the results are compared with experimental data taken from the literature. Finally the results are compared with data obtained from other theories of liquid mixtures.

## II. Theory

### a. General relations.

Before proceeding to the extension of the hole theory of pure simple liquids to binary liquid mixtures it is necessary to know the general relations which apply to a closed system, having its  $N$  molecules arranged in space according to a definite lattice structure. In this system we also assume that each molecule occupies only one lattice site. The sites may be considered as points or generally as cells, which centres form a regular lattice.

If the system is composed of  $n$  components, then the  $L=N$  lattice sites are occupied by  $N_1$  molecules of type 1,  $N_2$  molecules of type 2, ...,  $N_n$  molecules of type  $n$  and therefore we have:

$$N = N_1 + N_2 + \dots + N_n \quad (1)$$

We let  $N_{ij}$  be the number of the nearest-neighbour pairs of sites composed of one molecule of type  $i$  and one molecule of type  $j$ . If  $w_{ij}$  is the interaction energy between a pair of nearest-neighbouring molecules, namely  $i$  and  $j$ , then the total lattice energy is given by

$$E_{\text{lat.}} = \sum_{ij} N_{ij} w_{ij} \quad (2)$$

assuming that interactions between non nearest-neighbour molecules can be ignored (nearest-neighbour lattice statistics).

For an arbitrary lattice, we have

$$cN_i = 2N_{ii} + N_{i1} + N_{i2} + \dots + N_{i(i-1)} + N_{i(i+1)} + \dots + N_{in} \quad (3)$$

$$\text{or } N_{ii} = \frac{1}{2} c N_i - \frac{1}{2} (N_{i1} + N_{i2} + \dots + N_{in}) \quad (4)$$

where  $c$  is the number of the nearest-neighbour sites surrounding a given site. Therefore

$$E_{\text{lat.}} = \sum_i U_i + \sum_{i < j} N_{ij} w^{ij} \quad (5)$$

$$\text{where } U_i = \frac{1}{2} c N_i w_{ii} \quad (6)$$

$$\text{and } w^{ij} = w_{ij} - \frac{1}{2} (w_{ii} + w_{jj}) \quad (7)$$

The partition function of the  $i$ th molecule is

$$q_i = (q_{\text{int.}})_i \cdot (q_{\text{tr.}})_i \cdot \exp\left(-\frac{E_{\text{lat.}}}{NkT}\right) \quad (8)$$



where  $q_{int.}$  and  $q_{tr.}$  are the internal and the translational partition functions of this molecule, respectively. The canonical ensemble partition function can be obtained by multiplying  $q_i$  and adding over all permissible arrangements of the  $N$  molecules

$$Q = \sum_{\langle N \rangle} \prod_i q_i \tag{9}$$

Assuming that the internal degrees of freedom do not depend on the presence of other molecules in the lattice, then

$$\prod_{i=1}^N (q_{int.})_i = \prod_{j=1}^n (q_{int.})_j^{N_j} \tag{10}$$

and the general expression for the partition function  $Q$  is given by:

$$Q = \left\{ \prod_{i=1}^n (q_{int.})_i^{N_i} \right\} \cdot \exp\left(-\sum_i U_i/kT\right) \cdot \sum_{\langle N \rangle} \left( \prod_i q_{tr.} \right) \exp\left(-\sum_{i,j} N_{ij} w^{ij}/kT\right) \tag{11}$$

*b. Partition function for a binary liquid mixture on the basis of the hole theory*

The liquid mixture is regarded as a three-dimensional closed system which is composed of  $N_1$  molecules of type 1 and  $N_2$  molecules of type 2. We assume that the molecules are similar in size and we divide the volume  $V$  of the liquid mixture into  $L$  identical cells, where  $L \gg N_1 + N_2 = N$ . Furthermore, we assume that the centres of these cells follow the geometry of a regular face-centred cubic lattice and that each molecule moves in its own cell under the influence of the field of its nearest-neighbouring molecules. The cells are considered to be so small that the number of molecules per cell can be either one or zero.

To determine the partition function of this system according to the hole theory, as it has been developed in Ref.(1), and accounting for our conclusions of the previous section, we consider the empty cells as being the third component of the mixture. Then, from Eq.(11) we have

$$Q = q_{int.1}^{N_1} q_{int.2}^{N_2} \cdot \exp\left(-\frac{U_1 + U_2}{kT}\right) \cdot \sum_{\langle N \rangle} \left( \prod_{i=1}^n q_{tr.i} \right) \cdot \exp\left(-\frac{N_{12} w^{12} + N_{13} w^{13} + N_{23} w^{23}}{kT}\right) \tag{12}$$

because  $q_{int.3} = q_{tr.3} = 0$

and  $w_{33} = 0$

If  $v_{hi}$  is the free volume of the  $i$ th molecule of type 1, ( $i = 1, 2$ ), then

$$q_{tr.1i} = \lambda_1^{3/2} \cdot v_{f1i} \quad (13)$$

Furthermore, assuming that holes and molecules are randomly distributed in the mixture, the sum in Eq.(12) can be determined by the Bragg-Williams approximation, which yields

$$Q = \frac{L!}{N_1! N_2! (L-N)!} \cdot q_{int1}^{N_1} q_{int2}^{N_2} \exp\left(-\frac{U_1+U_2}{kT}\right) \cdot \lambda_1^{3N_1/2} \cdot \lambda_2^{3N_2/2} \cdot v_{f1}^{N_1} \cdot v_{f2}^{N_2} \exp\left(-\frac{\bar{N}_{12}w^{12} + \bar{N}_{13}w^{13} + \bar{N}_{23}w^{23}}{kT}\right), \quad (14)$$

$$\begin{aligned} \text{where } \bar{N}_{12} &= c N_1 N_2 / L \\ \bar{N}_{13} &= c N_1 N_3 / L \\ \bar{N}_{23} &= c N_2 N_3 / L \end{aligned} \quad (15)$$

Since  $w^{13} = -w_{11}/2$   
and  $w^{23} = -w_{22}/2$   
because  $w_{13} = w_{23} = w_{33} = 0$

it follows that

$$U_1 + U_2 + \bar{N}_{12}w^{12} + \bar{N}_{13}w^{13} + \bar{N}_{23}w^{23} = \frac{cN\theta}{2} \{ x_1^2 w_{11} + x_2^2 w_{22} + 2x_1 x_2 w_{12} \} \quad (16)$$

where  $\theta = N/L = \omega/v$ ,  $\omega = V/L$ ,  $v = V/N$ ,

and  $x_i = N_i/N$   $i=1,2$ .

If we assume that the interaction energy between a pair of molecules, namely  $i$  and  $j$ , can be satisfactorily represented by the Lennard-Jones 6:12 potential, then we have

$$w_{ij} = u_{ij}(\alpha) = 4\epsilon_{ij} \left\{ (\sigma_{ij}/\alpha)^{12} - (\sigma_{ij}/\alpha)^6 \right\} \quad (17)$$

where  $\alpha$  is the nearest-neighbour distance.

The parameters  $\epsilon_{11}$ ,  $\epsilon_{22}$ ,  $\sigma_{11}$  and  $\sigma_{22}$  are determined from the properties of the pure components. The common mixing rule for the collision diameters of unlike pairs is that given by the hard-sphere model i.e.

$$\sigma_{12} = \frac{1}{2} (\sigma_{11} + \sigma_{22}) \quad (18)$$

The usual mixing rule for the energy parameter  $\epsilon_{12}$  in the pair potential is

$$\epsilon_{12} = \epsilon_{12} (\epsilon_{11} \epsilon_{22})^{1/2}, \quad (19)$$

where  $\xi_{12}$  is an essentially empirical factor used to correct any deviations from the geometric mean. Although several theoretical treatments have been proposed for the calculation of mixed interaction energies they all involve assumptions which are difficult to justify. Here, for comparison purposes with the experimental data, we employ the practice of previous theories,<sup>2,3</sup> and we use  $\xi_{12}$  as an adjustable parameter.

If we introduce Eq.(17) into Eq.(16), we have

$$U_1 + U_2 + \bar{N}_{12} W^{12} + \bar{N}_{13} W^{13} + \bar{N}_{23} W^{23} = \frac{CN\theta}{2} \{ 4\langle \epsilon \rangle [ (\frac{\langle \sigma \rangle}{\alpha})^{12} - (\frac{\langle \sigma \rangle}{\alpha})^6 ] \} = \frac{N\theta}{2} \varphi(0) \quad (20)$$

where the average constants  $\langle \epsilon \rangle$  and  $\langle \sigma \rangle$  are functions of the Lennard-Jones constants for the individual types of molecular pairs and the mole fractions of the components:

$$\langle \epsilon \rangle = \frac{(x_1^2 \epsilon_{11} \sigma_{11}^6 + x_2^2 \epsilon_{22} \sigma_{22}^6 + 2x_1 x_2 \epsilon_{12} \sigma_{12}^6)^2}{x_1^2 \epsilon_{11} \sigma_{11}^{12} + x_2^2 \epsilon_{22} \sigma_{22}^{12} + 2x_1 x_2 \epsilon_{12} \sigma_{12}^{12}} \quad (21)$$

$$\langle \sigma \rangle = \left( \frac{x_1^2 \epsilon_{11} \sigma_{11}^{12} + x_2^2 \epsilon_{22} \sigma_{22}^{12} + 2x_1 x_2 \epsilon_{12} \sigma_{12}^{12}}{x_1^2 \epsilon_{11} \sigma_{11}^6 + x_2^2 \epsilon_{22} \sigma_{22}^6 + 2x_1 x_2 \epsilon_{12} \sigma_{12}^6} \right)^{1/6} \quad (22)$$

while  $\varphi(0)$  is given by

$$\varphi(0) = 12\langle \epsilon \rangle [ (1/\omega^*)^4 - 2(1/\omega^*)^2 ] \quad (23)$$

because  $\alpha^3 = \sqrt{2} \cdot \omega$ , and  $\omega^* = \omega / \langle \sigma \rangle^3$ .

By assuming a random distribution, things are markedly simplified. We considered all cells as equivalent and instead of  $v_{11}^{N_1} \cdot v_{12}^{N_2}$  in Eq.(14), we use a single free volume  $\langle v_f \rangle^N$  (one fluid model) which is given by

$$\langle v_f \rangle = \omega [1 - b(T)\theta] \quad (24)$$

$$b(T) = 1.1718 \cdot \exp(-0.1361/T^*)$$

where  $T^* = kT / \langle \epsilon \rangle$ .

From Eqs.(14), (20) and (24), the complete expression for the canonical ensemble partition function, by the single free volume approximation, is the following:

$$Q = \frac{L!}{N_1! N_2! (L-N)!} q_{\text{int},1}^{N_1} q_{\text{int},2}^{N_2} \lambda_1^{3N_1/2} \lambda_2^{3N_2/2} \langle v_f \rangle \cdot \exp\left(-\frac{N\theta\phi(0)}{2kT}\right) \quad (25)$$

$$\begin{aligned} \text{or} \quad N^{-1} \ln Q &= \left(1 - \frac{1}{\theta}\right) \ln(1 - \theta) - \ln\theta + \ln\langle v_f \rangle - \frac{\theta\phi(0)}{2kT} \\ &\quad - x_1 \ln x_1 - x_2 \ln x_2 + x_1 \ln \Lambda_1 + x_2 \ln \Lambda_2 \end{aligned} \quad (26)$$

$$\text{where} \quad \Lambda_1 = \lambda_1^{3/2} \cdot q_{\text{int},1} \quad (27)$$

### c. Thermodynamic Functions.

Once the partition function has been formulated the thermodynamic properties of a liquid mixture can be calculated by using the equations of the statistical thermodynamics.

Therefore:

The Helmholtz free energy is given by

$$\begin{aligned} \frac{A}{NkT} &= \ln\theta - \left(1 - \frac{1}{\theta}\right) \ln(1 - \theta) - \ln\langle v_f \rangle + \frac{\theta\phi(0)}{2kT} + x_1 \ln x_1 + x_2 \ln x_2 \\ &\quad - x_1 \ln \Lambda_1 - x_2 \ln \Lambda_2 \end{aligned} \quad (28)$$

where the volume per cell is determined by minimizing A:

$$\left(\frac{\partial A}{\partial \omega}\right)_{v,T} = 0 \quad (29)$$

The equation of state is calculated from

$$\frac{PV}{NkT} = \frac{b(T) \cdot \theta}{1 - b(T) \cdot \theta} - \frac{1}{\theta} \ln(1 - \theta) + \frac{6\theta\epsilon}{kT} \left(\frac{1}{\omega^{*4}} - \frac{2}{\omega^{*2}}\right) \quad (30)$$

From Eqs.(28), (29) and (30) the free energy A is determined as a function of P,T,N and  $x_1$ .

The internal energy of the liquid mixture is calculated from Eq.(28) and the relation

$$U = -T^2 \left( \frac{\partial A/T}{\partial T} \right)_{\omega, \nu}$$

$$U = \frac{3}{2}RT - \frac{0.1361b(T)\theta R\langle \epsilon \rangle}{1 - b(T)\theta} + \frac{6\theta\langle \epsilon \rangle}{k} \left( \frac{1}{\omega^{*4}} - \frac{2}{\omega^{*2}} \right) + R \cdot T^2 \frac{d \ln q_{int}}{dT} \quad (31)$$

The excess properties of a mixture are defined as the difference between the thermodynamic functions of mixing for a real solution in excess of those for an ideal solution. Some of the excess properties needed in our calculations are provided below

$$\bar{A}^E = A - (x_1 A_1^0 + x_2 A_2^0) - RT (x_1 \ln x_1 + x_2 \ln x_2)$$

$$U^E = U - (x_1 U_1^0 + x_2 U_2^0) \quad (32)$$

$$V^E = V - (x_1 V_1^0 + x_2 V_2^0)$$

where the superscript 0 corresponds to pure components. To calculate the excess properties, the thermodynamic functions of the pure components have been taken from Ref.(1).

Because in most cases the mixing process is considered to take place under constant pressure, the differences between the configurational enthalpy and energy, or between the configurational Helmholtz and Gibbs energies, are negligible.

Therefore we have

$$U^E = H^E \quad \text{and} \quad A^E = G^E \quad (33)$$

### III. Results and Discussion

The fundamental assumptions of the hole theory impose certain restrictions to the choice of the experimental system which could be used for a reasonable test of this theory. The liquid mixtures must be composed of spherical molecules of equal size, interacting with isotropic field forces. The mixtures Ar-O<sub>2</sub> and N<sub>2</sub>-CO with  $\sigma_{Ar} / \sigma_{O_2} = 1.005$  and  $\sigma_{N_2} / \sigma_{CO} = 0.993$  are considered as the most satisfactory experimental systems in what concerns the fulfillment of these requirements. Additionally, the systems CO-CH<sub>4</sub>, Kr-CH<sub>4</sub>, Ar-N<sub>2</sub>, Ar-CO, and N<sub>2</sub>-O<sub>2</sub>, although they are less satisfactory, they can be used for the test of the hole theory.

In order to be consistent with the other theories of mixtures<sup>2,3</sup> the calculation of the excess properties, reported in this paper, involve the potential parameters listed in table I. For Argon we use<sup>4</sup>  $\epsilon/k = 119.8$  K and  $\sigma = 3.405$  Å.

TABLE I. Potential parameters for pure substances

Substance	$\epsilon/\epsilon$ (argon)	$\sigma/\sigma$ (argon)
argon	1.000	1.000
krypton	1.387	1.070
nitrogen	0.836	1.063
oxygen	1.022	0.995
carbon monoxide	0.881	1.070
methane	1.266	1.099

In table II we compare the calculated and experimental excess properties of the equimolar mixtures, for the above systems at zero pressure. The adjustable parameter  $\xi_{12}$  was chosen in order to give the best agreement with the data of the excess Gibbs energy and was then used for the calculation of the other excess properties. In table II, the mixtures have been arranged at an order of increasing values of the

TABLE II. Comparison of theory and experiment ( $\xi_{12}$  adjusted) at  $P=0$  and  $x_1=x_2=1/2$ 

	$\xi_{12}$	$G^E$ J.mol. <sup>-1</sup>	$H^E$ J.mol. <sup>-1</sup>	$V^E$ cm <sup>3</sup> .mol <sup>-1</sup>
Ar-O <sub>2</sub> T= 84 K $\sigma_{Ar}/\sigma_{O_2} = 1.005$				
Experimental data <sup>a</sup>	0.99	37	60	0.14
vdW (a) <sup>b</sup>	0.978	37	50	0.12
vdW (b) <sup>d</sup>	0.978	37	50	0.12
G (b) <sup>b</sup>	0.987	37	59	0.09
APM <sup>c</sup>	0.989	36	55	0.14
Perturbation <sup>b</sup>	0.987	37	51	0.07
Present Calc.	0.988	37	59	0.08
CO-N <sub>2</sub> T=84 K $\sigma_{CO}/\sigma_{N_2} = 1.007$				
Experimental data <sup>c</sup>	0.99	23	--	0.13
vdW (a) <sup>b</sup>	0.983	23	34	0.16
vdW (b) <sup>b</sup>	0.983	23	35	0.17
G (b) <sup>b</sup>	0.989	23	40	0.12
APM				
Perturbation <sup>d</sup>	0.990	23	33	0.07
Present Calc.	0.991	23	38	0.10

TABLE II.- continued

	$\xi_{12}$	$G^E$ J.mol. <sup>-1</sup>	$H^E$ J.mol. <sup>-1</sup>	$V^E$ cm <sup>3</sup> .mol <sup>-1</sup>
<b>CH<sub>4</sub> - K    T= 116 K    <math>\sigma_{CH_4}/\sigma_K = 1.027</math></b>				
Experimental data <sup>f</sup>	--	29	55	± 0.01
vdW (a) <sup>f</sup>	1.00	21	25	- 0.14
vdW (b) <sup>f</sup>	1.00	15	17	- 0.11
G (b) <sup>f</sup>	1.00	18	22	- 0.03
APM <sup>f</sup>	1.00	38	56	+ 0.01
Perturbation <sup>d</sup>				
Present Calc.	1.00	32	50	+ 0.01
vdW (a) <sup>f</sup>	0.998	29	36	- 0.13
vdW (b) <sup>f</sup>	0.997	29	36	- 0.09
G (b) <sup>f</sup>	0.998	29	36	- 0.02
APM <sup>f</sup>	0.998	52	--	+ 0.03
Present Calc.	1.001	29	45	+ 0.01
<b>CO-CH<sub>4</sub>    T=91 K    <math>\sigma_{CH_4}/\sigma_{CO} = 1.027</math></b>				
Experimental data <sup>b</sup>	1.00	115	108	- 0.32
vdW (a) <sup>b</sup>	0.957	115	105	- 0.52
vdW (b) <sup>b</sup>	0.957	115	119	- 0.25
G (b) <sup>b</sup>	0.988	115	114	- 0.50
APM <sup>c</sup>	0.994	112	105	- 0.31
Perturbation <sup>d</sup>	0.983	115	92	- 0.51
Present Calc.	1.004	115	137	- 0.33
<b>N<sub>2</sub>-Ar    T=84 K    <math>\sigma_{N_2}/\sigma_{Ar} = 1.063</math></b>				
Experimental data <sup>b</sup>	1.00	34	51	- 0.18
vdW (a) <sup>b</sup>	0.991	34	38	- 0.29
vdW (b) <sup>b</sup>	0.987	34	40	- 0.18
G (b) <sup>b</sup>	0.997	34	41	- 0.26
APM <sup>c</sup>	1.054	35	45	- 0.20
Perturbation <sup>d</sup>	0.999	34	30	- 0.33
Present Calc.	1.027	33	52	- 0.11

TABLE II. - continued

	$\xi_{12}$	$G^E$ J.mol. <sup>-1</sup>	$H^E$ J.mol. <sup>-1</sup>	$v^E$ cm <sup>3</sup> .mol. <sup>-1</sup>
N <sub>2</sub> -O <sub>2</sub> T=78 K $\sigma_{N_2}/\sigma_{O_2} = 1.068$				
Experimental data <sup>i</sup>	--	42	44	- 0.21
vdW (a) <sup>d</sup>	1.003	42	41	- 0.34
vdW (b)				
G (b)				
APM <sup>c</sup>	1.009	47	47	- 0.20
Perturbation <sup>d</sup>	0.999	42	36	- 0.34
Present Calc.	1.032	42	65	- 0.10
Ar-CO    T=84 K $\sigma_{CO}/\sigma_{Ar} = 1.07$				
Experimental data <sup>i</sup>	0.99	57	--	+ 0.10
vdW (a) <sup>b</sup>	0.971	57	79	+ 0.00
vdW (b) <sup>b</sup>	0.968	57	79	+ 0.06
G (b) <sup>b</sup>	0.983	57	90	- 0.03
APM				
Perturbation <sup>d</sup>	0.985	57	71	- 0.15
Present Calc.	1.020	57	102	+ 0.24

a. Ref.(5),(6); b. Ref.(7); c. Ref.(8); d. Ref.(3); e. Ref.(6); f. Ref.(9); g. Ref.(10),(11),(12); h. Ref.(5); i. Ref.(6); j. Ref.(5),(13).

difference  $(1-\sigma_{11}/\sigma_{22})$ . In table II are also provided the corresponding theoretical data resulting from five other theories of mixtures, thus enabling the comparison with our calculations. These theories are: The "one-fluid" (a) and "two-fluid" (b) van der Waals models<sup>2,7,15</sup>, the "two-fluid" model of Guggenheim,<sup>7,14</sup> G(b), the average potential model<sup>2,18</sup> (APM), and the perturbation theory of L.H.B.<sup>3</sup> Except from the perturbation theory which is a rigorous mathematical theory, all the other theories contain an empirical element by which experimental information is introduced into them.

The comparisons and results of table II indicate that for  $\sigma_{11} / \sigma_{22} \approx 1$  the hole theory provides a quite satisfactory picture for the liquid mixtures. However, as the difference  $(1-\sigma_{11}/\sigma_{22})$  increases, the experimental system increasingly deviates from the assumptions of the theory (especially from the random distribution assumption), and the theory fails to describe successfully these systems, as this happens with Ar-O<sub>2</sub> and N<sub>2</sub>-CO mixtures.



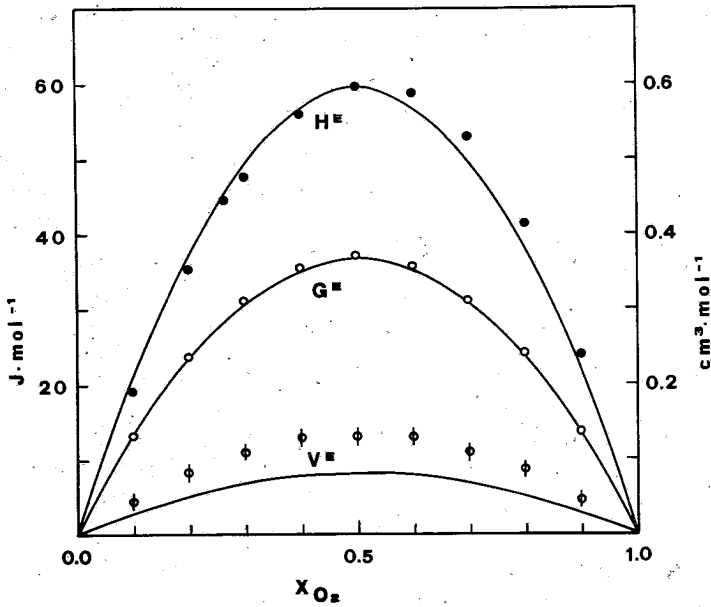


FIG. 1. Excess properties of Ar-O<sub>2</sub> at 84 K. The curves give the theoretical results and the points give the experimental results.

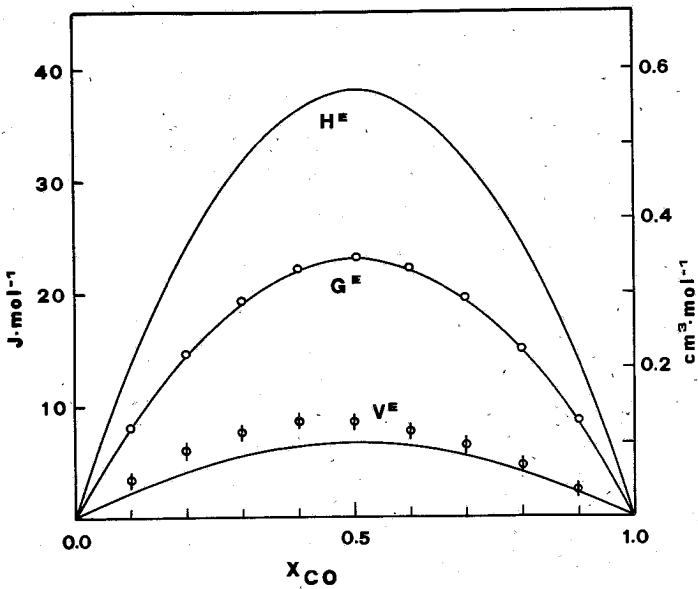


FIG. 2. Excess properties of N<sub>2</sub>-CO at 84 K. The curves give the theoretical results and the points give the experimental results.

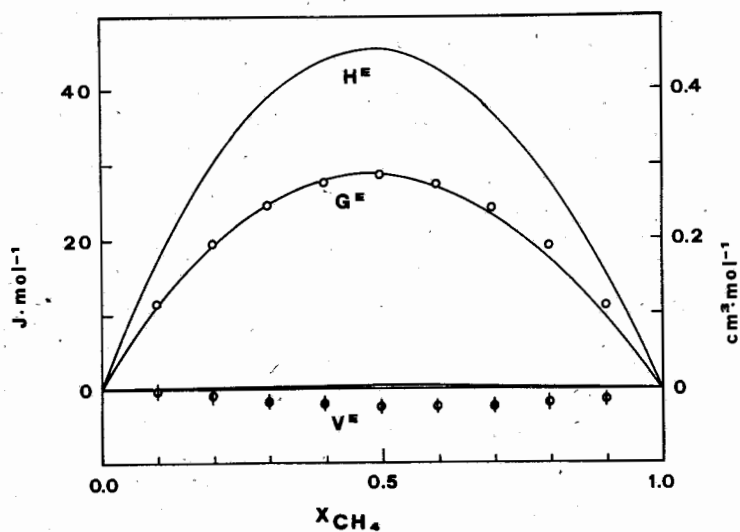


FIG. 3. Excess properties of Kr-CH<sub>4</sub> at 116 K. The curves give the theoretical results and the points give the experimental results.

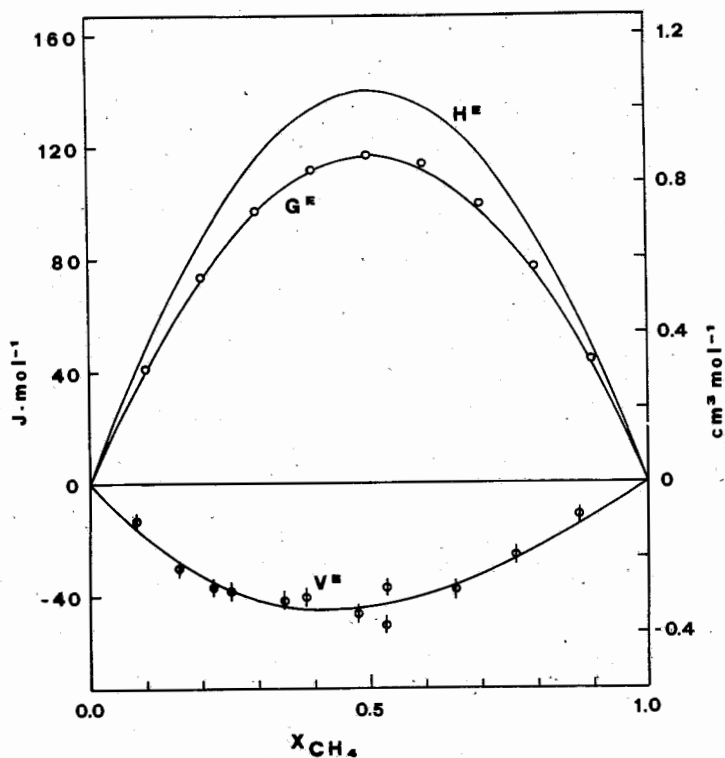


FIG. 4. Excess properties of CH<sub>4</sub>-CO at 91 K. The curves give the theoretical results and the points give the experimental results.

In figures 1-4 we have compared the calculated and experimental values of the excess Gibbs energy, the excess enthalpy and the excess volume over the entire composition range for the following systems: argon-oxygen (Figure 1), nitrogen-carbon monoxide (Figure 2), krypton-methane (Figure 3), and methane-carbon monoxide (Figure 4). From this comparison we conclude again that for  $\sigma_{11} \approx \sigma_{22}$  the hole theory provides an almost quantitative description of the liquid mixtures.

## Περίληψη

*Εφαρμογή μιᾶς νέας προσεγγιστικῆς μεθόδου τῆς θεωρίας ὁπῶν σέ ὑγρά δυαδικά μίγματα.*

Ἡ ἀναλυτικὴ συνάρτηση κατανομῆς ποῦ ἀναπτύχθηκε μέ βάση τή θεωρία ὁπῶν σέ προηγούμενη ἐργασία γιά καθαρά ἀλλά ρευστά ἐπεκτείνεται στήν ἐργασία αὐτή σά ὑγρά μίγματα. Τά συστατικά τοῦ μίγματος ὑποτίθεται ὅτι ἀποτελοῦνται ἀπό μόρια μέ ἴσες περίπου διαμέτρους, ἀλλά μέ διαφορετικά πεδία ἀλληλεπιδράσεως. Ἡ γενικευμένη συνάρτηση κατανομῆς προσδιορίζεται μέ τή βοήθεια τῆς προσεγγίσεως τῶν Bragg-Williams.

Ἀπό τή συνάρτηση κατανομῆς καί μέ τή βοήθεια τῶν θεμελιωδῶν σχέσεων τῆς Στατιστικῆς Θερμοδυναμικῆς προσδιορίζονται οἱ θεωρητικῆς σχέσεις γιά τήν ἐλεύθερη ἐνέργεια Gibbs, τήν ἐνθαλπία καί τό μοριακό ὄγκο τοῦ συστήματος.

Τά θεωρητικά ἀποτελέσματα συγκρίνονται μέ τά πειραματικά δεδομένα ἐπτά δυαδικῶν συστημάτων καί μέ τά θεωρητικά ἀποτελέσματα τῶν κυριότερων γνωστῶν θεωριῶν γιά μίγματα. Ἀπό τή σύγκριση προκύπτει τό συμπέρασμα ὅτι, ὅταν πληροῦνται ὅλες οἱ ὑποθέσεις, ἡ μέθοδος ποῦ ἀναπτύχθηκε περιγράφει ἱκανοποιητικά τίς ιδιότητες τῶν πραγματικῶν συστημάτων.

## References and Notes

1. Jannakoudakis, D.A. & Nikitas, P.J.: *Chimika Chronika*, New Series, in press.
2. Leland, T.W., Rowlinson, J.S. & Sather, G.A.: *Trans. Faraday Soc.* **64**, 1447 (1968).
3. Leonard, P.J., Henderson, D. & Barker, J.A.: *Trans. Faraday Soc.* **66**, 2439 (1970).
4. Michels, A., Wijker, H. & Wijker, Hk.: *Physica* **15**, 627 (1949).
5. Pool, R.A.H., Saville, G., Herington, T.M., Shields, B.D.C. & Staveley, L.A.K.: *Trans. Faraday Soc.* **58**, 1692 (1962).
6. Knobler, C.M., van Heijningen, R.J.J. & Beenaker, J.J.M.: *Physica* **27**, 296 (1961).
7. Marsh, K.N., McGlashan, M.L. & Warr, C.: *Trans. Faraday Soc.* **66**, 2453 (1970).
8. Bellemans, A., Mathot, V. & Simon, M.: *Adv. Chem. Phys.* **11**, 117 (1967).
9. Calado, J.C.G. & Staveley, L.A.K.: *Trans. Faraday Soc.* **67**, 1261 (1971).
10. Lambert, M. & Simon, M.: *Physica*, **28**, 1191 (1962).
11. Pool, R.A.H. & Staveley, L.A.K.: *Trans. Faraday Soc.* **53**, 1186 (1957).
12. Mathot, V., Staveley, L.A.K., Young, J.A. & Parsonage, M.G.: *Trans. Faraday Soc.* **52**, 1488 (1956).
13. Duncan, A.G. & Staveley, L.A.K.: *Trans. Faraday Soc.* **62**, 548 (1966).
14. Guggenheim, E.A.: *Mol. Phys.* **9**, 199 (1965).

# I. NEW SERIES OF N,N'-Bis(S-ALKYL-2-ETHANETHIO) ACETAMIDINES

## II. CYCLISATION OF S-ALKYL-BENZOYLAMINO-ALKYLENE-SULFIDES IN THE PRESENCE OF PHOSPHOROUS OXYCHLORIDE.

GEORGE PAPAIOANNOU and ASP. PAPADAKI-VALIRAKI.  
*Laboratory of Pharmaceutical Chemistry, University of Athens, Athens (Greece).*

(Received December 4, 1980; Revised April 22, 1981).

### Summary

A new series of N,N'-Bis(S-alkyl-2-ethanethio) acetamidines were synthesized. These derivatives were prepared by reacting equimolar quantities of S-alkyl-2-acetaminoethanesulfides and S-alkyl-2-aminoethanesulfides with phosphorous oxychloride. The same reaction when applied for the preparation of the analogous benzamidines failed to produce such compounds because cyclisation takes place. Thus, in all instances, by repeating the reaction, 2-phenyl-thiazoline and 5,6-dihydro-2-phenyl 4H-1,3-thiazine were obtained from S-alkyl-benzoylaminoethane- and propanesulfides respectively.

**Key words:** N,N'-Bis(S-alkyl-2-ethanethio) acetamidines- S-alkyl-benzoylamino-alkylene-sulfides.

### Introduction

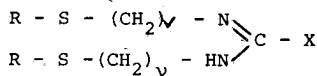
The fact that some amidines and their derivatives show various biological activities,<sup>1-3</sup> notably local anesthetic, antibacterial and antifungal, prompted the synthesis of the title amidines. It was thought that the presence of an alkyl-thio group would probably increase the antibacterial and antifungal activities.<sup>4</sup>

### Chemistry

The compounds formed correspond to the general formula I.

For the preparation of the above compounds, S-alkyl-2-aminoethanesulfides (Sch. I v=2) were used as the starting materials.

These compounds were synthesized by reacting the appropriate alkyl-mercaptans and ethylenimine<sup>5</sup>.



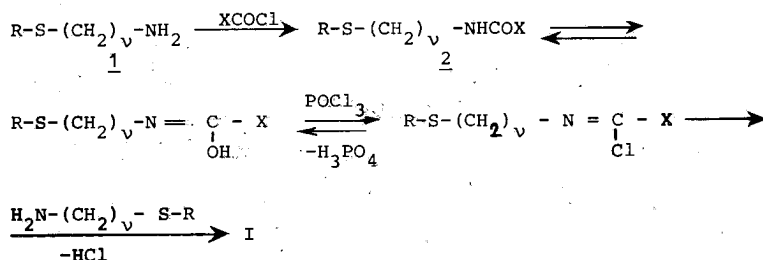
I

where R = CH<sub>3</sub>, C<sub>2</sub>H<sub>5</sub>, nC<sub>3</sub>H<sub>7</sub>, isoC<sub>3</sub>H<sub>7</sub> X=CH<sub>3</sub> v=2

The aminosulfides **1** were converted into their acetamino derivatives<sup>6</sup> **2** (Sch. I, v=2 X=CH<sub>3</sub>), by the reaction of acetyl chloride in chloroform in the presence of anh. sodium carbonate.

The compounds of the general formula I, were obtained by using equimolar quantities of **1** and **2** (Sch. I, v=2), which refluxed in benzene and in the presence of phosphorous oxychloride<sup>7</sup>.

The synthesis was performed as outlined in Scheme I:



Scheme I

The acetamidines so obtained, were characterized by their picrate or oxalate salts. Their analytical data and physical constants are given in Table I.

An attempt was made to farther synthesize a new series of benzamidines of the general formula I (R=C<sub>2</sub>H<sub>5</sub>, nC<sub>3</sub>H<sub>7</sub>, isoC<sub>3</sub>H<sub>7</sub>, nC<sub>4</sub>H<sub>9</sub>, v=2 or 3, X=C<sub>6</sub>H<sub>5</sub>. For that purpose, S-alkyl-3 aminopropanesulfides **1** (Sch. I, v=3) were also synthesized by the reduction of the appropriate nitriles<sup>8</sup> with Aluminium hydride<sup>9,10</sup>.

These, were converted into their benzoylamino derivatives **2** (Sch. I, v=2 or 3 X=C<sub>6</sub>H<sub>5</sub>) by reaction with benzoylchloride in pyridine:

All the prepared benzoylamino derivatives had the consistency of thick oils and failed to crystallize. The compounds were analyzed (N,S) following microdistillation (see Table II).

For the preparation of the desired benzamidines, a method similar to that described for the acetamidines was used. However, this reaction was ineffective due to the formation of unexpected cyclisation products. Repeated reactions with either S-alkyl-2-benzoylamino propanesulfides, always produced 2-phenylthiazoline **3** (Sch. II, v=2) and 5,6-dihydro-2-phenyl-4H-1,3-thiazine **3** (Sch. II, v=3) respectively.

TABLE I

N,N'-bis(S-alkyl-2-ethanethio)-acetamidines												
$\text{CH}_3-\text{C} \begin{cases} \text{=} \text{N}-\text{CH}_2\text{CH}_2-\text{S}-\text{R} \\ \text{=} \text{NH}-\text{CH}_2\text{CH}_2-\text{S}-\text{R} \end{cases}$												
R	Salt	Molecular Formula	Yield % (*)	M.P. °C (**)	Analyses							
					Calculated %				Found %			
					C	H	N	S	C	H	N	S
CH <sub>3</sub>	Picrate	C <sub>14</sub> H <sub>21</sub> N <sub>5</sub> O <sub>7</sub> S <sub>2</sub>	40	77-79	38,61	4,96	16,08	14,73	38,50	4,77	16,09	14,56
C <sub>2</sub> H <sub>5</sub>	Oxalate	C <sub>12</sub> H <sub>24</sub> N <sub>2</sub> O <sub>4</sub> S <sub>2</sub>	30	110-111	44,42	7,46	8,63	19,76	44,34	7,18	8,77	19,93
n-C <sub>3</sub> H <sub>7</sub>	Oxalate	C <sub>14</sub> H <sub>28</sub> N <sub>2</sub> O <sub>4</sub> S <sub>2</sub>	53	98-99	47,70	8,01	7,95	18,19	47,31	7,96	8,17	18,76
iso-C <sub>3</sub> H <sub>7</sub>	Oxalate	C <sub>14</sub> H <sub>28</sub> N <sub>2</sub> O <sub>4</sub> S <sub>2</sub> · 1/2 H <sub>2</sub> O	51	124-126	46,51	8,08	7,75	17,74	46,54	7,60	7,72	17,80

(\*) Yields refer to unpurified bases.

(\*\*) Recrystallisation from absolute ethanol-anhydrous ether.

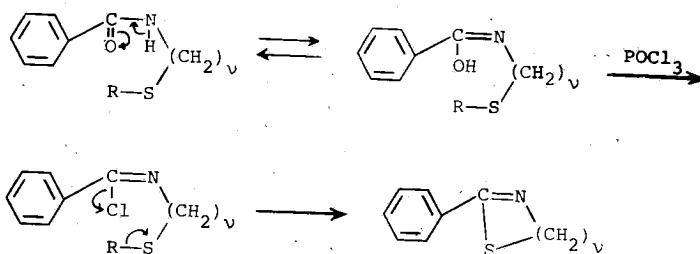
TABLE II

S-Alkyl-2-benzovlaminoethane and propanethiols.							
R-S-(CH <sub>2</sub> ) <sub>v</sub> -NHCOC <sub>6</sub> H <sub>5</sub>							
R	v	Molecular formula	Yield % (*)	Analyses			
				Calculated %		Found %	
				N	S	N	S
CH <sub>3</sub>	2	C <sub>10</sub> H <sub>13</sub> NOS	87,8	7,17	16,42	6,92	16,20
C <sub>2</sub> H <sub>5</sub>	2	C <sub>11</sub> H <sub>15</sub> NOS	97,8	6,69	15,32	6,58	15,25
C <sub>2</sub> H <sub>5</sub>	3	C <sub>12</sub> H <sub>17</sub> NOS	95,0	6,27	14,36	5,97	14,22
n-C <sub>3</sub> H <sub>7</sub>	3	C <sub>13</sub> H <sub>19</sub> NOS	95,4	5,90	13,51	5,72	13,37
iso-C <sub>3</sub> H <sub>7</sub>	2	C <sub>12</sub> H <sub>17</sub> NOS	87,4	6,27	14,36	6,11	14,12
iso-C <sub>3</sub> H <sub>7</sub>	3	C <sub>13</sub> H <sub>19</sub> NOS	96,6	5,90	13,51	5,54	13,28
n-C <sub>4</sub> H <sub>9</sub>	2	C <sub>13</sub> H <sub>19</sub> NOS	84,6	5,90	13,51	5,78	13,37
n-C <sub>4</sub> H <sub>9</sub>	3	C <sub>14</sub> H <sub>21</sub> NOS	89,0	5,57	12,75	5,49	12,52

(\*) Yields of unpurified products.

Litterature survey did not obtain similar formation of these heterocycles. (The synthetic methods used to prepare the thiazolines and dihydrothiazines followed standard procedures, described by Mac Farland<sup>14</sup>.

The sequence of reactions which probably takes place can be presented as follows (Scheme II).



where  $v=2$  or  $3$   $R=C_2H_5$ ,  $nC_3H_7$ ,  $iso C_3H_7$ ,  $nC_4H_9$

Scheme II

The structure of the above described products 3 (v=2 and 3) was confirmed by analytical data and by comparing their melting points with those of the derivatives 3 which were synthesized by a standard method.

The preparation of 2-phenylthiazoline was carried out by heating thiobenzamide with  $\beta$ -bromoethylamine<sup>11</sup> at 160-165°.

5,6-dihydro-2-phenyl-4H-1,3-thiazine was synthesized by heating thiobenzamide with 3-chloro-1-bromo-propane<sup>12,13</sup>.

### Experimental section

*S-alkyl-benzoylaminoethane and propanesulfides.*

*S-ethyl-2-benzoylaminoethane-sulfide.*

4,1 ml (0,035 mol) of benzoylchloride were added dropwise with stirring in a cooled solution of 3,6g(0,035 mol) S-ethyl-2-aminoethane-sulfide in 20 ml pyridine. Stirring was continued for 1hr after completion of the addition, at room temperature or with slight heating. The mixture was taken up with ether and the ethereal solution was washed successively with 5% HCl and water, dried and the solvent was evaporated to give an oily product (yield, 97%). This was used without further purification. The analytical sample was obtained after microdistillation.

All the derivatives of Table II were obtained in a similar manner.

*N,N'-bis(S-alkyl-2-ethanethio) acetamidines.*

*N,N'-bis(S-methyl-2-ethanethio) acetamidine.*

A mixture of 2,1g(0,023 mol) S-methyl-2-aminoethanesulfide, 3,1g(0,023 mol) of S-methyl-2-acetaminoethanesulfide and 6,8 ml(0,074 mol) of phosphorous oxychloride in 75ml benzene was refluxed for 3 hr. After evaporation of the benzene under reduced pressure, the residue was dissolved in a small quantity of water, alkalinized with 20% solution of NaOH and extracted with ether. After washing, drying and evaporating the ether, the amidine (1,8g) was obtained as an oily residue, yield 40% m.p. of the picrate 77-79° (EtOH).

All the amidines of Table I were prepared by the same procedure.

Their oxalates were prepared by adding an equimolar proportion of oxalic acid in abs. EtOH to a solution of the amidine in abs. EtOH.

### *2-phenyl thiazoline*

A mixture of 2,8g (0,03 mol) S-methyl-2-aminoethanesulfide, 6g(0,03 mol) of S-methyl-2-benzoylaminoethanesulfide and 9,2 ml (0,1 mol) POCl<sub>3</sub> in 50ml of benzene was treated according to the above described method to afford 2,8g of an oily base (yield 34%). The picrate formed corresponds to the formula C<sub>9</sub>H<sub>9</sub>NS · C<sub>6</sub>H<sub>3</sub>N<sub>3</sub>O<sub>7</sub> with a melting point in 176-70. This did not depress the m.p. of the picrate of the same compound prepared by the standard method.<sup>11</sup>



## Analysis

Calculated for  $C_{15}H_{12}N_4SO_7$ 

C 45,92 H 3,08 N 14,28 S 8,17

Found

C 45,81 H 2,94 N 14,55 S 7,66

*5,6-Dihydro-2-phenyl-4H-1,3-thiazine.*

A mixture of 2,6g(0,022 mol) S-ethyl-3-aminopropanesulfide, 5g(0,022 mol) of S-ethyl-3-benzoylamino-propanesulfide and 6,7ml(0,073 mol) of phosphorous oxychloride in 50ml benzene was treated as previously described to give an oily base with 69% yield. The picrate salt was melted at 184-5° and did not depress the m.p. of the picrate of the same product prepared by the standard method.<sup>12</sup>

## Analysis

Calculated for  $C_{16}H_{14}N_4SO_7$ 

C 47,29 H 3,47 N 13,79 S 7,89

Found

C 47,37 H 3,54 N 13,54 S 8,03

**Περίληψη**

*N,N'*-Δίς ύποκατεστημένες άλκυλο-αιθυλενοθειοακεταμιδίνες-Κυκλοποίηση των s-άλκυλο-βενζοϋλαμινο-άλκυλενοσουλφιδίων.

Στήν έργασία αυτή παρασκευάσθηκε μία σειρά δίς ύποκατεστημένων s-άλκυλο-αιθυλενοθειοακεταμιδινών. Τά παράγωγα αυτά παρασκευάσθηκαν δι' άντιδράσεως ίσομοριακών ποσοτήτων s-άλκυλο-2-ακεταμιοαιθυλενοσουλφιδίων και s-άλκυλο-2-αμινοαιθυλενοσουλφιδίων μέ δξυχλωριούχο φωσφόρο. Επιχειρήθηκε έπίσης ή σύνθεση μιās αναλόγου σειράς δίς ύποκατεστημένων s-άλκυλοθειοβενζαμιδινών. Όμως, τά παράγωγα αυτά δέν κατέστη δυνατό νά ληφθούν μέ τήν ίδια μέθοδο, λόγω κυκλοποιήσεως ή όποία λάμβανε χώρα κατά τήν θέρμανση των s-άλκυλο-βενζοϋλαμινοαιθυλενο-καί - προπυλενοσουλφιδίων μέ δξυχλωριούχο φωσφόρο.

Έτσι, όσες φορές έπανελήφθη ή άντίδραση από μέν τά s-άλκυλο-βενζοϋλαμινοαιθυλενοσουλφίδια προέκυπτε ή 2-φαινύλο-θειαζολίνη 3 (Σχ. 2, v=2) από δέ τά s-άλκυλο-βενζοϋλαμινοπροπυλενοσουλφίδια προέκυπτε ή 5,6-διϋδρο-2-φαινύλο-4H-1,3-θειαζίνη 3 (Σχ. 2, v=3).

Τό γεγονός αυτό διαπιστώθηκε μέ αναλύσεις και μέ συνθετική παρασκευή των παραγώνων 3, (v=2 και 3) μέ άλλη μέθοδο και σύγκριση του σημείου τήξεως των πικρικών άλάτων.

**References**

1. Okawa, K., Abe, J., Watanabe, T., Fujimoto, K.: *Pat. Japan*, 6726, 286, Dec. 1967, C.A., 69, 67130 (1968).
2. Caetzi, K.: *Pat.S.Africa*, 6803451 (1968), C.A., 74, 112446 (1969).
3. Hukki, J., Honkanen, E.: *Pat. Finn.* 33, 636, Jun. 1964, C.A., 61, 16020 (1964).

4. Solokovsky, M., Wisten, S., Ironson, E., Brown, H.: *Am. Rev. Tuberc.*, **74**, 59 (1956).
5. Wieland, T., Möeller, E., Diedelmann G.: *Chem. Ber.*, **85**, 1035 (1952).
6. Tsatsas, G., Sandris, C., Kontonassios, D.: *Bull. Soc. Chim. Franc.*, 3100 (1964).
7. Tsatsas, G., Delaby, R., Damiens, R.: *Ann. Pharm. Franc.*, **14**, 607 (1956).
8. Hurd, C., Gershbeim, L.: *J. Am. Chem. Soc.*, **69**, 2328 (1949).
9. Tsatsas, G., Sandris C., Kontonassios, D.: *Bull. Soc. Chim. Franc.*, 2160 (1963).
10. Lambrou, D., Tsatsas, G.: *Ann. Pharm. Franc.*, **32**, 295 (1974).
11. Hirsch, G.: *Ber.*, **29**, 2610 (1896).
12. Pinks, G.: *Ber.*, **26**, 1077 (1893).
13. Cherbuliez, E., Baehler, B., Espejo, O., Jindra, H., Willhalm, B., Rabinowitz, J.: *Helv. Chim. Acta*, **50**, I, 331 (1967).
14. McFarland, J.W., Howes, H.L., Conover, L.H., Lynch, J.E.: *J. Med. Chem.*, **13**, 113 (1970).

## A NOVEL ANGIOTENSIN II ANTAGONIST, [SAR<sup>1</sup>, DEHYDRO-ALA<sup>8</sup>]-A-II. PURIFICATION AND CHARACTERIZATION IN VITRO.

S.E. PAPAIOANNOU, P-C. YANG and F. FAGO  
*Searle Laboratories, P.O Box 5110 Chicago, Illinois, 60680 (USA)*

(Received January 30, 1981; Revised May 14, 1981).

### Summary

During the solid phase synthesis of the angiotensin II (A-II) analog SC-30824, [Sar<sup>1</sup>, S-benzyl-Cys<sup>8</sup>]-A-II, a heterogenous by product was shown to have high A-II antagonistic without agonistic activity. The active component (SN-790) of this by-product was purified by ion exchange chromatography. Structural studies of SN-790 by means of amino acid analysis, degradation with chymotrypsin and leucine aminopeptidase, and NMR, UV spectra of the C-terminal tripeptide, suggested the structure [Sar<sup>1</sup>, dehydro-Ala<sup>8</sup>]-A-II. The novel structure was confirmed by peptide synthesis of [Sar<sup>1</sup>, dehydro-Ala<sup>8</sup>]-A-II, (SC-33191), [Sar<sup>1</sup>, S-benzyl-Cys<sup>8</sup>]-A-II, (SC-30824), SN-790 and [Sar<sup>1</sup>, dehydro-Ala<sup>8</sup>]-A-II, (SC-33191) and the known A-II antagonists Saralasin and [Sar<sup>1</sup>, Ile<sup>8</sup>]-A-II were characterized in vitro for A-II receptor binding, and aldosterone production by isolated rat adrenal glomerulosa cells. The relative A-II receptor binding potencies of [Sar<sup>1</sup>, S-benzyl-Cys<sup>8</sup>]-A-II, (SC-30824) and [Sar<sup>1</sup>, dehydro-Ala<sup>8</sup>]-A-II, (SN-790) were 4.0 and 1.7 respectively, using A-II as a standard. Both analogs were highly antagonistic (ID<sub>50</sub>= $8.10 \times 10^{-8}$  M and  $5.7 \times 10^{-8}$  M, respectively) of aldosterone production stimulated by A-II at the cell level, but [Sar<sup>1</sup>, S-benzyl-Cys<sup>8</sup>]-A-II, (SC-30824) showed a partial agonist activity. SN-790 and [Sar<sup>1</sup>, dehydro-Ala<sup>8</sup>]-A-II, (SC-33191) had a superior in vitro profile as A-II blockers of pharmacological potential, when compared with Saralasin and [Sar<sup>1</sup>, S-benzyl-Cys<sup>8</sup>]-A-II, (SC-30824). They were found to be more potent than Saralasin both in terms of binding potency and antagonistic activity at the glomerulosa cell level. Apart from [Sar<sup>1</sup>, S-benzyl-Cys<sup>8</sup>]-A-II, (SC-30824), the above three antagonists showed no agonistic activity in vitro.

### Introduction

The first antagonists of angiotensin II (A-II) have been instrumental for structure-activity studies of the hormone.<sup>1,3,16</sup> Regoli et al<sup>2,3</sup> have reviewed the early pharmacological studies. The structure of the C-terminal residue was indentified as

most important for the agonistic and antagonistic properties of A-II analogs. More recently, Catt and coworkers<sup>5,6,8,9,25</sup> have demonstrated high affinity receptor binding sites for the hormone in bovine and rat adrenal cortex plasma membrane preparations, and correlated the specific binding to isolated canine and rat adrenal glomerulosa cells with aldosterone production. Apart from their importance for mechanistic studies, antagonists of A-II may be useful as diagnostic or therapeutic agents in the treatment of hypertension. Saralasin, [Sar<sup>1</sup>, Val<sup>5</sup>, Ala<sup>8</sup>]-A-II and [Sar<sup>1</sup>, Ile<sup>8</sup>]-A-II are potent antagonists in vitro,<sup>6,8</sup> and have been shown to lower the blood pressure in normal<sup>14,22</sup> and hypertensive subjects.<sup>1,15</sup> Both antagonists, however, have also shown an initial pressor effect.<sup>1,14,15,22</sup> In a search for A-II antagonists and as a result of a solid phase synthesis of [Sar<sup>1</sup>, S-benzyl-Cys<sup>8</sup>]-A-II, a heterogeneous by-product was obtained by counter current distribution.<sup>17</sup> Preliminary studies (unpublished observations, R.L. Novotney) indicated that this unknown by-product had no agonistic activity on blood pressure. We report here our studies on the purification and structural elucidation of a novel A-II antagonist from this by-product, as well as its characterization in vitro and comparison of its receptor binding and agonistic/antagonistic profile with those of known antagonists.

### Materials and methods

CM-Sephadex C-25 and Dextran T-70 were obtained from Pharmacia (Uppsala, Sweden). Silica gel 60F-254 was purchased from E. M. Laboratories, Inc. (Elmsford, NY), and silica gel (type H) for column chromatography from E. Merck, Darmstadt (Elmsford, NY). HEPES (N-2-hydroxy-ethylpiperazine-N'-2-ethane-sulfonic acid) and leucine aminopeptidase (type III-CP, 105 units/mg) were from Sigma Chemical Co. (St. Louis, MO). Bio-Gel P-2 was obtained from Bio-Rad Laboratories (Richmond, CA), and  $\alpha$ -chymotrypsin (3x crystallized, 53 units/mg) was from Worthington Biochemical Co. (Freehold, NJ). A-II and [Sar<sup>1</sup>, Ile<sup>8</sup>]-A-II were purchased from Beckman Instrument Co. (Palo Alto, CA), while [Sar<sup>1</sup>, Val<sup>5</sup>, Ala<sup>8</sup>]-A-II (P113, Saralasin acetate) was generously provided by Dr. K. O. Ellis, Norwich Pharmaceutical Co. (Norwich NY). SC-33191 i.e. [Sar<sup>1</sup>, dehydro-Ala<sup>8</sup>]-A-II, and SC-30824 i.e. [Sar<sup>1</sup>, S-benzyl-Cys<sup>8</sup>]-A-II were synthesized at Searle Laboratories by E.A. Hallinan. [<sup>125</sup>I] Monoiodo-A-II (specific activity, 1,000 m Ci/mg) was from New England Nuclear Co. (Boston, MA). EGWP filters were from Millipore (Bedford, MA). [1,2-<sup>3</sup>H] Aldosterone (specific activity 136 m Ci/mg) was purchased from Amersham-Searle (Arlington Heights, IL). Norit A (charcoal) was obtained from Fisher Scientific Co. (Pittsburgh, PA) and Medium 199 from Grand Island Biological Co. (Grand Island, NY).

### *Purification of SN-790*

Solid phase synthesis of [Sar<sup>1</sup>, S-benzyl-Cys<sup>8</sup>]-A-II<sup>17</sup> resulted in a heterogeneous by-product of unknown composition and structure(s). This by-product (440 mg) was subjected to ion exchange chromatography using a CM-

Sephadex C-25 column (2.5×29 cm) equilibrated with 0.05M ammonium acetate pH 5.6. The column was eluted with a gradient of ammonium acetate, eight ml fractions were collected and the optical density determined at 280 nm. The peak fractions were pooled, lyophilized and tested for homogeneity by ascending thin-layer chromatography (TLC) on Merck Silica Gel 60-F-254 plates developed by one of the following two solvents: n-propanol-ethylene dichloride-water-ammonium hydroxide (24:8:8:1 by vol.), or ethanol-ethylene dichloride-water-ammonium hydroxide (28:8:8:1 by vol.). The spots were visualized by short wave UV light, and stained with ninhydrin or starch-potassium iodide<sup>18</sup>. The first sharp peak (fractions 80-86) off the CM-Sephadex column was lyophilized and designated SN-790.

#### *Structural characterization of SN-790*

Sixty mg SN-790 were dissolved in twelve ml of one percent ammonium bicarbonate buffer pH 8.3 and two mg chymotrypsin were used for hydrolysis at 37°C. Progress of hydrolysis was followed by TLC as above. After one hour the solution was acidified to pH 4 with 1M acetic acid and lyophilized. This hydrolysate was further fractionated on a (0.8×40 cm) column, packed with Merck H silica gel. The column was prewashed with ethanol, water, ethylene dichloride and 0.1% ammonia. The hydrolysate dissolved in 1.5 ml of eluting solvent made of 60% ethanol, 10% water, 0.1% ammonium hydroxide and 29.9% ethylene dichloride, was applied to the column followed by elution until three ml eluate were collected in 75 fractions. The elution continued with a mixture of 60% ethanol, 20% water, 0.1% ammonium hydroxide and 19.9% ethylene dichloride, until another 3.3 ml eluate were collected. The column chromatography was monitored by means of TLC as above. Fractions 8-15 were pooled and lyophilized. The lyophilizate was hydrolyzed at pH 8.6 with one percent by weight of leucine aminopeptidase, after activation of the enzyme on the basis of an earlier method<sup>27</sup>. Progress of hydrolysis was followed by TLC as above. After one hundred min at 40°C the hydrolysate was lyophilized. This product was fractionated by gel filtration using a (0.9×90 cm) column packed with Bio-Gel P-2, 200-400 mesh in 1% ammonium bicarbonate, and 1.2 ml fractions were collected. Five µl from each fraction were spotted on TLC plates (as above) and the column eluted material visualized by short wave UV light and after spraying with ninhydrin. Fractions 33-36 were visible by UV, while fractions 38-40 were ninhydrin positive. These fractions were pooled, lyophilized and tested for homogeneity by the above described TLC method. The lyophilizate of fractions 33-36 was further characterized by amino acid analysis<sup>20</sup>, as well as UV and NMR spectroscopy. SN-790 and the lyophilizate from the silica gel column (fractions 8-15) were also analyzed for amino acid content<sup>20</sup>.

#### *Angiotensin II receptor binding assay*

The radioligand-receptor assay was performed as by Saltman et al<sup>25</sup>, with the

following minor modifications. The rat whole adrenals were homogenized in 50 mM Tris-HCl buffer (pH 7.4) For incubation, 0.1 mg protein of the crude plasma membrane preparation were used in 50 mM Tris-HCl, 0.6M sucrose and 0.2% BSA. Filtration was through Millipore EGWP (0.20  $\mu$ m) filters. The initial binding of [ $^{125}$ I]-monoiodo-A-II tracer in the absence of unlabeled hormone was approximately ten percent, and the nonspecific binding was less than one percent.

#### *Aldosterone production assay by isolated adrenal glomerulosa cells*

Glomerulosa cell suspensions were prepared by collagenase digestion and physical dispersion of the capsular layer from rat adrenal glands essentially as described by Fredlund and coworkers (8). The tissue was minced, washed and dispersed in buffer A: 10mM HEPES-25 mM NaHCO<sub>3</sub> - 118 mM NaCl - 1.18mM MgSO<sub>4</sub>, pH 7.4. Dispersion was carried out by repeated pipetting through a ten ml plastic pipette in buffer B: Medium 199 made 10 mM with HEPES, 0.065% with NaHCO<sub>3</sub> and 0.1% with BSA, pH 7.4. For the agonistic assay the glomerulosa cells were incubated in buffer B at 37°C for one hour. The antagonistic data were obtained in the presence of  $5 \times 10^{-8}$  M A-II. The aldosterone RIA was performed by the direct method as in (8) except that 5 mg/ml BSA were used instead of gamma globulin, and the bound tracer separated by the addition of 0.8 ml charcoal-dextran suspension (250 mg Norit A and 25 mg dextran per 100 ml of 50 mM sodium phosphate - 140 mM NaCl, pH 7.4).

## Results

#### *Purification and enzymatic degradation of SN-790*

Ion exchange chromatography (Fig. 1) was effective in separating several UV absorbing peaks from the by-product of solid phase synthesis of [Sar<sup>1</sup>, S-benzyl-

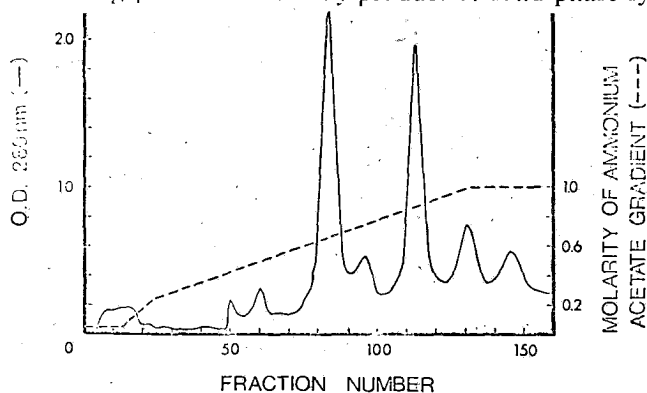


FIG. 1. Elution profile of a heterogeneous by-product from solid phase synthesis of [Sar<sup>1</sup>, S-benzyl-Cys<sup>8</sup>]-A-II, on a CM-Sephadex C-25 column. The flow rate was 42 ml/hr. Fractions 80-86 were pooled and lyophilized.

Cys<sup>8</sup>]-A-II.<sup>17</sup> The first sharp peak (fractions 80-86), designated SN-790, was homogeneous as judged by TLC. It was estimated that SN-790 was only two percent of the crude mixture from the solid phase synthesis of [Sar<sup>1</sup>, S-benzyl-Cys<sup>8</sup>]-A-II. The results of amino acid analysis (Table 1) indicated a heptapeptide with

TABLE 1. Amino Acid Composition of SN-790 and its Purified C-terminal Peptides

Amino Acid	SN-790	C-terminal Tetrapeptide	C-terminal Tripeptide
ASP	0	0	0
THR	0	0	0
SER	0	0	0
PRO	0.99	1.22	1.13
GLU	0.19	0	0
GLY	0	0	0
ALA	0	0	0
VAL	1.02	0	0
MET	0	0	0
ILE	0.91	1.02	0.01
LEU	0	0	0
TYR	0.95	0	0
PHE	0	0	0
S-benzyl-Cys <sup>8</sup>	0.07	0	0
Sarcosine	0.85	0	0
LYS	0	0	0
HIS	1.00	1.00	1.00
ARG	1.01	0	0

The peptides were hydrolyzed for 24 h at 110°C as described in the text. The number of residues per mol of peptide was calculated by assuming one residue of histidine/mol.

only traces of S-benzyl-cysteine. The strong binding to the adrenal A-II receptor (Table 2), however, did not agree with proline being the C-terminal residue of SN-

TABLE 2. Angiotensin II, (A-II) Receptor Binding and Aldosterone Production Properties of SN-790 and Related Antagonists.

Compound	Structure	Receptor Binding RP	Agonistic Activity %	Antagonistic Activity ID50 (M)
A-II	Asp <sup>1</sup> Arg <sup>2</sup> Val <sup>3</sup> Tyr <sup>4</sup> Ile <sup>5</sup> His <sup>6</sup> Pro <sup>7</sup> Phe <sup>8</sup>	1.00	100	---
SC-30824	[Sar <sup>1</sup> , S-benzyl-Cys <sup>8</sup> ]-A-II	4.00	44	8.0 × 10 <sup>-8</sup>
SN-790	[Sar <sup>1</sup> , dehydro-Ala <sup>8</sup> ]-A-II	1.7	0	5.7 × 10 <sup>-8</sup>
SC-33191	[Sar <sup>1</sup> , dehydro-Ala <sup>8</sup> ]-A-II	1.4	0	5.2 × 10 <sup>-8</sup>
Saralasin (P113)	[Sar <sup>1</sup> , Val <sup>3</sup> , Ala <sup>8</sup> ]-A-II	0.7	0	3.5 × 10 <sup>-7</sup>
---	[Sar <sup>1</sup> , Ile <sup>8</sup> ]-A-II	1.2	0	1.0 × 10 <sup>-8</sup>

Receptor binding studies were carried out on crude adrenal membrane preparations, while the agonistic and antagonistic properties were based on aldosterone production by isolated glomerulosa cells. RP stands for binding potency relative to A-II. The agonistic activity is expressed as percent of A-II activity. The data are from dose-response curves, each dose point representing the mean of duplicate determinations with 5% max. intra-assay variability for the receptor binding assay and 10% for the aldosterone release assay.

790. The enzymatic degradations of SN-790, shown schematically in Fig. 2, were pursued in order to isolate the C-terminal tripeptide for further structural characterization.

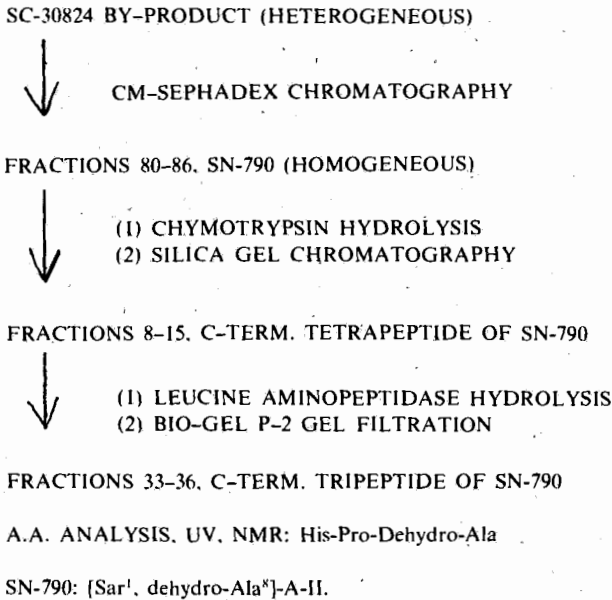


FIG. 2. Diagram of purification, degradation and structural characterization of SN-790.

Hydrolysis of SN-790 with chymotrypsin (as in Methods) resulted in the disappearance of the substrate material on TLC and the appearance of two new spots. The reaction was complete in two minutes with no further TLC changes during hydrolysis for one hour. Resolution of the chymotrypsin hydrolysate was achieved by silica gel column chromatography monitored by TLC. The early fractions from the column showed one major spot with high R<sub>f</sub> value, while the later fractions showed lower R<sub>f</sub> values. The early fractions (8-15) were pooled and the amino acid analysis (Table 1) showed the presence of equimolar isoleucine, histidine and proline, identifying the material as the C-terminal peptide of SN-790.

Hydrolysis of this peptide with leucine aminopeptidase (as in Methods) resulted in two spots by monitoring with TLC. One of the two spots was isoleucine.



Gel filtration of the above hydrolysate in Bio-Gel P-2 separated the N-terminal isoleucine (fractions 38-40) from the C-terminal peptide (fractions 33-36).

### *Structural characterization of C-terminal tripeptide of SN-790*

The lyophilizate of the above fractions 33-36 was estimated to be about ninety percent pure by TLC. Amino acid analysis (Table 1) indicated proline and histidine in equimolar amounts. The UV and NMR spectra of this peptide are shown in Fig. 3 and 4, respectively. The 248 nm shoulder of the UV spectrum was similar to the 250 nm absorption characteristics of  $\alpha,\beta$ -unsaturated amino acid residues as shown by Gross and Kiltz<sup>10</sup>. The pronounced olefinic peaks at 5.99 and 5.74 ppm of the NMR spectrum (Fig. 4) were a further evidence of a dehydroamino acid residue in

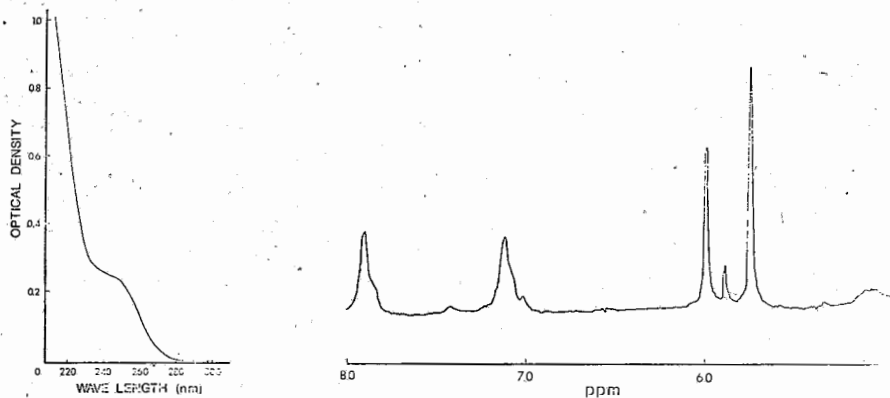


FIG. 3. Ultraviolet absorption spectrum of the C-terminal tripeptide of SN-790. The concentration was 50  $\mu$ g per ml water.

FIG. 4. Proton nuclear magnetic resonance spectrum of the C-terminal tripeptide of SN-790 using a Varian XL-100 spectrometer at 100 MHz. The sample concentration was 33 mg per ml D<sub>2</sub>O (99.7%), and the number of scans was 9,000.

the above C-terminal tripeptide of SN-790 (fractions 33-36). On the basis of the above results the structures of SN-790 and its C-terminal tripeptide were tentatively identified as shown at the bottom of Fig. 2. More recently, this structure of SN-790 was positively identified by solid phase synthesis of SC-33191, i.e. [Sar<sup>1</sup>, dehydro-

Ala<sup>8</sup>]-A-II. (E.A. Hallinan, unpublished work).

### *Receptor binding and effects on aldosterone production*

Specific binding to crude rat adrenal membrane receptor preparations was comparable to the binding observed with similar bovine<sup>25</sup> and rat<sup>5</sup> preparations. Thus, [Des-Asp<sup>1</sup>]-A-II was essentially equipotent to A-II. AI was 2% as potent, and the [Des-Asp<sup>1</sup>, Des-Arg<sup>2</sup>]-A-II was only 0.4% as potent. The binding of Saralasin and [Sar<sup>1</sup>, Ile<sup>8</sup>]-A-II antagonists (Table 2) was also comparable to that reported previously<sup>5,25</sup>. The fifty percent effective dose for A-II binding was  $6.6 \pm 1.8 \times 10^{-9}$  M, (n=13) similar to recent binding studies<sup>5</sup> using the 20,000xg pellet without DTT and EDTA additives.

The aldosterone production results were also comparable to the original methodology<sup>5,8</sup>. The endogenous aldosterone production and inter-assay variability in absence of added A-II was  $2.0 \pm 1.1$  ng/10<sup>5</sup> cells (n=8). A 3- to 7-fold increase above this control value was obtained by addition of  $5 \times 10^{-8}$  M A-II. The A-II concentration for half maximal stimulation of aldosterone was  $1.8 \pm 1.2 \times 10^{-9}$  M from five separate experiments. SN-790, SC-33191, ie the synthetic [Sar<sup>1</sup>, dehydro-Ala<sup>8</sup>]-A-II, and the early synthetic antagonist [Sar<sup>1</sup>, S-benzyl-Cys<sup>8</sup>]-A-II, (SC-30824), were compared with A-II and model antagonists as shown in Table 2. The relative binding potency of [Sar<sup>1</sup>, S-benzyl-Cys<sup>8</sup>]-A-II, (SC-30824) was the highest reported to date<sup>4,25</sup>, but it is a partial agonist since it showed considerable agonistic activity (Table 2). The profiles of SN-790 and [Sar<sup>1</sup>, dehydro-Ala<sup>8</sup>]-A-II, (SC-33191) were very similar, as expected. They bound strongly to the A-II receptor, had high antagonistic activity and no agonistic activity. These antagonists were more potent than Saralasin, both in terms of receptor binding and steroidogenic antagonistic activity.

### **Discussion**

The present studies were prompted from early preliminary data indicating that a crude by-product of [Sar<sup>1</sup>, S-benzyl-Cys<sup>8</sup>]-A-II synthesis had no agonistic activity, while the above peptide was a partial agonist. It was decided to purify the active constituent of the above by-product and characterize structurally, as well as in terms of its binding to the A-II receptors, and its effects on aldosterone production at the cell level. The existence of highly sensitive, specific *in vitro* methodology<sup>5,6,8,9,25</sup> that correlated well with *in vivo* data, made possible the relevant monitoring for the purification and characterization of SN-790, a novel A-II antagonist.

SN-790 showed superior *in vitro* profile (Table 2) as a potential diagnostic or therapeutic antihypertensive agent, when compared with the originally designed [Sar<sup>1</sup>, S-benzyl-Cys<sup>8</sup>]-A-II, (SC-30824). Amino acid analysis (Table 1) showed the seven residues of SC-30824 with only a trace of S-benzyl-cysteine. It was suspected however that a residue at the eighth position was present in SN-790, since removal

of the C-terminal phenylalanine residue from A-II and its active analogs causes complete inactivation<sup>23,25</sup>. It was decided to identify this hypothetical C-terminal residue that was undetectable by amino acid analysis. The enzymatic degradation of SN-790 with chymotrypsin and leucine aminopeptidase proceeded as expected from the sequence of [Sar<sup>1</sup>, S-benzyl-Cys<sup>8</sup>]-A-II, (SC-30824). Thus chymotrypsin hydrolyzed SN-790 at the peptide bond of the [Tyr<sup>4</sup>] carboxyl group, while leucine aminopeptidase removed isoleucine from the C-terminal tetrapeptide, resulting at the C-terminal tripeptide, the amino acid analysis of which (Table 1) was consistent with the above interpretation.

The first hint about the structure of the C-terminal residue came from the UV spectrum of the tripeptide. On the basis of earlier studies<sup>10</sup>, the spectrum in Fig. 3 was interpreted as indicating the existence of an  $\alpha,\beta$ -unsaturated amino acid residue in the C-terminal tripeptide of SN-790. The NMR spectrum of this peptide added more evidence to support the hypothesis that the C-terminal residue was dehydroalanine. The formation of such a residue could be explained by elimination of benzylmercaptan from the S-benzyl-cysteine during the synthesis of [Sar<sup>1</sup>, S-benzyl-Cys<sup>8</sup>]-A-II, (SC-30824), as documented in similar cases.<sup>21,24</sup> Acid hydrolysis of dehydroalanine peptides resulted in pyruric acid that is not ninhydrin positive<sup>2</sup>. This explained why dehydroalanine was not detected by amino acid analysis of SN-790 or its C-terminal peptides (Table 1). The structure of SN-790 was finally confirmed by solid phase synthesis of [Sar<sup>1</sup>, dehydro-Ala<sup>8</sup>]-A-II, (SC-33191). Dehydroamino acid residues have been earlier reported in the literature as constituents of peptide antibiotics nicin<sup>12</sup>, subtilin<sup>11</sup>, and other natural products<sup>3,19</sup>.

The structure-activity relationships for [Sar<sup>1</sup>, dehydro-Ala<sup>8</sup>]-A-II, (SN-790) and [Sar<sup>1</sup>, S-benzyl-Cys<sup>8</sup>]-A-II, (SC-30824) were in agreement with the literature<sup>23,25,26</sup>. Both peptides bound to be A-II receptor with higher potency than A-II, probably due to the N-terminal sarcosine<sup>25</sup>. The S-benzyl-cysteine residue in [Sar<sup>1</sup>, S-benzyl-Cys<sup>8</sup>]-A-II, (SC-30824) resulted in an A-II antagonist with partial agonistic activity (Table 2). In this aspect SC-30824 resembled the thienylamine derivative of A-II<sup>25</sup>. When the phenyl ring at the eighth position of A-II was substituted with a short aliphatic chain, the analogs like Saralasin and [Sar<sup>1</sup>, Ile<sup>8</sup>]-A-II showed strong antagonistic activity<sup>23,25</sup>. The results of the present study on these antagonists are in agreement with the literature<sup>25,26</sup>. The dehydroalanine at position eight of [Sar<sup>1</sup>, dehydro-Ala<sup>8</sup>]-A-II, (SN-790) resulted in even stronger antagonistic activity than Saralasin and higher binding potency than Saralasin and [Sar<sup>1</sup>, Ile<sup>8</sup>]-A-II. On the basis of the correlation between the antagonistic activities of A-II antagonists on rabbit aortic strip and the aldosterone production in isolated glomerulosa cells<sup>26</sup>, it would be anticipated that [Sar<sup>1</sup>, dehydro-Ala<sup>8</sup>]-A-II, (SN-790) would possess antihypertensive properties. SN-790, Saralasin and [Sar<sup>1</sup>, Ile<sup>8</sup>]-A-II showed no agonistic activity in vitro (Table 2) in spite of the definite agonistic activity of the latter two antagonists in vivo<sup>1,14,15,22</sup>. Due to the more potent binding and antagonistic activities of SN-790 compared to Saralasin, it is possible that the in vivo hemodynamic profile of SN-790 would be superior. Furthermore, dehydroamino acid residues offer increased resistance to hydrolysis by proteolytic

enzymes<sup>7</sup>, resulting in possible prolonged activity in vivo. The present work is also an example of the usefulness of specific and sensitive in vitro methodology for identification, isolation and characterization of novel by-products from crude mixtures resulting from solid phase synthesis.

### Acknowledgements

We are grateful to Dr. R. Mazur and Ms. E. A. Hallinan for the synthesis of SC-30824 and SC-33191, and their contribution in identifying the dehydroalanine residue of SN-790. We also acknowledge the interpretation of NMR spectrum by Dr. R. Bible, the early in vivo data by Dr. R. Novotney, and the amino acid analyses by Miss E. deGuzman.

### Περίληψη

*Ένας νέος ανταγωνιστής της άγγειοτονίνης II, [Sar<sup>1</sup>, dehydro-Ala<sup>8</sup>]-A-II.\* Καθαρισμός και Χαρακτηρισμός in vitro.*

Κατά την πεπτιδική σύνθεση του αναλόγου SC-30824 της άγγειοτονίνης II, [Sar<sup>1</sup>, S-benzyl-Cys<sup>8</sup>]-A-II, ανιχνεύθηκε ένα ετερογενές παραπροϊόν με ανταγωνιστικές ιδιότητες χωρίς αγωνιστική δράση. Το ένεργό συστατικό (SN-790) του παραπροϊόντος αυτού άπεμονώθη χρωματογραφικά. Δομική μελέτη του SN-790 δι' ανάλυσεως των αμινοξέων του, ύδρολύσεως διά χυμοθρυψίνης άμινοπεπτιδάσης, NMR, και με ύπεριώδη φασματοσκοπική ανάλυση του καρβοξυ-τελικού τριπεπτιδίου του, κατέληξε στην πιθανή δομή [Sar<sup>1</sup>, dehydro-Ala<sup>8</sup>]-A-II, που επιβεβαιώθηκε με πεπτιδική σύνθεση της δομής αυτής (SC-33191). Οί ενώσεις [Sar<sup>1</sup>, S-benzyl-Cys<sup>8</sup>]-A-II, (SC-30824), τό άπομονωθέν παραπροϊόν SN-790 και τό συνθετικό [Sar<sup>1</sup>, dehydro-Ala<sup>8</sup>]-A-II, (SC-33191), καθώς και οί γνωστοί ανταγωνιστές Saralasin ή [Sar<sup>1</sup>, Val<sup>5</sup>, Ala<sup>8</sup>]-A-II, και [Sar<sup>1</sup>, Ile<sup>8</sup>]-A-II έμελετήθησαν in vitro δι' άλληλεπιδράσεως με τούς άδρενεργικούς ύποδοχείς της άγγειοτονίνης II, και διά της παραγωγής άλδοστερόνης σε πρωτογενείς κυτταρικές καλλιέργειες έκ φλοιού έπινεφριδίων άρουραίου. Οί σχετικές δραστηριότητες του [Sar<sup>1</sup>, S-benzyl-Cys<sup>8</sup>]-A-II, (SC-30824) και του άπομονωθέντος παραπροϊόντος [Sar<sup>1</sup>, dehydro-Ala<sup>8</sup>]-A-II, (SN-790), με μονάδα την δραστηριότητα συνδέσεως της άγγειοτονίνης II με τούς ύποδοχείς της, προσδιορίστησαν άντιστοιχως ώς 4,0 και 1,7. Καί τά δύο αυτά ανάλογα είχαν ισχυρή ανταγωνιστική δράση στην διά της άγγειοτονίνης II παραγωγή άλδοστερόνης, ενώ τό [Sar<sup>1</sup>, S-benzyl-Cys<sup>8</sup>]-A-II, (SC-30824) έδειξε μερική αγωνιστική δράση. Τό άπομονωθέν παραπροϊόν [Sar<sup>1</sup>, dehydro-Ala<sup>8</sup>]-A-II, (SN-790) και τό συνθετικό [Sar<sup>1</sup>, dehydro-Ala<sup>8</sup>]-A-II, (SC-33191) είχαν βελτιωμένες ιδιότητες σαν ανταγωνιστές της άγγειοτονίνης II in vitro με πιθανές φαρμακολογικές ιδιότητες έν συγκρίσει με την Saralasin και τό [Sar<sup>1</sup>, S-benzyl-Cys<sup>8</sup>]-A-II, (SC-30824). Συγκεκριμένα τά δύο πρώτα ανάλογα ήταν δραστικότερα της Salalasin, όσον άφορά την σύνδεση με τούς ύποδοχείς της άγ-

γειοτονίνης II και την αγωνιστική δράση στα κύτταρα του φλοιού επινεφριδίων. Εκτός του [Sar<sup>1</sup>, S-benzyl-Cys]-A-II, (SC-30824), οι πίο πάνω τρεις ανταγωνιστές δέν είχαν αγωνιστική δράση in vitro.

---

## References

1. Anderson, Jr., C. H., Streeten, D.H.P. & Dalakos, T.G.: *Cir. Res.* **40**, 243 (1977).
2. Bayer, E. & Parr, W.: *Angew. Chem. Int. Ed.* **5**, 840 (1966).
3. Bodansky, M. & Scozzie, J.A. & Muramatzu, I.: *J. Antibiot.* **23**, 9 (1970).
4. Bumpus, F.M.: *Fed. Proc.* **36**, 2128 (1977).
5. Douglas, J., Aguilera, C., Kondo, T. & Catt, K.J.: *Endocrinol.* **102**, 685 (1978).
6. Douglas, J., Saltman, S., Fredlund, P., Kondo, T. & Catt, K. J.: *Cir. Res. (Suppl II)* **38**, 108 (1976).
7. English, M.L. & Stammer, C.H.: *Biochem. Biophys. Res. Commun.* **83**, 1464 (1978).
8. Fredlund, P., Saltman, S. & Catt, K.J.: *Endocrinol.* **97**, 1577 (1975).
9. Glossman, H., Baukal, A. J. & Catt, K.J.: *J. Biol. Chem.* **249**, 825 (1974).
10. Gross, E. & Kiltz, H.H.: *Biochem. Biophys. Res. Comm.* **50**, 559 (1973).
11. Gross, E., Kiltz, H.H. & Craig, L.C.: *Hoppe-Seler's Z. Physiol. Chem.* **354**, 799 (1973).
12. Gross, E. & Morell, J. L.: *J. Am. Chem. Soc.* **93**, 4634 (1971).
13. Khairallal, P.A., Toth, A. & Bumpus, F.M.: *J. Med. Chem.* **13**, 181 (1970).
14. MacGregor, G. A. & Dawes, P.M.: *Br. J. Clin. Pharmac.* **3**, 483 (1976).
15. Marks, L.S., Maxwell, M.H. & Kaufman, J.J.: *Lancet II*, 784 (1975).
16. Marshall, G.R., Vine, W. & Needleman, P.: *Proc. Natl. Acad. Sci. USA*, **67**, 1624 (1970).
17. Mazur, R.H. (G. D. Searle & Co.): *U.S. Patent* 3, 975, 365 Aug. 17. (1976).
18. Mazur, R.H., Ellis, B.W. & Cammarata, P.S.: *J. Biol. Chem.* **237**, 1619 (1962).
19. Meyer, W.L., Knyper, L.F., Lewis, R.B., Templeton, G.E. & Woodhead, S.H.: *Biochem. Biophys. Res. Commun.* **56**, 234 (1974).
20. Moore, S. & Stein, W.H.: *Methods Enzymol.* **6**, 819 (1963).
21. Nicolet, B.H.: *J. Am. Chem. Soc.* **53**, 3066 (1931).
22. Oghihara, T., Hata, T., Mikami, H., Mandai, T. & Kumahar, Y.: *Life Sci.* **20**, 1855 (1977).
23. Regoli, D., Park, W.K. & Rioux, F.: *Pharmacol. Rev.* **26**, 69 (1974).
24. Rich, D.H. Tarn, J., Mathiaparanam, P., Grand, J.A. & Mabuni, C.: *J.C.S. Chem. Comm.* 897 (1974).
25. Saltman, S., Baukal, A., Waters, S., Bumpus, F.M. & Catt, K.J.: *Endocrinol.* **97**, 275 (1975).
26. Saltman, S., Fredlund, R., & Catt, K.J.: *Endocrinol.* **98**, 894 (1976).
27. Spackman, D.H., Smith, E.L. & Brown, D.M.: *J. Biol. Chem.* **212**, 255 (1955).

---

\*"Άλλοι όροι για την ίδια όρμόνη είναι: άγγειοτενσίνη, άγγειοτασίνη, άγγειοπιεσίνη, ύπερτασίνη, angiotensin, hypertensin, και ή σύντμηση A-II.

---

## Short Papers

---

*Chimika Chronika, New Series, 10, 381-383 (1981)*

### DIETHYLAMINOETHYL ESTERS OF THE p-[(N'-ALKYL)- CARBAMOYLAMINO] - BENZOIC ACID

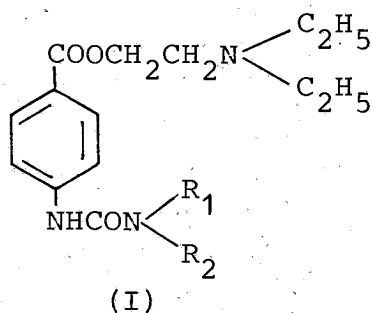
GEORGE PAPAIOANNOU

*Laboratory of Pharmaceutical Chemistry, University of Athens, Athens (Greece)*

(Received December 17, 1980; Revised April 22, 1981)

The fact that several basic carbamates have shown interesting pharmacodynamic activity as local anesthetics<sup>1,2,3</sup> has prompted the synthesis of the title compounds, in order to facilitate the increase of the local anesthetic properties of diethylaminoethyl ester of p-aminobenzoic acid.

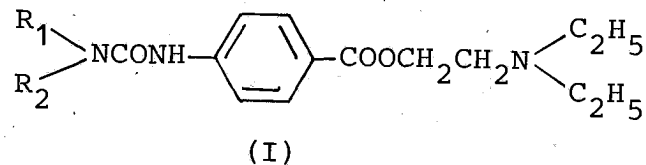
The new carbamates correspond to the general formula (I).



where  $\text{R}_1$  : H,  $\text{CH}_3$ .

$\text{R}_2$  :  $\text{CH}_3$ ,  $\text{C}_2\text{H}_5$ ,  $\text{nC}_3\text{H}_7$ ,  $\text{nC}_4\text{H}_9$ .

These were synthesized by the reaction of diethylaminoethylester of p-aminobenzoic acid with alkyl-isocyanates or dimethylcarbamoylchloride in benzene, according to the method of G. Tsatsas et al<sup>4</sup>. The prepared compounds were characterized by the picrate or HCl salts. Their physical constants and analytical data are cited in Table I.

TABLE I. Diethylaminoethyl esters of *p*-[(*N*'-alkyl)-carbamoylamino]-benzoic acid.

No Ref	R <sub>1</sub>	R <sub>2</sub>	Yield %	Salt	Molecular formula	M.p. °C	Analyses							
							Calculated %				Found %			
							C	H	Cl	N	C	H	Cl	N
T4132	H	CH <sub>3</sub>	91,4	Picrate	C <sub>21</sub> H <sub>26</sub> N <sub>6</sub> O <sub>10</sub>	143-144 (b)	48,27	5,02	—	16,09	48,31	5,02	—	16,03
T4133	H	C <sub>2</sub> H <sub>5</sub>	92,3	Picrate	C <sub>22</sub> H <sub>28</sub> N <sub>6</sub> O <sub>10</sub>	129 (b)	49,25	5,26	—	15,67	49,16	5,29	—	15,54
T4134	H	nC <sub>3</sub> H <sub>7</sub>	93,1	Picrate	C <sub>23</sub> H <sub>30</sub> N <sub>6</sub> O <sub>10</sub>	128-129 (b)	50,18	5,49	—	15,27	49,98	5,37	—	15,21
T4135	H	nC <sub>4</sub> H <sub>9</sub>	89,2	Picrate	C <sub>24</sub> H <sub>32</sub> N <sub>6</sub> O <sub>10</sub>	139-140 (b)	51,06	5,71	—	14,89	51,02	5,83	—	14,83
T4137	CH <sub>3</sub>	CH <sub>3</sub>	84,6	Hydrochlorid	C <sub>16</sub> H <sub>26</sub> ClN <sub>3</sub> O <sub>3</sub>	142-143 (c)	55,89	7,62	10,31	12,22	55,53	7,56	10,23	12,35

(a) Yields of unpurified bases.

(b) Recrystallization from abs. ethanol.

(c) Recrystallization from abs. ethanol-anh.ether.

The diethylaminoethyl esters of p-[(N'-methyl)-carbamoylamino]-benzoic acid, were prepared as follows: 3g (0.0127 mol) of diethylaminoethylester of the p-aminobenzoic acid were dissolved in 30 ml anhydrous benzene and to this solution 0.94g (0.0165 mol, 30% excess) of methyl isocyanate were added. The mixture was left for 4 days at room temperature and the solvent was evaporated in vacuum. The resulting oily base gave picrate salt melting at 143-4° (EtOH abs) (T4132).

All the carbamate compounds appearing in the Table were prepared in the same way, with the exception of T4137, which was prepared by the addition of dimethylcarbamoylchloride instead of alky-isocyanate.

### Abstract

A series of diethylaminoethyl esters of the p-[(N'-alkyl)-carbamoylamino]-benzoic acid were synthesized by the reaction of the diethylaminoethyl ester of the p-aminobenzoic acid, with alkyl-isocyanates or dimethylcarbamoylchloride.

### Περίληψη

*Καρβαμιδικά παράγωγα του διαιθυλαμινοαιθυλεστέρος του ρ-αμινοβενζοϊκού οξέος.*

Στήν εργασία αυτή συνετέθη μία σειρά καρβαμιδικών παραγώγων του διαιθυλαμινοαιθυλεστέρος του ρ-αμινοβενζοϊκού οξέος με τόν σκοπό όπως ενισχυθῆ ἡ τοπική αναισθητική δράση τοῦ ἐν λόγω ἐστέρος.

Τά παράγωγα αὐτά ἐλήφθησαν δι' ἀντιδράσεως τοῦ διαιθυλαμινοαιθυλεστέρος τοῦ ρ-αμινοβενζοϊκού οξέος μέ ἰσοκυανικούς ἐστέρας ἢ διμεθυλαμινοκαρβαμοῦλοχλωρίδιο ἐντός ἀνύδρου βενζολίου καί ἐχαρακτήρισθησαν διά σχηματισμοῦ τῶν πικρικῶν ἢ ὑδροχλωρικῶν τῶν ἀλάτων.

### References and Notes.

1. Sekera, A.: *J. Mond. Pharm.*, 5, 1 (1962).
2. Haring, M.: *Helv. Chim. Acta*, 42, 1916 (1959).
3. Rushig, Stein, L.: *Germ. Pat.*, 949, 947 (1956).
4. Tsatsas, G., Papadaki-Valiraki, A., Benson, W., Ferguson, S.: *J. Med. Chem.*, 13, 648 (1970).